2019

# Endothelial N-Glycan Hypoglycosylation Enhances Cd16+ Monocyte Adhesion: A Role For Alpha-Mannosidases

Kellie Regal McDonald
*University of Alabama at Birmingham*

# ENDOTHELIAL *N*-GLYCAN HYPOGLYCOSYLATION ENHANCES CD16$^{+}$ MONOCYTE ADHESION: A ROLE FOR ALPHA-MANNOSIDASES

by

KELLIE REGAL MCDONALD

RAKESH PATEL, COMMITTEE CHAIR
SCOTT BALLINGER
JARROD BARNES
SUSAN BELLIS
SILVIO LITOVSKY
JAN NOVAK
C. ROGER WHITE

A DISSERTATION

Submitted to the graduate faculty of The University of Alabama at Birmingham,
in partial fulfillment of the requirements for the degree of
Doctor of Philosophy

BIRMINGHAM, ALABAMA

2019

ENDOTHELIAL *N*-GLYCAN HYPOGLYCOSYLATION ENHANCES CD16$^{+}$ MONOCYTE ADHESION: A ROLE FOR ALPHA-MANNOSIDASES

KELLIE REGAL MCDONALD

GRADUATE BIOMEDICAL SCIENCES

## ABSTRACT

Monocyte extravasation through the endothelial layer is a hallmark of atherosclerotic plaque development and is mediated by heavily glycosylated surface adhesion molecules, such as intercellular adhesion molecule-1 (ICAM-1). Human monocytes have been classified into three distinct groups – classical (anti-inflammatory; CD14+/CD16-), nonclassical (patrolling; CD14+/CD16++), and intermediate (pro-inflammatory; CD14++/CD16+). The CD16+ nonclassical / intermediate monocytes have been implicated in atherosclerosis progression and their levels positively associate with adverse cardiac events. However, there is a relative lack of understanding as to whether there are distinct mechanisms that regulate CD16+ vs. CD16- monocyte adhesion to the inflamed endothelium. Our previous data identified a high-mannose (HM) glycoform of ICAM-1 present during inflammation, but the function of different endothelial N-glycoforms is not yet known. Here, we test the hypothesis that distinct ICAM-1 N-glycoforms mediate recruitment of different monocyte subsets and specifically that endothelial HM-ICAM-1 promotes adhesion of CD16+ monocytes. We measured monocyte rolling and adhesion to i) TNFα-activated HUVEC, in which N-glycosylation was modulated by inhibiting α-mannosidase activity or by lectin-based blocking or ii) Cos-1 cells expressing HM- or complex ICAM-1. Expression of HM-ICAM-1 selectively enhanced CD16+ monocyte adhesion under flow with no effect on CD16- monocytes noted. This effect was dependent upon both HM epitopes and ICAM-1; adhesion was abrogated by blocking either.

Further, using the proximity ligation assay (PLA) we show that HM-ICAM-1 is present in human and mouse atherosclerosis, increasing with disease severity and positively correlating with CD68 macrophage staining. Finally, we addressed the mechanism behind the formation of HM-ICAM-1 during inflammation by studying endothelial α-mannosidases, a class of enzymes responsible for early N-glycan processing. We show that TNFα decreases class I α-mannosidase activity in a time-dependent manner, resulting in formation of HM-ICAM-1 on the cell surface. We also show that this decrease in activity is independent of NF-κB, suggesting a parallel mechanism of N-glycan regulation distinct from up-regulation of adhesion molecule protein expression. Together, these data highlight a high-mannose ICAM-1 present in human and mouse atherosclerotic lesions as a key mediator of $CD16^+$ monocyte recruitment to the endothelium, and identify α-mannosidases as a potential therapeutic target in atherosclerosis.

Keywords: monocytes, intercellular adhesion molecule 1 (ICAM-1), glycosylation, mannosidases, endothelium

# DEDICATION

I dedicate this dissertation to my husband, Jeff, without whom this would not have been possible. You have been my rock throughout this journey; understanding the late nights and early mornings, the obscene amounts of time spent writing, and being a springboard for ideas. Your constant support and love for me even at the most difficult of times is too great to put into words. There is something great to be said about having someone to come home to at the end of the day; who understands the frustration of lab work and who loves me even if my western blots don't. This journey is just one of many we will have in our lives, and I could not be happier to have anyone else by my side.

ACKNOWLEDGEMENTS

There are many people in which I have to thank for making this journey possible. First and foremost, I cannot say enough about my mentor, Dr. Rakesh Patel, who has simply gone above and beyond for me, and all of his students. You embody what it is to be a mentor; pushing me past any limits I thought I had, pushing me to do better science, to think critically, to work harder than I ever have before. But at the same time, truly caring about your students and what happens to them, and never forgetting that life is still happening outside of the lab. The amount of time you have poured into my training is unfathomable, and I finish my degree as a more confident and competent scientist because of you. Thank you for always pushing me, and for always being in my corner.

Along similar lines, I thank my labmates. Grad school is a bit easier when you enjoy the people you work around every day. You have all been integral to my growth as a scientist by pushing me in my technical and presentation skills, and have always been there at the end of a long day to encourage me to keep going, and to share in my OCD and laughter over silly things. I am grateful I had such a great environment to work in.

To my committee members (all six of you!), I thank you for your time and your contribution to this project. Your insight has been invaluable over the years and I am grateful for the expertise and conversations we've had around that conference table.

I have several former mentors without whom I would not have ended up in research. My undergraduate mentor, Dr. Joseph Deweese, took a chance on a sophomore

who had not even completed organic chemistry to work on a pharmacology research project. You mentored me through my first lab experience, first poster, first oral presentation, first conference, and first publication. Without your guidance and willingness to take on such a young student for years, I would not have fallen in love with research the way I did.

The other former mentor I have to thank is Dr. Michael Karlstad, who I worked for during my year off between undergrad and graduate school. From teaching me everything I know about animal work to how heat pumps work, you guided me through a crossroads in my life and propelled me towards a career in research. Without that time, I may have ended up in a completely different route of life. Both of these mentors I have so much respect for, and am eternally grateful for their impact on both my career and my life.

Away from the bench, I must thank my friends. I am surrounded by an amazing group of people, whether here in Birmingham, or all the way to different countries, you all have been supportive since day one; either blowing off steam with me or listening to my latest frustration even if they don't know what I'm talking about. I have been so blessed to have so many wonderful friends and wonderful life events to be involved in over the past few years to keep grounded to life outside of science.

Last but not least, I thank my family. For as long as I can remember, my parents have supported me and pushed me to aim for the stars. I would be remiss not to acknowledge the sacrifices you both made so that I could pursue my dreams; as I grow older I recognize more and more what you did so that your kids had a pathway to success.

I hope to one day to be able to pay back those sacrifices you made so that we could be successful.

They say it takes a village; and I have the best village of them all.

TABLE OF CONTENTS

*Page*

ABSTRACT ..... iii

DEDICATION ..... v

ACKNOWLEDGEMENTS ..... vi

LIST OF TABLES ..... xi

LIST OF FIGURES ..... xii

INTRODUCTION ..... 1

- Overview ..... 1
- Vascular Inflammation ..... 3
- Atherosclerosis ..... 6
- Endothelial Dysfunction: a Hallmark of Atherosclerosis ..... 7
- Monocytes: Not All Created Equal ..... 8
- Monocytes in Cardiovascular Disease and Atherosclerosis ..... 10
- Monocyte Adhesion to the Endothelium ..... 12
- Sweet Protein: N-glycosylation ..... 14
- Mannosidases: Key Regulators of N-glycosylation ..... 15
- Role of N-glycans in ICAM-1 Regulation and Function ..... 17
- ICAM-1 N-glycosylation and Monocyte Recruitment ..... 18
- Research Overview ..... 19

HIGH-MANNOSE INTERCELLULAR ADHESION MOLECULE-1 (ICAM-1) ENHANCES CD16+ MONOCYTE ADHESION TO THE ENDOTHELIUM ..... 27

ASSESSMENT OF ICAM-1 N-GLYCOFORMS IN MOUSE AND HUMAN MODELS OF ENDOTHELIAL DYSFUNCTION ..... 58

TNFα-INDUCED HYDROGEN PEROXIDE INHIBITS ENDOTHELIAL α-MANNOSIDASE ACTIVITY AND INCREASES SURFACE HIGH-MANNOSE N-GLYCANS ..... 90

DISCUSSION ..... 119

GENERAL LIST OF REFERENCES .....130

APPENDIX

A: COPYRIGHT STATEMENT AMERICAN JOURNAL OF PHYSIOLOGY .....142

B: INSTITUTIONAL REVIEW BOARD APPROVAL.....144

LIST OF TABLES

*Table* *Page*

INTRODUCTION

1 Endothelial adhesion molecules and their cognate receptors .....12

ASSESSMENT OF ICAM-1 N-GLYCOFORMS IN MOUSE AND HUMAN MODELS OF ENDOTHELIAL DYSFUNCTION

1 Atherosclerosis patient demographics .....85

2 AVF patient demographics .....88

LIST OF FIGURES

*Figure* *Page*

INTRODUCTION

1 Monocyte adhesion cascade....21

2 General mechanisms that regulate monocyte-endothelial interactions....22

3 N-glycan biosynthesis pathway....23

4 Potential isomers generated by class I α-mannosidases....24

5 ICAM-1 N-glycoforms and structure....25

6 Schematic overview of the questions focused around this dissertation....26

HIGH-MANNOSE INTERCELLULAR ADHESION MOLECULE-1 (ICAM-1) ENHANCES CD16+ MONOCYTE ADHESION TO THE ENDOTHELIUM

1 Lectins used in this study and their specificity for N-glycan structures....49

2 TNFα forms endothelial HM-ICAM-1 in a time-dependent manner....50

3 Kifunensine and Swainsonine selectively form HM and hybrid N-glycans on the activated endothelium....52

4 $CD16^{+}$ monocyte adhesion is enhanced by endothelial HM epitopes....53

5 $CD16^{+}$ monocyte adhesion is dependent on endothelial HM epitopes and ICAM-1....54

6 HM-ICAM-1 enhances $CD16^{+}$ monocyte adhesion under flow....55

ASSESSMENT OF ICAM-1 N-GLYCOFORMS IN MOUSE AND HUMAN MODELS OF ENDOTHELIAL DYSFUNCTION


1 Proximity-Ligation assay (PLA) schematic and lectin specificity .....80

2 HM epitopes co-localize with ICAM-1 in high fat-induced mouse atherosclerosis .....81

3 HM / hybrid, HM, and α-2,6-sialylated ICAM-1 are increased in mouse atherosclerosis after induction of disturbed flow *in vivo*.....83

4 CD68 macrophage staining positively correlates with HM-ICAM-1 in mouse models of atherosclerosis .....84

5 HM / hybrid ICAM-1 is increased in human atherosclerosis .....86

6 CD68 macrophage staining positively correlates with HM / hybrid ICAM-1 .....87

7 HM / hybrid, HM, α-2,6-sialylated, ICAM-1 are increased CKD patients with failed arteriovenous fistulas.....89


TNFα-INDUCED HYDROGEN PEROXIDE INHIBITS ENDOTHELIAL α-MANNOSIDASE ACTIVITY AND INCREASES SURFACE HIGH-MANNOSE N-GLYCANS


1 TNFα inhibition of α-mannosidase activity and HM N-glycan formation occurs early .....113

2 TNFα inhibition of α-mannosidase activity is class-I dependent .....115

3 Hydrogen peroxide inhibits α-mannosidase activity in a time and dose dependent manner.....116

4 ERO1-α inhibition abrogates TNFα-inhibition of α-mannosidase activity and HM N-glycan formation.....117

5 HOCl and $ONOO^-$ have no effect on α-mannosidase activity .....118


DISCUSSION


1 Formation of HM N-glycans on the cell surface recruit $CD16^+$ monocytes..129

# INTRODUCTION

Vascular inflammation is a carefully orchestrated process critical for innate immunity, but also underlies several acute and chronic diseases afflicting all major organ systems. The focus of this dissertation is endothelial dysfunction, which is key feature in chronic inflammatory diseases including atherosclerosis, the disease focused on in this dissertation, as well as chronic kidney disease (CKD), diabetes, and autoimmune diseases such as lupus (9-12).

Endothelial dysfunction can be characterized by a number of biochemical, molecular, and functional changes, one of which is the upregulation of surface adhesion molecules. Adhesion molecules are proteins induced by inflammation that recruit circulating leukocytes, such as monocytes and neutrophils, to the endothelium (8-10), and the primary focus of my research. Leukocytes have well-studied cognate receptors that recognize surface adhesion molecules and can use these to roll, firmly adhere, and migrate through the endothelial layer to the intima of the vessel (13). There, depending on the disease state, leukocytes can have several roles. This dissertation will primarily focus on monocytes, since monocytes in the intima differentiate into macrophages and give rise to the foci for foam cells that lead to plaque development during atherosclerosis (1, 14). Further, in CKD, monocyte recruitment can contribute to restenosis of the vessel wall after the formation of an arteriovenous fistula (AVF), resulting in AVF failure (15-18).

Abrogating monocyte adhesion, therefore, would be a viable method to therapeutically intervene in atherosclerotic plaque development and vessel restenosis. Since we know the adhesion molecules on the cell surface and their cognate receptors, therapeutically targeting this process should be straightforward. In animal models, atherosclerosis has been successfully abrogated by inhibition of adhesion molecules, including intercellular adhesion molecule 1 (ICAM-1) and P-selectin (19-22). Translation into humans, however, has not yet had therapeutic efficacy, and in some cases has even had increased mortality and adverse clinical events (23, 24).

Therapeutics targeting monocyte-endothelial interactions used in these trials were developed at a time before monocyte and endothelial heterogeneity were appreciated, which may explain their lack of success. We know now that monocytes are heterogeneous; consisting of 2-3 subsets in humans and mice that have varying roles in disease (25-27), and also that endothelial beds are heterogeneous, responding differently to inflammatory stimuli (28-30). More on that will be discussed later. Despite this understanding, it is still not known how the endothelium may recruit specific monocyte subsets during inflammation. In this dissertation, I hypothesize that the key mediators of monocyte subset adhesion are endothelial N-glycans, which are regulated by inflammatory stimuli.

To this end, I show in **chapter 2** that a hypoglycosylated, high-mannose (HM) N-glycoform of intercellular adhesion molecule-1 (ICAM-1) specifically recruits pro-inflammatory monocyte subsets to the inflamed endothelium. In **chapter 3**, I show that this HM-ICAM-1 is present in human and mouse models of endothelial dysfunction, including atherosclerotic lesions and failed AVFs in CKD patients. In **chapter 4**, I present data

to demonstrate a role for inflammatory stimuli and reactive species in regulating N-glycosylation in endothelial beds via α-mannosidases, a class of early N-glycan processing enzymes. Taken together, these data support the hypothesis that inflammation inhibits N-glycosylation pathway enzymes, leading to increased surface HM epitopes, and specifically HM-ICAM-1, in vascular beds which will selectively recruit pro-inflammatory monocytes, exacerbating inflammatory disease.

Next, I will provide a broad introduction into vascular inflammation, monocyte subsets, mechanisms governing monocyte-endothelial interactions, N-glycosylation, and our current understanding of the endothelial "zip-code".

## Vascular inflammation

Atherosclerotic plaque development in the vessel wall occurs in part via a low-level chronic vascular inflammation, characterized by endothelial dysfunction (9, 10). Exposure of the endothelial cell layer to pro-inflammatory factors such as hyperlipidemia or hyperglycemia, pro-oxidant and inflammatory stimuli, or turbulent blood flow results in endothelial dysfunction. Cardinal amongst the changes in the endothelium during inflammation is a more adhesive surface that is key to the recruitment and extravasation of monocytes into the sub-endothelial space (31-33). Circulating monocytes are captured onto the endothelium via a process of rolling, firm adhesion, and ultimately migration through to the intima where they can differentiate into macrophages and form foci for foam cells. (4, 8, 32, 34, 35).

Specific binding between adhesion molecules expressed on the surface of the endothelium and cognate receptors on monocytes is the established mechanism for mediating monocyte rolling, adhesion and transmigration. The specific adhesion molecules, their roles in the adhesion cascade, and their respective leukocyte cognate receptors have been identified, discussed further below. In addition, how their function is controlled is also largely understood. On the endothelial side, the most appreciated mechanism involves surface expression levels. Pro-inflammatory stimuli induce signaling cascades, typically via NF-κB, that either up-regulate gene, protein, and then surface expression, and / or mobilize, pre-formed intracellular stores of adhesion molecules, to the cell surface. This paradigm is supported by many years of research from multiple labs (36-38).

As mentioned earlier, much of our knowledge of endothelial adhesion molecule function, and how they bind with their cognate receptors on the monocyte, were elucidated at a time when both monocyte and vascular endothelial heterogeneity was not as appreciated as it is now. Human monocytes exist in at least 3 distinct subtypes, each having different surface marker expression, chemokine secretion, and adhesive properties that will be discussed at length later (14, 25, 27, 39). Importantly, these monocytes are differentially correlated with disease severity across atherosclerosis and other diseases such as diabetes and CKD (14, 39, 40). Moreover, the mechanisms governing endothelial responses to inflammation vary depending on the vascular bed in which these cells reside (28, 29). These newer insights collectively underscore, in our opinion, a relatively less understood aspect of monocyte-endothelial interactions; if there are there mechanisms that regulate monocyte subset adhesion differently and in a manner that allows vascular bed and / or disease selectivity.

This dissertation focuses on the concept of an endothelial “zip code”, i.e., that there are molecular and/or biochemical signatures across vascular beds that control the homing of monocyte subsets to specific endothelial surfaces (28, 29, 41). Specifically, I focus on endothelial adhesion molecule N-glycosylation, which our lab feels remains a relatively under-explored facet of the mechanisms regulating adhesion molecule function.

Our lab and others have shown that N-glycosylation of adhesion molecules vary across endothelial beds during inflammation and may be key for leukocyte homing (41, 42). For example, Renkonen et al (43), used three different antibodies against epitopes of sialyl-Lewis X, sulfated sialyl-Lewis X, and sulfated lactosamine structures on L-selectin ligands and measured their expression levels across several inflammatory diseases including thyroiditis, vasculitis, myocarditis, and colitis (41). When compared to non-inflamed tissue, the inflamed endothelium contained higher amounts of sialyl-Lewis X and sulfated sialyl-Lewis X structures. Also, the relative expression of each epitope varied by disease with vessels that were positive for all three glycan epitopes measured, and this was suggested to be associated with L-selectin-dependent lymphocyte homing. The investigators then assigned each disease a three-number code based on the positive staining for each epitope tested, deeming it an organ-specific “zip code” (41, 44).

This study is one of the few studies looking at N-glycans providing an endothelial “zip code”, and it is worth noting that their assignment of zip codes are based primarily on the level of each epitope stained for, but all epitopes are forms of sialyl-LewisX structures. We propose that an endothelial zip code may exist based on different types of N-glycan structures in different endothelial beds.

I provide evidence in this dissertation, that HM N-glycans, specifically on ICAM-1, are key mediators of pro-inflammatory monocyte adhesion during inflammation and together, these data demonstrate the presence N-glycan endothelial "zip code" made up of hypoglycosylated, or less complex, structures that are critical to selective recruitment of pro-inflammatory monocytes to specific vascular beds (43).

## Atherosclerosis

Cardiovascular disease (CVD) is the leading cause of death in the United States, with approximately 600,000 deaths attributed to it each year (45, 46). Atherosclerosis is the most common underlying cause of mortality attributed to CVD (46), which is the narrowing of the blood vessels due to the accumulation of fatty plaque in the vessel wall. Starting out as fatty streaks in the early decades of life, this plaque grows throughout a lifetime to where it can block blood flow almost entirely in the vessel, or rupture and block a smaller vessel downstream, resulting in a heart attack or stroke (47, 48). Hypocholesteremia, hyperlipidemia, and high blood pressure are all contributors to plaque development, and risk factors such as smoking and diabetes further increase the prevalence of disease.

At the molecular level, excess lipids are stored in the intima of the blood vessel wall, promoting a local inflammatory response (33, 48, 49). Resident macrophages in the intima are loaded with the excess lipids, and a failure in lipid recycling in these lipid-laden macrophages, as well as a lack of apoptotic clearance of these cells, results in the formation foam cells that are hallmark of plaque production (50, 51). In addition, the endothelial cell responds via mechanosensors to inflammatory stimuli, such as turbulent

blood flow (9, 10), causing the endothelium to release cytokines such as TNFα and IL-1β that will further activate the endothelium (33, 47, 49). The resulting endothelial dysfunction occurs early and ongoing throughout atherosclerosis due to the sustained inflammatory signaling. Next I will discuss what we know about endothelial dysfunction and propose what we may be overlooking.

## Endothelial dysfunction: a hallmark of atherosclerosis

During vascular inflammation, the endothelium responds with several phenotypic changes that define endothelial dysfunction: 1) the decrease of nitric oxide (NO) availability, 2) the increase of surface adhesion molecules, and 3) the increase of monocyte extravasation through the endothelial layer (9, 10). These changes contribute to the vascular inflammation seen in the diseases briefly discussed in the introduction. Here, I will elaborate on the role of endothelial dysfunction in atherosclerosis.

Under non-inflamed conditions, the endothelium acts as a tight barrier to the vessel wall, keeping cells from migrating in or out (9, 10). When exposed to inflammation, the barrier changes to allow cells in and out as need be. Acute inflammation can result in "leaky" vessels; allowing cells and fluids to pass through freely, while chronic inflammation is a more controlled process; selectively recruiting and releasing cells through the vessel wall.

Monocytes cross the endothelial layer and differentiate into macrophages during inflammation that in turn fuel plaque development. The more adhesion molecules on the

cell surface, the more monocytes will adhere and contribute to lesion formation. As mentioned, monocyte adhesion to the endothelium, therefore, has been well-described, yet it has not yet been therapeutically targeted.

The endothelium is heterogeneous, as mentioned earlier. Monocytes, as will be discussed in the next section, are also heterogeneous. The mechanism that recruits monocyte subsets to specific vascular beds remains unknown, and that is the focus of this project. I propose that one major aspect of endothelial dysfunction that we have overlooked is the N-glycosylation of the endothelium. While we know N-glycans exist on the cell surface, little is understood of their regulation, changes, and function in inflammation. This project proposes the model that endothelial heterogeneity during disease is due to these N-glycans, specifically under-processed, hypoglycosylated N-glycans, that can recruit specific monocyte subsets.

## Monocytes: not all created equal

Monocytes are myeloid-derived immune cells integral to the innate immune system and make up 5-10% of total circulating leukocytes in the average adult. Once mature and released from the bone marrow, they circulate for several days before undergoing cell death or infiltrating injured tissues, where they differentiate into macrophages and dendritic cells to resolve inflammation (52, 53).

Since their discovery, human monocytes have been categorized into three different categories based on surface expression of the lipopolysaccharide receptor CD14 and the Fcγ receptor III CD16. 90% of the typical circulating human monocyte population is

made up of classical monocytes (CD14++/CD16-) while the remaining 10% consists of non-classical (CD14+/CD16++) and intermediate (CD14++/CD16+) monocytes (25, 54).

Of the three subsets, classical monocytes are considered the most anti-inflammatory due to producing the highest levels of anti-inflammatory cytokines, such as IL-10 (14). Classical monocytes also differ the most in transcriptional and surface marker profiling compared to the non-classical and intermediate monocytes (55). They have little to no detectable levels of the chemokine receptor CX3CR1, which is expressed on the other monocyte subsets and thought to play a role in monocyte recruitment to damaged endothelial beds (55, 56). Further, classical monocytes have high expression of genes encoding phagocytic, antimicrobial, and wound healing activities, highlighting their importance in tissue repair (57-59).

Non-classical monocytes express genes associated with cytoskeletal rearrangement, allowing for their patrolling behavior along the endothelium to survey tissues (55, 60). Further, while classical and intermediate monocytes can secrete various levels of cytokines and reactive oxygen species (ROS), the non-classical monocytes have little secretory activity, only triggered by viruses or nucleic acids (57).

As implied by their name, intermediate monocytes fall on a middle ground between the classical and non-classical monocytes. They have the greatest inflammatory potential and are the greatest producers of ROS (57, 59, 61, 62). Intermediate monocytes harbor the highest expression of MHC-II (HLA-DR), which in turn gives them a strong capability of inducing CD4+ T-cell proliferation (14, 55). However, these studies have been contradictory, with some studies also claiming that intermediate monocytes are robust producers of the anti-inflammatory cytokine, IL-10 (27, 63). This speaks to the true

intermediate nature of these monocytes; that they can produce both pro- and anti- inflammatory cytokines. In the context of disease, however, it seems that the pro-inflammatory function of intermediate monocytes dominates any anti-inflammatory capabilities.

## Monocytes in cardiovascular disease and atherosclerosis

As already mentioned, monocyte extravasation through the endothelial cell layer of the vessel wall is key in atherosclerotic plaque development. Monocytes are recruited to the endothelium during inflammation and migrate through to the intima of the vessel, where they mature into macrophages and provide foci for foam cells, which are the main components of atherosclerotic plaque (see **Figure 1A**). Historically, this process was thought to be an early event in atherosclerosis (31, 32), as demonstrated by scanning electron microscopy of pre-atherosclerotic human aortas showing increasing adhesion of monocytes compared to athero-resistant vessels (64-66). However, we know now that monocytes are also continually recruited throughout lesion formation, especially if the lesion undergoes neovascularization (65, 67, 68). As monocytes contribute to both initial lesion formation and lesion advancement, understanding the dynamics of monocyte homing and infiltration was and remains a critical focus of atherosclerosis research.

Specific monocyte subsets have been associated with advanced disease states. Multiple studies have demonstrated that circulating intermediate monocytes correlate with more advanced atherosclerosis, peripheral artery disease, and independently predict adverse cardiac events in at-risk patients (61, 69-73). Results from the HOM SWEET HOMe (69) and the CARE FOR HOMe (74) studies show positive correlations between the levels of intermediate and non-classical monocytes subsets with disease severity,

prevalence of adverse cardiac events, and cardiac-related mortality in patients at-risk for cardiovascular disease and in chronic kidney disease patients. In both of these studies, large cohorts of patients at increased cardiovascular risk were followed for 3-4 years, and after adjustments for confounders, both studies found that intermediate monocytes were the only subset to independently correlate with cardiovascular events in these at-risk patient populations (69, 74). These data may be explained by selective recruitment of non-classical/intermediate $CD16^+$ monocytes to inflamed endothelial cells over classical $CD16^-$ monocytes. An important consideration in understanding how monocytes adhere is their relative cell numbers, greater numbers increase probability of adhesion by the law of mass action. Indeed, in atherosclerosis, total monocyte numbers are increased, but importantly, $CD16^+$ monocytes can expand to ~20-30% of the total monocyte population while $CD16^-$ monocyte levels can decrease to ~70-80% (40, 69, 71, 75, 76).

In addition to cell number, the affinity and avidity of adhesive interactions may also regulate how different monocyte subsets bind to the endothelium. Supporting this concept, are experiments that demonstrate that $CD16^+$ monocytes adhere to endothelial cells more strongly than $CD16^-$ monocytes during TNFα stimulated inflammation. Increased $CD16^+$ monocyte adhesion was observed under conditions where this subtype was either equal to or even lower in cell number relative to $CD16^-$ monocytes (77-79) 51-53. However, the mechanism regulating $CD16^+$ vs. $CD16^-$ adhesion remains unclear; potential mechanisms are discussed later.

Monocyte adhesion to the endothelium

Adhesion molecules are multidomain transmembrane proteins that are basally expressed at low levels or packaged in intracellular vesicles (80, 81). Once the endothelium is exposed to inflammatory stimuli, adhesion molecules are rapidly become transcribed or mobilized to be expressed on the cell surface (33, 35, 82). Endothelial adhesion molecules and cognate monocyte receptors involved in monocyte adhesion include are summarized in the table below, as well as illustrated in **Figures 1A-C**.

| **Endothelial Adhesion Molecule** | **Monocyte Receptor** |
|---|---|
| Intercellular adhesion molecule 1 (ICAM-1) | Lymphocyte function-associated antigen 1 (LFA-1)<br>Macrophage-1 antigen (MAC-1) |
| Vascular cell adhesion molecule 1 (VCAM-1) | Very late antigen-4 (VLA-4) |
| Platelet endothelial cell adhesion molecule (PECAM) | Platelet endothelial cell adhesion molecule (PECAM) |
| Mucosal addressin cell adhesion molecule 1 (MAdCAM-1) | Integrin α4β7 (LPAM) |
| E- and P- Selectin | P-selectin glycoprotein ligand-1 (PSGL-1) |

**Table 1.** Endothelial adhesion molecules and their cognate receptors.
(1-4), (2, 5-8).

Broadly speaking, there are several models, illustrated in **Figure 2**, by which interactions between these receptors are regulated. At the cellular levels, these include (**A**) Leukocyte cell number, and (**B**) Platelet bridging and chemokine-based recruitment (6, 33, 35, 83-87). On the leukocyte receptor side, these include (**C**) Receptor density or amount per cell, and (**D**) Binding affinity and avidity between cognate receptors (6, 7, 88-90). One example of ligand affinity is LFA-1, which can exist in low, intermediate, or

high affinity states defined by conformations that correlate with binding affinity to ICAM-1; the high affinity state increases binding to ICAM-1 by ~10,000 fold compared to the low affinity state (91). Another well-characterized example is leukocyte PSGL-1 and its post-translational modification with sialyl-Lewis X sugars that provide the actual ligands for endothelial E- or P-selectins; blocking the sialyl-Lewis X structure alone, without changing PSGL-1 expression, is sufficient to attenuate adhesion (89, 92).

How these models apply to the mechanisms controlling how different monocyte subsets adhere to endothelial cells remains unclear. This is an interesting question especially since both $CD16^-$ and $CD16^+$ monocytes express similar ligands for endothelial adhesion molecules. In some studies, intermediate monocytes have been reported to express higher levels of CD11b (Mac-1 integrin) compared to classical and nonclassical, yet other data shows that all three subsets express similar levels, and another has shown that nonclassical subsets express the lowest amount while intermediate and classical monocytes express similar levels (25, 55, 70, 93). Regardless, we have shown in our studies when we match cell-for-cell that baseline adhesion to TNFα-treated ECs is not different at least between the nonclassical/intermediate combination and classical subsets (79). In this case, increased adhesion to HM N-glycans is due to the endothelial N-glycan changes, and not monocyte ligand expression levels

We hypothesize that one potential mechanism for the selective recruitment of $CD16^+$ monocytes over $CD16^-$ cells is via an inflammation dependent regulation of endothelial adhesion molecule post-translational modification via N-glycosylation that occurs independently of inflammation-induced expression of these proteins.

## Sweet proteins: N-glycosylation

N-glycosylation is a co- and post- translational modification that occurs in the endoplasmic reticulum (ER) and Golgi and is necessary for correct protein folding, transport, and cell-to-cell interactions (e.g., immune responses) (94). During translation in the ER and Golgi, surface and secreted proteins with the appropriate consensus sequence Asn-X-Ser/Thr, where X is any amino acid except Pro, are adorned with a 14-mer sugar consisting of 2GlcNAc (*N*-acetylglucosamine), 3Glucose, and 9Mannose residues ($Glc_3Man_9GlcNAc_2$). As the protein is processed through the ER and Golgi, some sugar residues are sequentially trimmed and other sugar residues added through a series of enzymatic processes catalyzed by enzymes such as the α-mannosidases and the α-1,3-mannosyl-glycoprotein 2-β-N-acetylglucosaminyltransferase (MGAT) family. Finally, the addition of galactose, sialic acid, and fucose are catalyzed by transferases in the trans-Golgi and the fully-processed protein is trafficked to the cell surface to be expressed or secreted (94). See **figure 3** for the N-glycan biosynthesis pathway.

Second to phosphorylation, N-glycosylation is the most abundant post-translational modifications in proteins, and is restricted to surface and secreted proteins (95). Many of these proteins contain more than one N-glycosylation site; for example, ICAM-1, which will be discussed at length in the following sections, contains 8 N-glycosylation sites. Given that each of these sites can be modified by a different sugar, the possibilities of structures increase logarithmically with each site added. Lau et. al. calculated that a protein with one N-glycosylation site can have up to 14 different glycoforms, while a protein with 8 N-glycosylation sites can have >200,000 different glycoforms (96). For how many possible N-glycoforms there are, their functions remain vastly unexplored.

**Chapter 2** in this dissertation addresses some of the functional changes different N-glycoforms exhibit in monocyte adhesion. It is also worth noting that the idea of N-glycosylation mediating leuckoyte adhesion is not a new one (e.g., sialyl-LewisX ligands mediating selectin-dependent adhesion), but rather the novelty in the presented work lies in the endothelial N-glycans changing during inflammation and mediating monocyte subset adhesion.

## Mannosidases: key regulators of N-glycosylation

An important part of this project was looking at the regulation of N-glycans during inflammation. My data in **chapter 4** shows that α-mannosidases, enzymes involved in early N-glycan processing, are targets for inflammation-induced changes in surface N-glycans. I limit my introduction here on discussing α-mannosidases, but there are many other N-glycan processing enzymes not discussed further here, such as N-acetylglucosaminyltransferases (MGATs) and sialyltransferases (i.e., ST6GAL1) that can all play a role in disease status, especially in cancer (97, 98).

α-mannosidases are a class of enzymes responsible for the trimming of terminal mannose residues from early N-glycan structures in the ER and Golgi (99-103). There are two classes of α-mannosidases; class I enzymes cleave α−1,2-linked mannose residues while class II cleave α−1,3- and α−1,6- linked mannose residues. Together, these enzymes transform a high-mannose structure (5-9 mannose residues) into a hybrid (3-5 mannose residues), and finally into a complex structure (3 mannose residues).

Each class of α-mannosidases consist of multiple isoforms. Class I contains 5 different isoforms (MAN1A1, 1A2, 1B1, 1B2, and 1C1), while class II contains 4 isoforms

(MAN2A1, 2A2, 2B1, 2C1) (94, 103, 104). Class I α-mannosidases sequentially trim a 9-mannose structure to a 5-mannose structure one residue at a time. As outlined in **figure 4,** it has been shown that different class I isoforms can generate different high-mannose N-glycan structures; i.e., each α-mannosidase isoform cleaves a terminal mannose off different branches of the initial 9-mannose structure (104, 105). Each branch is assigned a number, and the resulting isomer is labeled based on the branch from which the terminal mannose is cleaved. For example, if the terminal mannose from the "A" branch in the 9-Mann structure is cleaved, the resulting 8-Man isomer is labeled M8A.

Class II α-mannosidases employ a two-step mechanism to cleave α-1,3 and α-1,6-mannose linkages. Their method of cleavage has been more well-defined compared to class I α-mannosidases as they sequentially cleave in the same catalytic site, and only have two possible residues to cleave (101).

We know very little about the regulation of α-mannosidases as well as their expression and activity across different tissues. What we do know is that N-glycosylation is a linear process, and given that α-mannosidases are early enzymes in the pathway, their inhibition will prematurely truncate N-glycosylation and the result will be proteins on the cell surface in a variety of under processed, hypoglycosylated N-glycoforms. In **chapter 4**, I show that endothelial α-mannosidases have decreased activity during inflammation and in turn, form hypoglycosylated, high-mannose (HM) structures on the cell surface.

## Role of N-glycans in ICAM-1 regulation and function

Endothelial adhesion molecules are heavily N-glycosylated; with some molecules harboring upwards of 10 N-glycan sites. For example, approximately 50% of the observed molecular weight of ICAM-1 is due to N-glycans (106). ICAM-1 has a predicted molecular weight of 50kDa, but is typically reported at a molecular weight around 100kDa (107, 108). Oftentimes, there is also a secondary band that appears around 75kDa and is largely ignored (107, 108). We have shown, however, that this secondary band is in fact a hypoglycosylated, or HM, form of ICAM-1 (**Figure 5A**) (106). The impacts of this N-glycoform and others on the endothelium during disease have remained largely unexplored.

This project has focused on ICAM-1 because of its known hypoglycosylation in inflammation but it is worth noting that other adhesion molecules, such as VCAM-1, are still heavily glycosylated. However, whether or not they have hypoglycosylated forms during inflammation remains unseen (106, 109).

ICAM-1 is a five-domain adhesion molecule responsible for the firm adhesion of leukocytes to the endothelium (**Figure 5B**). It is constitutively expressed on the cell surface at low levels until stimulation with inflammatory signals, such as TNFα, induce NF-κB activation to transcribe ICAM-1. Once on the cell surface, it can interact with circulating leukocytes (5, 7, 110-112).

Monocytes adhere to ICAM-1 through the integrins Mac-1 (CD11b/CD18) and LFA-1 (CD11a/CD18) at domains 3 and 1, respectively (**Figure 5B**) (5-7). Blocking of either inhibits leukocyte adhesion to ICAM-1 (5). Interestingly, monocyte subsets basally

express similar levels of CD11a/b and CD18 complexes (70, 93). If monocyte subsets express similar levels of adhesion molecule receptors, yet specific subsets are implicated in disease over others, there must be another mechanism selectively recruiting monocyte subsets to the endothelium. We propose that this mechanism is differential N-glycosylation.

## ICAM-1 N-glycosylation and monocyte recruitment

Interestingly, domain 1 of ICAM-1 is devoid of N-glycans, while domain 3 contains an N-glycosylation site. Furthering this point, Mac-1 binding to ICAM-1 can be regulated by altering glycosylation of the latter (110). Diamond, et. al., showed that Mac-1 adhesion could be eliminated by the deletion of domain 3 on ICAM-1, while LFA-1 binding was unaffected (5, 110). Most interestingly, Diamond et. al., demonstrated that Mac-1 binding to ICAM-1 was increased when ICAM-1 was treated with deoxymannojiriycin (DMJ), an α-mannosidase class I inhibitor that will cause the accumulation of HM structures on the cell surface. LFA-1 binding to ICAM-1 was not affected by treatment with DMJ, and treatment with neuraminidase to remove sialic acid residues from ICAM-1 had no effect on binding on either LFA-1 or Mac-1 to ICAM-1 (110). These data have several conclusions; that domain 3 mediates Mac-1 binding to ICAM-1, Mac-1 binding to ICAM-1 can be increased by the generation of a HM-ICAM-1, and that sialic acid residues, which are terminal sugars on complex N-glycan structures, have no impact on Mac-1 dependent adhesion. That said, there has been little follow-up on these early findings published over 20 years ago.

We and others (106, 109, 110, 113, 114) have shown that N-glycans on the endothelial surface are key modulators for monocyte adhesion. Specifically, hypoglycosylated N-glycans increase on the endothelial surface in atherosclerosis with ICAM-1 being the adhesion molecule harboring these structures. Blocking these HM epitopes with lectins or providing alternative HM epitopes attenuated monocyte adhesion (109). Importantly, the total levels of surface ICAM-1 did not change in these experiments; monocyte adhesion was attenuated only by changing the type of sugar on ICAM-1. The following chapters demonstrate these changes *in vivo* (**chapter 3**) and the impact they have on monocyte adhesion (**chapter 2**).

The data presented in this dissertation revolve around questions highlighted in **Figure 6 –** the expression of ICAM-1 N-glycans *in vivo*, the role of these N-glycans in mediating monocyte subset adhesion, the regulation of N-glycans, and which enzymes are responsible**.** Specifically, it is shown that hypoglycosylated ICAM-1 enhances adhesion of $CD16^+$ monocyte subsets via domain 3 (Mac-1), and can be abrogated by lectin blocking. Further, the data herein show a presence of these varied N-glycans *in vivo*; especially highlighting the presence of HM-ICAM-1 in advanced atherosclerotic lesions. Finally, some insight is gleaned into the mechanism of N-glycan hypoglycosylation on the cell surface by demonstrating a decrease in activity of α-mannosidases in the presence of inflammatory stimuli like TNFα and is due, at least in part, to the generation of ER-produced hydrogen peroxide. Taken together, the data presented in this dissertation

demonstrate a key role for hypoglycosylated N-glycans *in vivo* and present druggable targets for the generation of glyco-therapeutic drugs for the treatment of cardiovascular disease.

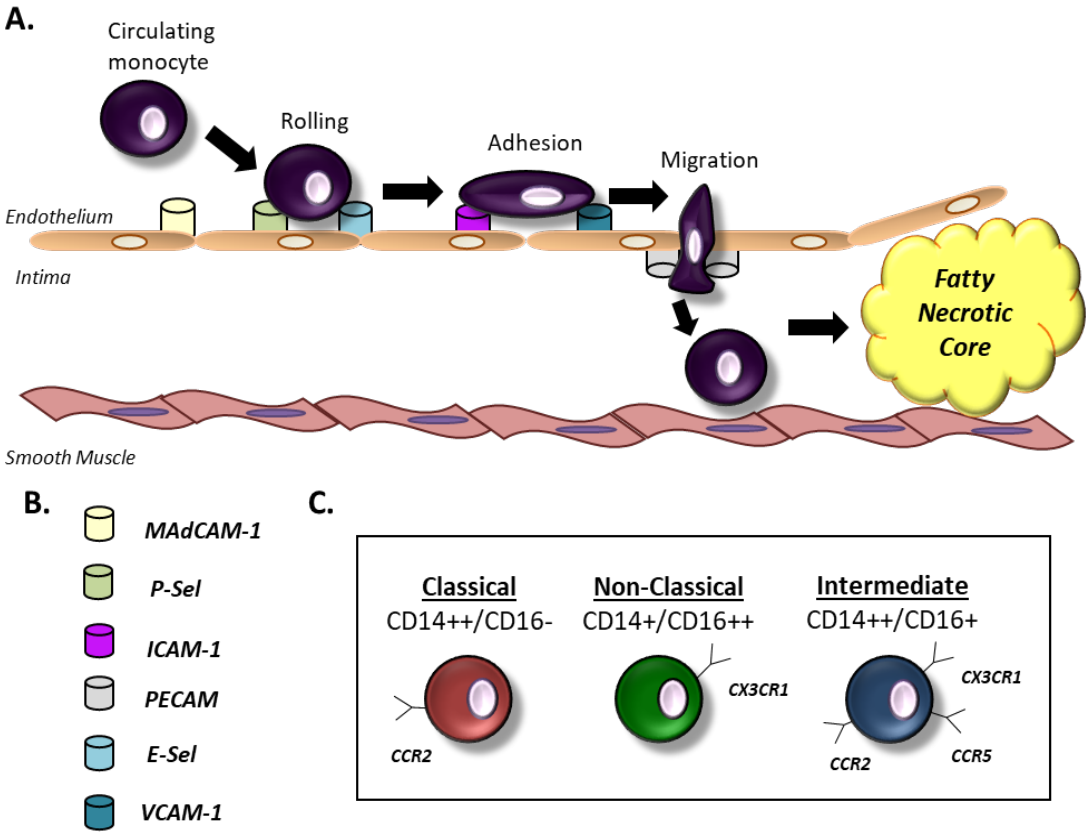


**Figure 1**. **Monocyte adhesion cascade.** **A**. Simplified cascade of monocyte rolling, adhesion, and migration into the intima of the vessel to fuel plaque development during atherosclerosis. **B.** Adhesion molecules on the endothelium. **C.** Monocyte subsets and their receptors classified into classical, nonclassical, and intermediate based on CD14 and CD16 surface markers

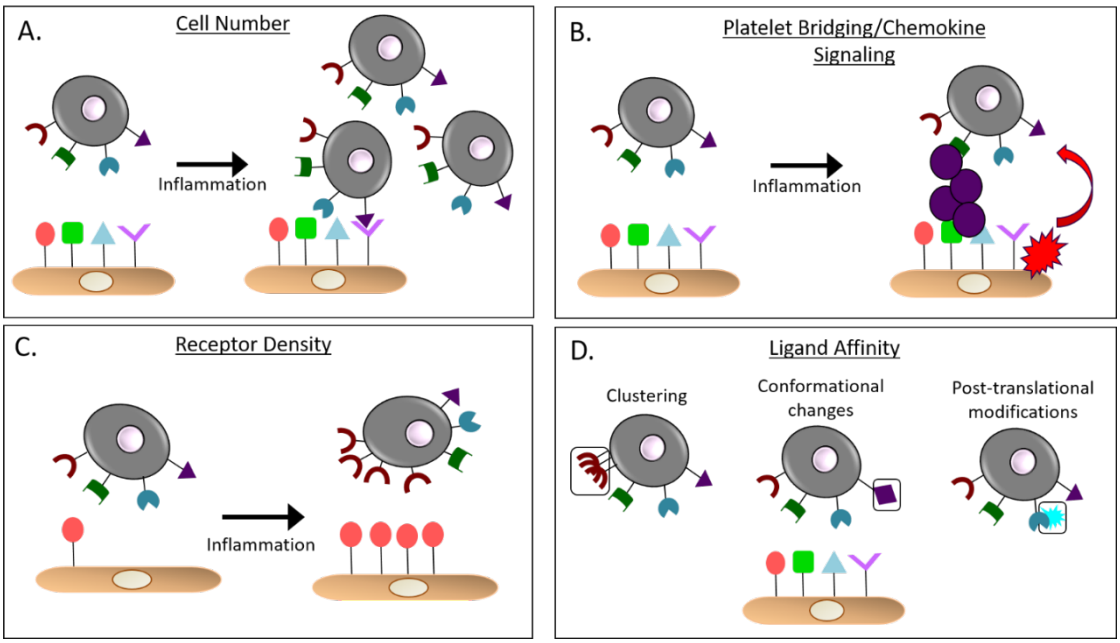


**Figure 2**. **General mechanisms that regulate monocyte-endothelial interactions. Panel A** illustrates an increase in cell number that will increase leukocyte binding via the laws of mass action. **Panel B** shows platelet bridging and chemokine secretion by the endothelium to recruit leukocytes. **Panel C** shows receptor density; that during inflammation there may be an increase in either leukocyte or endothelial ligands that facilitates binding. **Panel D** illustrates potential mechanisms that regulate affinity and avidity for binding between adhesion molecules. These include post-translational modifications, change in receptor confirmation, localization, and/or binding and clustering with other surface, cytosolic or matrix proteins.

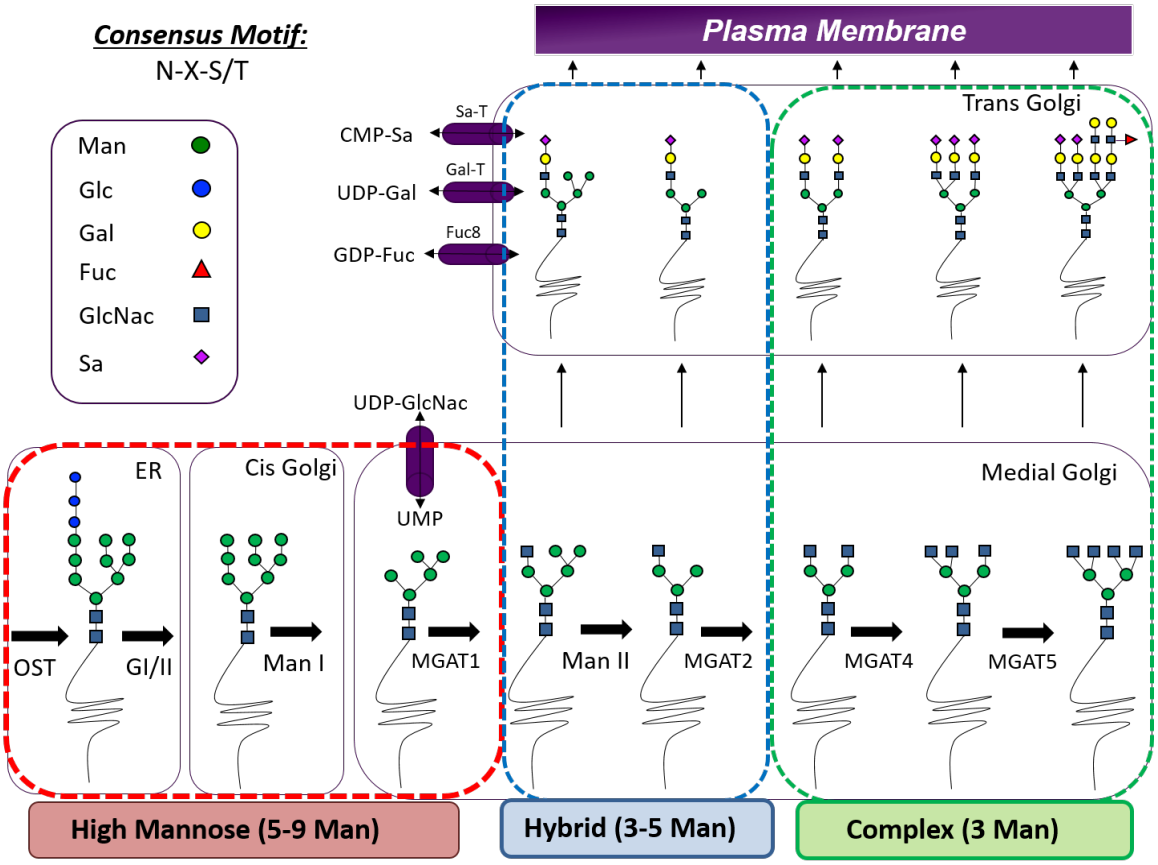


**Figure 3**. **N-glycan biosynthesis pathway.** A 14-mer sugar is added to Asn residues of proteins with the appropriate consensus sequence in the ER. The sugar is enzymatically processed through the ER and Golgi, adding and removing mannose (Man), glucose (Glc), galactose (Gal), Fucose (Fuc), N-acetylglucosamine (GlcNac), and sialic acid (Sa) residues until the protein is expressed on the cell surface in a fully processed, complex N-glycoform. Structures with 5-9 mannose residues are considered high-mannose; with 3-5 mannose considered hybrid; and with 3 mannose capped with other sugars considered complex.

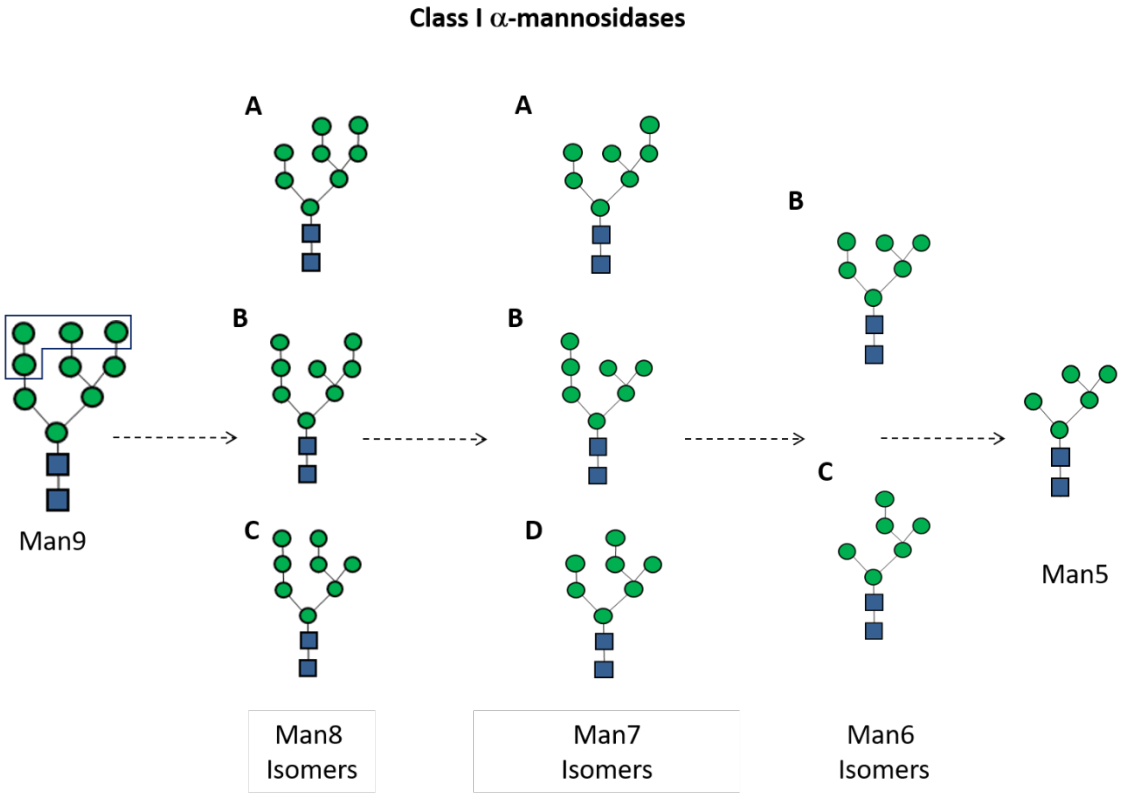


**Figure 4**. **Potential isomers generated by class I α-mannosidases.** Starting with a Man9 sugar structure, class I α-mannosidases will sequentially cleave one terminal mannose residue at a time until a Man5 structure is reached. Depending on the α-mannosidase isoform present and acting on the protein, the sequential steps can result in a variety of intermediate isomers.

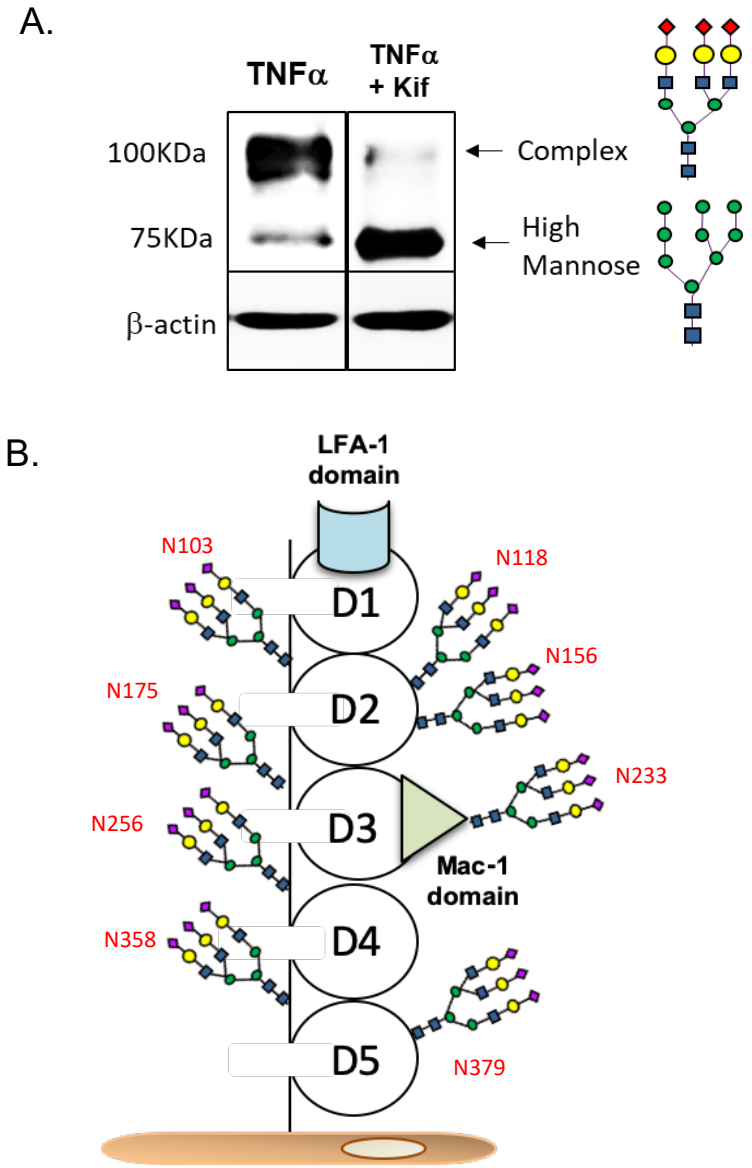


**Figure 5**. **ICAM-1 N-glycoforms and structure. A.** Western blot of ICAM-1 from TNFα-treated HUVECs with Kif pretreatment to demonstrate HM-ICAM-1 formation. Glycoforms are labeled. **B.** ICAM-1 contains 8 N-glycans sites over its 5 domains. LFA-1 binding site is in domain 1 while Mac-1 binding site is in domain 3.

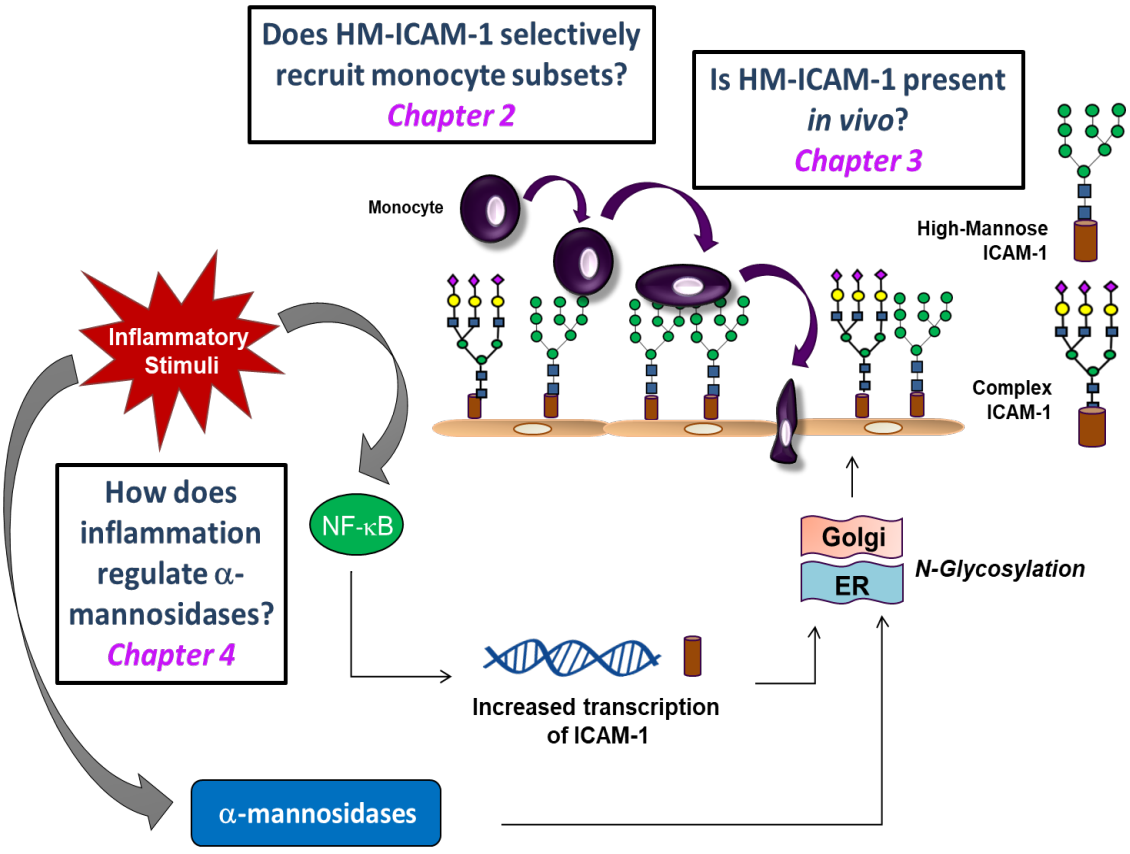


**Figure 6**. **Schematic overview of the questions focused around this dissertation.** The data contained in this dissertation will tease out some of the fundamental questions surrounding endothelial hypoglycosylation, the function of it in regards to monocytes subset adhesion (**chapter 2**), if it's present *in vivo* (**chapter 3**) and how it may be regulated during inflammation (**chapter 4**).

# HIGH-MANNOSE INTERCELLULAR ADHESION MOLECULE-1 (ICAM-1) ENHANCES CD16+ MONOCYTE ADHESION TO THE ENDOTHELIUM

by

KELLIE REGAL MCDONALD, BRITTNEY XU, JARROD W. BARNES, AND RAKESH P. PATEL

*American Journal of Physiology – Heart and Circulatory Physiology.*

## Abstract

Human monocytes have been classified into three distinct groups – classical (anti-inflammatory; $CD14^{+}/CD16^{-}$), non-classical (patrolling; $CD14^{+}/CD16^{++}$), and intermediate (pro-inflammatory; $CD14^{++}/CD16^{+}$). Adhesion of non-classical / intermediate monocytes with the endothelium is important for innate immunity, and also vascular inflammatory disease. However, there is an incomplete understanding of the mechanisms that regulate $CD16^{+}$ vs. $CD16^{-}$ monocyte adhesion to the inflamed endothelium. Here, we tested the hypothesis that a high mannose (HM) N-glycoform of intercellular adhesion molecule-1 (ICAM-1) on the endothelium mediates the selective recruitment of $CD16^{+}$ monocytes. Using TNFα treatment of human umbilical vein endothelial cells (HUVECs), and using proximity ligation assay (PLA) for detecting proximity of specific N-glycans and ICAM-1, we show that TNFα induces HM-ICAM-1 formation on the endothelial surface in a time-dependent manner. Next, we measured $CD16^{-}$ or $CD16^{+}$ monocyte rolling and adhesion to TNFα treated HUVECs in which HM- or hybrid ICAM-1 N-glycoforms were generated using the α-mannosidase class I and II inhibitors, Kifunensine and Swainsonine, respectively. Expression of HM-ICAM-1 selectively enhanced $CD16^{+}$ monocyte adhesion under flow with no effect on $CD16^{-}$ monocytes noted. $CD16^{+}$ monocyte adhesion was abrogated by blocking either HM-epitopes or ICAM-1. A critical role for HM-ICAM-1 in mediating $CD16^{+}$ monocyte rolling and adhesion was confirmed using Cos-1 cells engineered to express HM- or complex ICAM-1 N-glycoforms. These data suggest that HM-ICAM-1 selectively recruits non-classical/intermediate $CD16^{+}$ monocytes to the activated endothelium.

# Introduction

Monocyte adhesion and migration through the endothelial cell (EC) layer is a key process during inflammation (9). Monocyte trafficking is mediated by EC surface adhesion molecules, the surface expression of which are induced by inflammatory stimuli (8, 15). Once inflammation is resolved, adhesion molecule expression returns to basal levels. However, in chronic inflammation as seen in diseases such as atherosclerosis, diabetes, and autoimmune disorders, adhesion molecule expression remains elevatedα leading to excessive adhesion and accumulation of monocytes into the vessel wall (8, 16, 17, 42).

Relative to the understanding that monocytes are important drivers of inflammation, the appreciation that human monocytes are heterogeneous is a more recent advance in knowledge. Human monocytes are grouped into three categories based on the surface markers CD14 and CD16: classical (anti-inflammatory; $CD14^{++}/CD16^{-}$), non-classical (patrolling; $CD14^{+}/CD16^{++}$), and intermediate (pro-inflammatory; $CD14^{++}/CD16^{+}$) (7, 44). At rest, classical monocytes are most abundant, accounting for 90% of total monocytes. During chronic inflammation, non-classical and intermediate subsets can expand from ~10% to 20-30% (39, 40), depending on the disease. Further, higher levels of non-classical and intermediate monocytes are associated with poorer prognoses in atherosclerosis, diabetes, asthma, stroke, and other diseases (18, 21, 28, 29, 39). Recent studies have extensively characterized the biochemical, molecular and genetic profiles of the different monocytes (7, 19, 38, 41) and associated these with the distinct functions each monocyte subset mediates (30, 42, 43). Surprisingly however, little is known about mechanisms that govern how distinct monocyte subsets roll and adhere to an inflamed endothelial surface.

Endothelial intercellular adhesion molecule-1 (ICAM-1) is an important adhesion molecule that recognizes CD11a/CD18 (lymphocyte function-associated antigen 1; LFA-1) and CD11b/CD18 (macrophage-1 antigen; Mac-1) on monocytes to regulate the latter's rolling, firm adhesion and transmigration (3, 6, 11, 23, 27). ICAM-1 is heavily N-glycosylated; ~50% of its observed mass is due to N-glycans (5, 20). Protein N-glycosylation is an enzyme-driven, co-translational modification that attaches a core, branched tetradecasaccharide [$Glucose_3$-$Mannose_9$-N-Acetylglucosamine $(GlcNAc)_2$] onto the amide residues of Asn in the consensus sequence N-X-S/T (where X cannot be proline). Sugars from this core are sequentially cleaved by a series of glucosidases and mannosidases leading to high mannose and hybrid N-glycan structures in the endoplasmic reticulum. Thereafter, fucose, galacatose, GlcNAc, and sialic acid are added, resulting in complex N-glycoproteins (34). While most glycoproteins are assumed to be processed to complex forms for cell-surface expression, we have previously demonstrated that the endothelial cell surface expresses increased high mannose (HM) and/or hybrid N-glycans during inflammation (10, 33). In particular, using a model cell system where expression of ICAM-1 N-glycoforms could be controlled, we showed that ICAM-1 expressing HM/hybrid N-glycans resulted in increased adhesion of monocytes when compared to ICAM-1 bearing more complex type N-glycans (31). The current study tests (i) whether HM/hybrid ICAM-1 is formed and expressed on the surface of activated endothelial cells and if so, how this compares to complex N-glycoforms, (ii) whether HM/hybrid or complex ICAM-1 N-glycoforms selectively mediate adhesion of classical vs. non-classical / intermediate monocytes.

## Experimental procedures

### *Materials*

Human umbilical vein endothelial cells (HUVEC) were isolated from umbilical veins via collagenase as described (12). Cos-1 cells were a generous gift from Dr. Joanne Murphy-Urlich (University of Alabama at Birmingham). MCDB131, RPMI1640, DMEM, HI-FBS, trypsin, L-glutamine, and Penicillin/Streptomycin were purchased from Invitrogen (Carlsbad, CA). DuoLink® proximity ligation assay kit was purchased from ThermoFisher (Waltham, MA). CD14 and CD16 magnetic beads and magnetic columns were purchased from Miltenyi Biotec (Bergisch Gladbach, Germany). Parallel plate flow chambers were purchased from GlycoTech (Gaithersburg, MD). Concanavalin A (ConA), Sambucus Nigra (SNA), Hippeastrum Hybrid Amaryllis (HHL), and Maackia Amurensis Lectin II (MAL-II) lectins were purchased from Vector laboratories (Birlingame, CA). Where indicated, ConA or HHL were denatured by heating for 15min, at 95°C. Ki-funensine (Kif) and Swainsonine (Swain) were purchased form Cayman Chemicals (Ann Arbor, MI). Cell Trackers green (CMFDA) and blue (CMAC) were purchased from Thermo Fisher (Waltham, MA). All other reagents were purchased from Sigma-Aldrich (St. Louis, MO) unless otherwise noted.

### *Cell culture and treatment*

HUVEC were cultured as previously described (31). Cells were used within one day of reaching confluence and were serum-starved in MCDB-131 media containing 1% FBS for 2 hours prior to treatment. In some experiments, cells were pre-treated (2h) with the class I and II α-mannosidase inhibitors, Kifunensine or Swainsonine, respectively,

prior to addition of TNFα (10ng/ml, 4-18h). Cos-1 cells were transfected with human ICAM-1 as described(31). Once stably transfected, Cos-1 cells were cultured in DMEM media containing 10% FBS and 1x Pen/Strep with or without Kifunensine.

*Western blotting*

Cells were treated as described and lysed in RIPA buffer for 10 min on ice. 20 μg protein was loaded onto a 10% SDS-PAGE gel and subject to electrophoresis before being transferred to a 0.2 μm nitrocellulose membrane and probed for the described protein O/N at 4 degrees C with rocking. Membranes were incubated with HRP-linked, species-appropriate secondary antibodies for 2 hours at RT prior to chemiluminescence measurement. Images were analyzed using ImageQuant software (GE Healthcare Life Sciences).

*Proximity-ligation assay (PLA)*

Following treatment as described, HUVECs or Cos-1 cells were washed with ice-cold PBS with 1mM $MgCl_2$ and $CaCl_2$ prior to fixation with 4% PFA for 15 min at RT. After fixation, PLA staining was carried out as per the manufacturer's protocols. Briefly, 20 μg of the following biotinylated lectins: HM and hybrid N-glycan-specific lectin *Concanavalin A* (ConA), the α2,6-sialyation specific lectin *Sambucus nigra* (SNA), the HM-specific lectin *Hippeastrum hybrid* (HHL), or the α2,3-sialylation specific lectin *Maackia amurensis* (MAL-II) were added for 30 minutes at 4°C (see **figure 1**). These lectins were chosen to provide broad coverage of different N-glcyan structures. After 30min, cells were washed twice with PBS, samples were blocked with 1X Carbo-Free blocking solution (Vector Labs) for 30 min at 20-25°C. Immediately following blocking,

samples were incubated with oligo-tagged anti-ConA, avidin or anti-ICAM-1 (10 µg/mL) for one hour at 37°C followed by ligation and amplification steps as per the protocol. Human ICAM-1 (clone RR1/1) antibody recognizes the N-glycan devoid extracellular domain 1 epitopes on ICAM-1. Slides were left to dry and mounted using the DuoLink® mounting medium containing DAPI. To quantify, 3 random fields per group, per experiment were selected and average fluorescence intensity calculated and plotted per counted nuclei.

*α-mannosidase activity assay*

Total (class I and II) α-mannosidase activity was determined as described (33) with minor modifications. Cells were washed with PBS before lysis in PBS containing 1% Triton X-100 for 10 min on ice before clarification at 10,000 x g for 10 min. 50 uL cell lysate (corresponding to 30-40 ug protein) was prepared, in a microtiter plate, in 100 mM acetate buffer (pH 6.5) and 200 uM of the α-mannosidase substrate, resorufin-α-d-mannopyranoside added to start the reaction. Plates were read continuously at 550 nm and 595 nm in a Biotek Synergy plate reader for 18 h at 37°C.

*Surface N-glycan immunoprecipitation*

To label surface N-glycans only, after treatment, cells were washed with ice-cold PBS containing 1mM $CaCl_2$ and $MgCl_2$ prior to incubation with 10µg biotinylated ConA for 15 min at 4 degrees C. Cells were lysed with 1% TritonX-100 in PBS and incubated with avidin resin for 2 hours at RT. Samples were washed 3x and boiled at 95 degrees C

for 10 minutes in 5X SDS loading buffer to release biotin complexes. Samples were then treated as western blot as described above.

*Monocyte and neutrophil isolation*

Primary human monocytes and neutrophils were isolated from freshly drawn whole blood collected by venipuncture from healthy volunteers using magnetic beads as described (32). Briefly, after removal of the plasma layer, blood was layered on top of a Histopaque 1119 to 1077 gradient and centrifuged at 700 x g for 20 minutes at RT. Monocytes appear at the interface of media and the 1077 layer while neutrophils appear between the two Histopaque layers. Monocytes were incubated with a CD16 antibody and isolated using positive selection via a magnetic column. The flow-through ($CD16^-$ cells) was then incubated with a CD14 antibody to isolate distinct $CD16^+$ and $CD16^-$ monocyte populations. Neutrophils were incubated with a CD15 antibody and isolated in the same manner. All cell separations were confirmed via flow cytometry analysis (not shown). All protocols were approved by the UAB Institutional Review Board.

*Monocyte and neutrophil rolling and adhesion assay*

Isolated monocyte populations were incubated with 1μM fluorescent CellTracker™ dyes; $CD16^-$ cells were labeled with CellTracker™ green (CMFDA) and $CD16^+$ cells were labeled with CellTracker™ blue (CMAC) for 30 min at 37°C. Cells were pelleted and supernatant aspirated to remove any unincorporated dye. $CD16^-$ and $CD16^+$ monocytes were then were combined in equal amounts (final cell count 250,000 cells/mL; 125,000 cell/ml of each subtype), unless otherwise stated. Treated HUVEC or

Cos-1 cells were exposed to fluorescent monocytes or neutrophils at a flow rate of 100 μL/min, corresponding to 1 dyne/cm$^2$, in a GlycoTech parallel plate flow chamber. Neutrophils were treated with 100 ng/mL PMA (15 min) prior to adhesion assay. Images were captured on a Biotek Lionheart live cell imager over 2 minutes at 30 frames/sec. Any cell that was stationary for ≥ 5 sec was considered firmly adhered as described (23)(32). Where indicated 10 min prior to adhesion assay, HUVEC were treated with ConA or HHL lectins (10 μg/ml) to block surface hybrid and HM-N-glycans.

*Statistics*

All statistical analyses were performed using GraphPad Prism software. Paired t-test or one-way ANOVA followed by Tukey's post hoc test were performed as indicated in the figure legends. A minimum of three independent experiments were performed for each replicate.

## Results

*HM-ICAM-1 formation is transient in TNFα treated endothelial cells*

Our previous studies have shown that the luminal surface of atherosclerotic lesions is characterized by increased HM/hybrid N-glycan structures that parallel with severity of disease (10, 31, 32). Moreover, we identified ICAM-1 as a candidate adhesion molecule that may harbor HM-structures on the endothelial surface. To determine if endothelial inflammation leads to formation of ICAM-1 harboring HM/hybrid N-glycan structures, we used western blot analysis and the proximity-ligation assay (PLA). Treatment of HUVECs with TNFα led to a time-dependent increase in ICAM-1 indicated by

100kD band (**Fig 2A**). Also seen is a ~75kD band that transiently appears at 4h, comprising ~25% of the total ICAM-1 at this time (**Fig 2B)**, after which it returns to basal levels by 18h. We have shown previously that the ~100kDa and ~75kD bands correspond to complex and HM/hybrid ICAM-1 N-glycoforms respectively(31).

To determine if different ICAM-1 N-glycoforms [HM, hybrid, and complex (via α-2,3-sialylated, and α-2,6-sialylated identification)] were expressed on the cell-surface, we used PLA. HUVECs were treated with TNFα and cell surface N-glycans labeled with biotinylated lectins (see **figure 1** for structures recognized by each lectin) followed by treatment with avidin and an anti-ICAM-1 antibody, both tagged with complementary oligonucleotides. Red puncta indicate positive staining where the two epitopes (ICAM-1 and the lectin-identified N-glycan structures) are within 40nm of each other. **Figs 2C & D** show representative images and **Fig 2E** quantitation. Surface HM/hybrid ICAM-1 transiently increased at 4 hours, whereas α-2,6-sialylated (SNA) ICAM-1 continued to increase over 18h. No α-2,3-sialyated ICAM-1 (MAL-II) was observed. HUVECs that were not exposed to TNFα had no detectable staining (data not shown) similar to the staining controls in which one of the PLA reagents was absent (**Fig. 2D**).

In order to test whether HM structures selectively bind $CD16^+$ vs. $CD16^-$ monocytes, we first established conditions to selectively express HM and hybrid structures on the endothelial surface using the α-mannosidase class I and II inhibitors, Kifunensine (Kif) and Swainsonine (Swain) respectively (**Fig. 3A**). Kif and Swain each inhibited α-mannosidase activity in HUVECs to similar extents indicating ~equal class I and class II α-mannosidase activities (**Fig. 3B**). Further, Kif and Swain produced HM and hybrid N-glycoforms of ICAM-1 indicated by the bands at 75 and 100Kd respectively, (**Fig. 3C-**

**D**). Importantly, Kif and swain did not change total ICAM-1 expression (**Fig. 3E**) nor surface ICAM-1 expression (**Fig. 3F**).

*Endothelial HM-epitopes and ICAM-1 enhance CD16$^+$ monocyte rolling and adhesion*

To test if HM or hybrid N-glycans had an effect on monocyte subset adhesion, HUVECs were treated as described and exposed to isolated monocytes under flow. As shown in **Figure 4A,** TNFα increased adhesion for both CD16$^-$ and CD16$^+$ monocytes. Pre-treatment of HUVECs with Kif or Swain had no effect on TNFα-dependent CD16$^-$ monocyte adhesion. However, Kif pre-treatment, but not Swain, significantly further increased CD16$^+$ monocyte adhesion by ~1.7-fold (**Fig. 4A**) suggesting that endothelial HM-epitopes have higher affinity for CD16$^+$ monocytes. Since neutrophils also adhere to endothelial ICAM-1 we tested the effects of Kif on neutrophil adhesion. Kif did not affect neutrophil adhesion to TNFα-treated HUVECs (**Fig. 4B**).

Physiologically, the relative abundance of circulating CD16$^+$ and CD16$^-$ monocytes is ~10% and ~90%, respectively. To evaluate if HM-epitopes can selectively recruit CD16$^+$ cells at these physiologic cell number ratios, we performed the same experiment as above using a 10:1 ratio of CD16$^-$ to CD16$^+$ monocytes. **Figure 4C** shows that TNFα increased both CD16$^-$ and CD16$^+$ monocyte adhesion relative to control. Swain had no effect, whereas Kif treatment significantly further increased CD16$^+$ monocyte adhesion relative to TNFα alone. This effect of Kif was not observed with CD16$^-$ monocyte adhesion. **Figure 4D** shows fold change in monocyte adhesion relative to CD16$^-$ cell adhesion to TNFα treated ECs. These data suggest that, while there are less CD16$^+$ cells relative to CD16$^-$ cells, the former are more likely to adhere to HM glycan epitopes.

*CD16+ adhesion to activated ECs is dependent on HM-epitopes and ICAM-1*

Next, we tested the effects of ConA or HHL dependent blocking of endothelial HM/hybrid type N-glycans on monocyte adhesion. **Figure 5A** shows ConA decreased adhesion of $CD16^-$ cells by 49% and $CD16^+$ cells by 75%. However, blocking with HHL only decreased adhesion of $CD16^+$ monocytes (by ~80%). Similar inhibitory effects of both lectins were observed in Kif pretreated cells, although only trends were noted with $CD16^-$ cell adhesion. Prior denaturation of Con A or HHL resulted in a loss in their ability to inhibit monocyte adhesion suggesting that this effect is not due to non-specific binding of lectins to the endothelium.

We hypothesized that ICAM-1 is the primary adhesion molecule harboring HM-epitopes that mediate $CD16^+$ adhesion. To test this we compared the effects of two anti-ICAM-1 blocking antibodies that recognize the LFA-1 (domain 1, D1) or Mac-1 (domain 3, D3) binding domains on ICAM-1 with an IgG control antibody. **Fig. 5B** shows that D1 and D3 blockade inhibits $CD16^-$ monocyte adhesion by ~75% and ~35% respectively. In Kif treated cells, D1 blockade still inhibited $CD16^-$ monocyte adhesion; however, D3 blockade had no effect. With $CD16^+$ monocyte adhesion, in the absence or presence of Kif, D1 blockade had no effect, whereas D3 blockade significantly (75-90%) decreased adhesion.

*HM-ICAM-1 enhances $CD16^+$ monocyte adhesion under flow*

To evaluate the potential for ICAM-1 N-glycoforms to regulate $CD16^+$ vs $CD16^-$ monocyte rolling and adhesion in the absence of other adhesion molecules, we utilized

Cos-1 cells, which inherently do not express ICAM-1. Cells were transfected with (WT) or without (EV) human ICAM-1 and grown in the presence or absence of Kif. **Fig. 6A** shows that total ICAM-1 expression was similar, but with Kif, all ICAM-1 migrated at ~75kDa consistent with a HM-ICAM-1 N-glycoform. Immunoprecipitation of surface proteins with ConA confirmed that HM-ICAM-1 was present on the cell surface with the levels being greater in Kif-treated cells (**Fig. 6B**). Furthermore, PLA analysis demonstrated the presence of HM-ICAM-1 in Kif-treated WT Cos-1 cells, with complex (α2,6-sialyated) ICAM-1 predominating in WT Cos-1 cells not treated with Kif (**Figs. 6C & D**).

$CD16^+$ monocyte adhesion is higher and rolling velocity is significantly slower to HM-ICAM-1 compared to complex ICAM-1 expressing Cos1 cells (**Figs. 6E & F**). $CD16^-$ monocyte adhesion was higher in ICAM-1 expressing Cos1 cells compared to empty vector control. Modulating N-glycoforms using Kif had no effect on $CD16^-$ monocyte rolling or adhesion. Treatment of WT or Kif exposed Cos-1 cells with ConA or HHL lectins, prior to assessing monocyte adhesion, had no effect on $CD16^-$ monocyte adhesion but significantly abrogated $CD16^+$ monocyte adhesion (**Fig. 6G**). Notably, both ConA and HHL abrogated $CD16^+$ cell adhesion to Cos-1 cells expressing predominantly complex ICAM-1 also; i.e. without prior Kif treatment (**Fig. 6G**). This indicates that a basal level of HM epitopes are present on the cell surface for HHL to block, which leads to inhibition of $CD16^+$ monocyte adhesion. Consistent with this conclusion, longer exposure times of PLA staining with HHL and ICAM-1 in WT ICAM-1 transfected Cos-1 cells, without Kif treatment, demonstrate clear HM-ICAM-1 staining (**Fig. 6H**). Further, ConA

and HHL had no effect on monocyte rolling velocities in $CD16^-$ cells. However, HHL rescued rolling velocity of $CD16^+$ cells in the presence of Kif (**Fig 6I**).

Finally, since $CD16^+$ monocytes were purified using positive selection by CD16-magnetic beads, these cells may have been activated leading to increased adhesivity. Therefore, monocyte adhesion to Cos-1 cells was also assessed using monocytes without CD16 based selection. In these experiments, at the end of the adhesion assay, cells were fixed and levels of CD62L and CD16 determined to assess relative adhesion of $CD16^-$ or $CD16^+$ cells respectively. **Fig 6J** shows that both CD62L and CD16 levels increased in ICAM-1 expressing Cos-1 cells, with only CD16 levels increasing further in Kif treated cells.

## Discussion

The process of monocyte adhesion to and migration across the EC layer is a key component of inflammatory responses, as is the more recent concept that there are distinct monocyte populations that have pro-inflammatory or anti-inflammatory (reparative) functions. However, there remains limited insight into whether the mechanisms that govern how $CD16^-$ vs $CD16^+$ monocytes adhere to inflamed endothelial cells are the same or are regulated differently. Both $CD16^-$ and $CD16^+$ cells express VLA4, LFA-1 (CD11a/18), and Mac-1 (CD11b/18), which comprise the main monocytic ligands for adhesion to endothelial VCAM-1 and ICAM-1. Since both monocyte subsets express similar levels of these ligands, it is unlikely their abundance accounts for differential recruitment of $CD16^-$ vs $CD16^+$ monocytes to the endothelium during inflammation(36, 39).

Some studies have demonstrated a role for $CX_3CR1/CX_3CL1$ (fractalkine) in the recruitment of $CD16^+$ monocytes (1, 2, 4); here we provide evidence that high-mannose (HM) N-glycans, specifically residing on endothelial ICAM-1, may selectively recruit $CD16^+$ monocytes.

A role for HM-epitopes is indicated by elevated $CD16^+$ monocyte adhesion in EC or Cos-1 cells treated with the α-mannosidase class I inhibitor Kif. This was confirmed by data showing that HHL or ConA, lectins that recognizes terminal mannose residues, abrogated $CD16^+$ monocyte adhesion. A role for surface HM epitopes was confirmed using Cos-1 cells transfected with ICAM-1. $CD16^+$ cell adhesion was higher in Cos-1 cells expressing higher levels of HM-ICAM1, and blocking surface HM using HHL, completely inhibited $CD16^+$ monocyte interactions. Interestingly, this inhibition was observed with control ICAM-1 transfected Cos-1 cells also where HM-ICAM-1 was still detectable, albeit at lower levels compared to Kif-treated cells (see **Fig 5H**). These data suggest that surface HM-sugars are primary mediators of $CD16^+$ cell adhesion. ConA also, albeit to lesser extent inhibited $CD16^-$ cell adhesion (**Fig 4A**) which is likely due to the fact that ConA also recognizes terminal glucose and galactose residues in addition to mannose residues (35). Indeed, ConA inhibited $CD16^-$ adhesion with or without Kif treatment suggesting for this monocyte subset, the anti-adhesive effect of this lectin is HM-independent.

Our previous studies identified ICAM-1 as the primary endothelial adhesion molecule whose N-glycosylation is modulated during inflammation (31). We therefore focused on determining the role of HM- and complex ICAM-1 N-glycoforms in mediating $CD16^-$ and $CD16^+$ monocyte adhesion in this study. A dependence on ICAM-1 was

demonstrated using ICAM-1-blocking antibodies. We show that $CD16^+$ monocyte adhesion occurs at the D3 ICAM-1 domain (where Mac-1 binds). These data are consistent with previous reports showing that the Mac-1 binding domain is N-glycosylated, while the LFA-1 binding domain is not (13, 26). Notably, a HM-dependence was not observed for PMN adhesion consistent with studies showing a dominant role for LFA-1 dependent interactions in mediating PMN- ICAM-1 adhesion (14, 24, 25). The mechanisms by which PMNs preferentially utilize LFA-1 dependent mechanisms, whereas CD16+ monocytes use Mac-1, remains to be determined and likely important in understanding how different leukocytes traffic to sites of injury.

A role for HM-ICAM-1 in mediating $CD16^+$ monocyte adhesion was demonstrated with both a mixture of naïve monocytes (without prior CD16 ligation) and with $CD16^+$ monocytes purified by positive selection using anti-CD16 coated magnetic beads. Moreover, in all experiments, total levels of ICAM-1 were similar, but HM composition of ICAM-1 was altered, and the latter regulated $CD16^+$ cell adhesion. This supports the conclusion that while ICAM-1 is necessary, HM-glycoforms on ICAM-1 confer selectivity for $CD16^+$ monocyte binding. This conclusion is further supported by experiments in which $CD16^+$ monocyte adhesion was determined at physiological ratios with $CD16^-$ cells (Fig 2C-D). If binding of $CD16^-$ and $CD16^+$ cells was equivalent, based on relative abundance, a 10-fold less adhesion of $CD16^+$ cells is expected. However, only a 2-fold decrease in $CD16^+$ cells, compared to $CD16^-$ cells was observed in TNFα treated ECs, and no difference in Kif-treated cells. Collectively, these data suggest that HM-ICAM-1 se-

lectively recruits low abundant $CD16^+$ monocytes to the endothelium. Since $CD16^+$ monocyte numbers expand during chronic inflammation, we speculate that HM-ICAM-1 plays a significant role in disease settings also (18, 39).

$CD16^+$ monocyte rolling velocity was selectively slowed when Cos-1 expressed HM-ICAM-1, consistent with earlier reports of a role for ICAM-1 in both the rolling and adhesion processes (16, 22, 37). However, the effects of HM glycoforms were greater in the firm adhesion step. Further studies are required to identify the precise interactions between HM-ICAM-1 and $CD16^+$ monocyte receptors. Current studies are focusing primarily on the ICAM-1 ligands Mac-1 and LFA-1, their activation states, and the role of CD16 itself.

Notably, surface expression of HM-ICAM-1 on cultured endothelial cells was transient providing an intriguing insight into the timing of inflammation. Based on our data, we speculate that an initial wave of pro-inflammatory monocyte infiltration is mediated by the formation of HM-ICAM-1. Thereafter, HM-ICAM1 levels decline preventing further $CD16^+$ monocyte recruitment and allowing resolution. Further studies testing how HM-ICAM-1 may change in chronic inflammation are warranted and may shed insights into how recruitment of pro-inflammatory monocytes continues in disease settings. While we have not investigated the mechanisms by which HM-N-glycan are transiently incorporated into induced ICAM-1, our prior data show that TNFα inhibits α-mannosidase activity (33). Given that N-glycan biosynthesis is a linear process, and data with Kif treatment, inhibition of α-mannosidase activity likely mediates formation of HM-N-glycans. Ongoing studies are determining the role of TNFα on the transient inhibition of α-mannosidase activity. Future studies are also required to map the specific N-glycan sites on ICAM-1

where HM-structures reside. The term ‘high-mannose’ does not imply that ICAM-1 exclusively expresses HM structures. ICAM-1 contains 8 N-glycosylation sites, and any single ICAM-1 is likely to harbor an array of N-glycans, from HM to complex structures. Our data simply demonstrates that a form of ICAM-1 harboring HM structures enhances $CD16^{+}$ monocyte adhesion.

In conclusion, the presented data suggest that endothelial HM-ICAM-1 is a key mediator for recruiting $CD16^{+}$ monocytes to the activated endothelium, and in turn may present a novel therapeutic target to modulate pro-inflammatory monocyte trafficking during innate immunity and inflammatory disease.

References

1. Ancuta P, Rao R, Moses A, Mehle A, Shaw SK, Luscinskas FW, and Gabuzda D. Fractalkine preferentially mediates arrest and migration of CD16+ monocytes. *J Exp Med* 197: 1701-1707, 2003.

2. Ancuta P, Wang J, and Gabuzda D. CD16+ monocytes produce IL-6, CCL2, and matrix metalloproteinase-9 upon interaction with CX3CL1-expressing endothelial cells. *J Leukoc Biol* 80: 1156-1164, 2006.

3. Argenbright LW, Letts LG, and Rothlein R. Monoclonal antibodies to the leukocyte membrane CD18 glycoprotein complex and to intercellular adhesion molecule-1 inhibit leukocyte-endothelial adhesion in rabbits. *J Leukoc Biol* 49: 253-257, 1991.

4. Aspinall AI, Curbishley SM, Lalor PF, Weston CJ, Blahova M, Liaskou E, Adams RM, Holt AP, and Adams DH. CX(3)CR1 and vascular adhesion protein-1-dependent recruitment of CD16(+) monocytes across human liver sinusoidal endothelium. *Hepatology* 51: 2030-2039, 2010.

5. Bloom JW, Madanat MS, and Ray MK. Cell line and site specific comparative analysis of the N-linked oligosaccharides on human ICAM-1des454-532 by electrospray ionization mass spectrometry. *Biochemistry* 35: 1856-1864, 1996.

6. Bourdillon MC, Poston RN, Covacho C, Chignier E, Bricca G, and McGregor JL. ICAM-1 deficiency reduces atherosclerotic lesions in double-knockout mice (ApoE(-/-)/ICAM-1(-/-)) fed a fat or a chow diet. *Arterioscler Thromb Vasc Biol* 20: 2630-2635, 2000.

7. Boyette LB, Macedo C, Hadi K, Elinoff BD, Walters JT, Ramaswami B, Chalasani G, Taboas JM, Lakkis FG, and Metes DM. Phenotype, function, and differentiation potential of human monocyte subsets. *PLoS One* 12: e0176460, 2017.

8. Carlos TM, and Harlan JM. Leukocyte-endothelial adhesion molecules. *Blood* 84: 2068-2101, 1994.

9. Cejkova S, Kralova-Lesna I, and Poledne R. Monocyte adhesion to the endothelium is an initial stage of atherosclerosis development. *Cor et Vasa* 58: e419-425, 2015.

10. Chacko BK, Scott D, Chandler RT, and Patel RP. Endothelial surface N-Glycans mediate monocyte adhesion and are targets for anti-inflammatory effects of peroxisome proliferator-activated receptor Y ligands. *J Biol Chem* 286: 38738-38747, 2011.

11. Collins RG, Velji R, Guevara NV, Hicks MJ, Chan L, and Beaudet AL. P-Selectin or intercellular adhesion molecule (ICAM)-1 deficiency substantially protects against atherosclerosis in apolipoprotein E-deficient mice. *J Exp Med* 191: 189-194, 2000.

12. Crampton SP, Davis J, and Hughes CCW. Isolation of Human Umbilical Vein Endothelial Cells. *J Vis Exp* 3: 183, 2007.

13. Diamond MS, Staunton DE, Marlin SD, and Springer TA. Binding of the integrin Mac-1 (CD11b/CD18) to the third immunoglobulin-like domain of ICAM-1 (CD54) and its regulation by glycosylation. *Cell* 65: 961-971, 1991.

14. Ding ZM, Babensee JE, Simon SI, Lu H, Perrard JL, Bullard DC, Dai XY, Bromley SK, Dustin ML, Entman ML, Smith CW, and Ballantyne CM. Relative contribution of LFA-1 and Mac-1 to neutrophil adhesion and migration. *J Immunol* 163: 5029-5038, 1999.

15. Galkina E, and Ley K. Vascular adhesion molecules in atherosclerosis. *Arterioscler Thromb Vasc Biol* 27: 2292-2301, 2007.

16. Gerhardt T, and Ley K. Monocyte trafficking across the vessel wall. *Cardiovasc Res* 107: 321-330, 2015.

17. Hilgendorf I, Swirski FK, and Robbins CS. Monocyte fate in atherosclerosis. *Arterioscler Thromb Vasc Biol* 35: 272-279, 2015.

18. Idzkowska E, Eljaszewicz A, Miklasz P, Musial WJ, Tycinska AM, and Moniuszko M. The role of different monocyte subsets in the pathogenesis of atherosclerosis and acute coronary syndromes. *Scan J of Immun* 82: 163-173, 2015.

19. Ingersoll MA, Spanbroek R, Lottaz C, Gautier EL, Frankenberger M, Hoffmann R, Lang R, Haniffa M, Collin M, Tacke F, Habenicht AJ, Ziegler-Heitbrock L, and Randolph GJ. Comparison of gene expression profiles between human and mouse monocyte subsets. *Blood* 115: e10-19, 2010.

20. Jimenez D, Roda-Navarro P, Springer TA, and Casanovas JM. Contribution of N-linked glycans to the conformation and function of intercellular adhesion molecules (ICAMs). *J Biol Chem* 280: 5854-5861, 2005.

21. Kapinsky M, Torzweski M, Buchler C, Duong CQ, Rother G, and Schmitz G. Enzymatically degraded LDL preferentially binds to $CD14^{high}$ CD16+ monocytes and induces foam cell formation mediated only in part by the class B scavenger-receptor CD36. *Arterioscler Thromb Vasc Biol* 21: 1004-1010, 2001.

22. Kevil CG, Chidlow JH, Bullard DC, and Kucik DF. High-temporal-resolution analysis demonstrates that ICAM-1 stabilizes WEHI 274.1 monocytic cell rolling on endothelium. *Am J Physiol Cell Physiol* 285: C112-118, 2003.

23. Kevil CG, Patel RP, and Bullard DC. Essential role of ICAM-1 in mediating monocyte adhesion to aortic endothelial cells. *Am J Physiol Cell Physiol* 281: C1442-1447, 2001.

24. Lefort CT, and Ley K. Neutrophil arrest by LFA-1 activation. *Front Immunol* 3: 157, 2012.

25. Li N, Yang H, Wang M, Lu S, Zhang Y, and Long M. Ligand-specific binding forces of LFA-1 and Mac-1 in neutrophil adhesion and crawling. *Mol Biol Cell* 29: 408-418, 2018.

26. Otto VI, Damoc E, Cueni LN, Schurpf T, Frei R, Ali S, Callewaert N, Moise A, Leary JA, Folkers G, and Przybylski M. N-glycan structures and N-glycosylation sites of mouse soluble intercellular adhesion molecule-1 revealed by MALDI-TOF and FTICR mass spectrometry. *Glycobiology* 16: 1033-1044, 2006.

27. Patel SS, Thiagarajan R, Willerson JT, and Yeh ET. Inhibition of alpha4 integrin and ICAM-1 markedly attenuate macrophage homing to atherosclerotic plaques in ApoE-deficient mice. *Circulation* 97: 75-81, 1998.

28. Rogacev KS, Cremers B, Zawada AM, Seiler S, Binder N, Ege P, Grosse-Dunker G, Heisel I, Hornof F, Jeken J, Rebling NM, Ulrich C, Scheller B, Bohm M, Fliser D, and Heine GH. CD14++CD16+ monocytes independently predict cardiovascular events: a cohort study of 951 patients referred for elective coronary angiography. *J Am Coll Cardiol* 60: 1512-1520, 2012.

29. Rogacev KS, Ulrich C, Blomer L, Hornof F, Oster K, Ziegelin M, Cremers B, Grenner Y, Geisel J, Kohler ASH, Fliser D, Girndt M, and Heine GH. Monocyte heterogeneity in obesity and subclinical atherosclerosis. *European Heart Journal* 31: 369-376, 2009.

30. Sampath P, Moideen K, Ranganathan UD, and Bethunaickan R. Monocyte Subsets: Phenotypes and Function in Tuberculosis Infection. *Front Immunol* 9: 1726, 2018.

31. Scott D, Dunn T, Ballestas M, Litovsky S, and Patel RP. Identification of a high-mannose ICAM-1 glycoform: effects of ICAM-1 hypoglycosylation on monocyte adhesion and outside in signaling. *Am J Physiol Cell Physiol* 305: C228-237, 2013.

32. Scott DW, Chen J, Chacko BK, Traylor JG, Orr AW, and Patel RP. Role for endothelial N-glycan mannose residues in monocyte recruitment during atherogenesis. *Arterioscler Thromb Vasc Biol* 32: 2012.

33. Scott DW, Vallejo MO, and Patel RP. Heterogenic Endothelial Responses to Inflammation: Role for Differentital N-Glycosylation and Vascular Bed of Origin. *J American Heart Association* 2: 2013.

34. Stanley P, Schachter H, and Taniguchi N. N-Glycans. In: *Essentials of Glycobiology*, edited by nd, Varki A, Cummings RD, Esko JD, Freeze HH, Stanley P, Bertozzi CR, Hart GW, and Etzler ME. Cold Spring Harbor (NY): 2009.

35. Stanley P, Schachter H, and Taniguchi N. N. Glycans. In: *Essentials of Glycobiology*, edited by Varki A, Cummings R, Esko J, Freeze H, Stanley P, Bertozzi C, Hart G, and Etzler M. New York: Cole Sping Harbor, 2009.

36. Stec M, Weglarczyk K, Baran J, Zuba E, Mytar B, Pryjma J, and Zembala M. Expansion and differentiation of CD14+CD16(-) and CD14+ +CD16+ human monocyte subsets from cord blood CD34+ hematopoietic progenitors. *J Leukoc Biol* 82: 594-602, 2007.

37. Steeber DA, Campbell MA, Basit A, Ley K, and Tedder TF. Optimal selectin-mediated rolling of leukocytes during inflammation in vivo requires intercellular adhesion molecule-1 expression. *Proc Natl Acad Sci U S A* 95: 7562-7567, 1998.

38. Weber C, Belge KU, von Hundelshausen P, Draude G, Steppich B, Mack M, Frankenberger M, Weber KS, and Ziegler-Heitbrock HW. Differential chemokine receptor expression and function in human monocyte subpopulations. *J Leukoc Biol* 67: 699-704, 2000.

39. Wildgruber M, Aschenbrenner T, Wendorff H, Czubba M, Glinzer A, Haller B, Schiemann M, Zimmermann A, Berger H, Eckstein HH, Meier R, Wohlgemuth WA, Libby P, and Zernecke A. The "Intermediate" CD14(++)CD16(+) monocyte subset increases in severe peripheral artery disease in humans. *Sci Rep* 6: 39483, 2016.

40. Wildgruber M, Czubba M, Aschenbrenner T, Wendorff H, Hapfelmeier A, Glinzer A, Schiemann M, Zimmermann A, Eckstein HH, Berger H, Wohlgemuth WA, Meier R, Libby P, and Zernecke A. Increased intermediate CD14(++)CD16(++) monocyte subset levels associate with restenosis after peripheral percutaneous transluminal angioplasty. *Atherosclerosis* 253: 128-134, 2016.

41. Wong KL, Tai JJ, Wong WC, Han H, Sem X, Yeap WH, Kourilsky P, and Wong SC. Gene expression profiling reveals the defining features of the classical, intermediate, and nonclassical human monocyte subsets. *Blood* 118: e16-31, 2011.

42. Wong KL, Yeap WH, Tai JJY, Ong SM, Dang TM, and Wong SC. The three human monocyte subsets: implications for health and disease. *Immunologic Research* 53: 41-57, 2012.

43. Woollard KJ, and Geissmann F. Monocytes in atherosclerosis: subsets and functions. *Nat Rev Cardiol* 7: 77-86, 2010.

44. Ziegler-Heitbrock L. Blood Monocytes and Their Subsets: Established Features and Open Questions. *Front Immunol* 6: 423, 2015.

*Funding:* This study was supported by HL007918 (KRM), and the K99/R00 Pathway to

Independence Award (R00HL131866, to J.W.B.).

*Acknowledgements:* N/A.

*Conflict of Interest:* None declared.

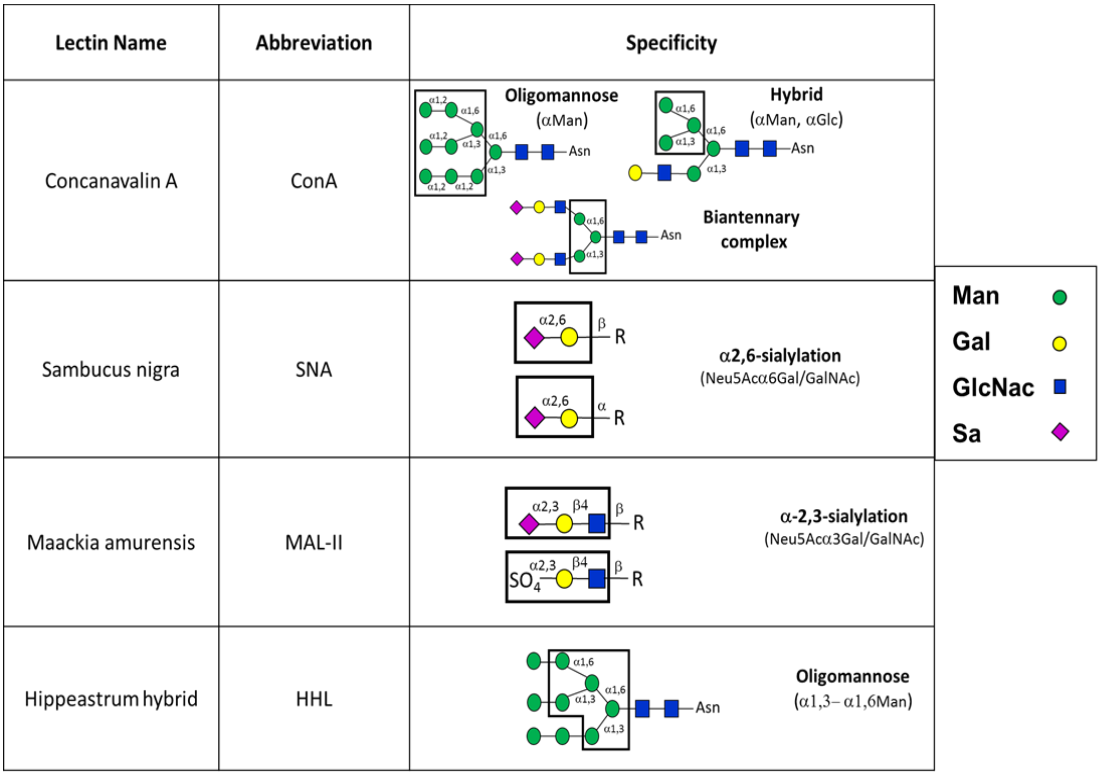


**Figure 1.** Lectins used in this study and their specificity for N-glycan structures (Adapted from(34)). Man= Mannose; Gal = Galactose; GlcNac = N-acetylglucosamine; Sa = Sialic acid; R= varying N-glycan structures.

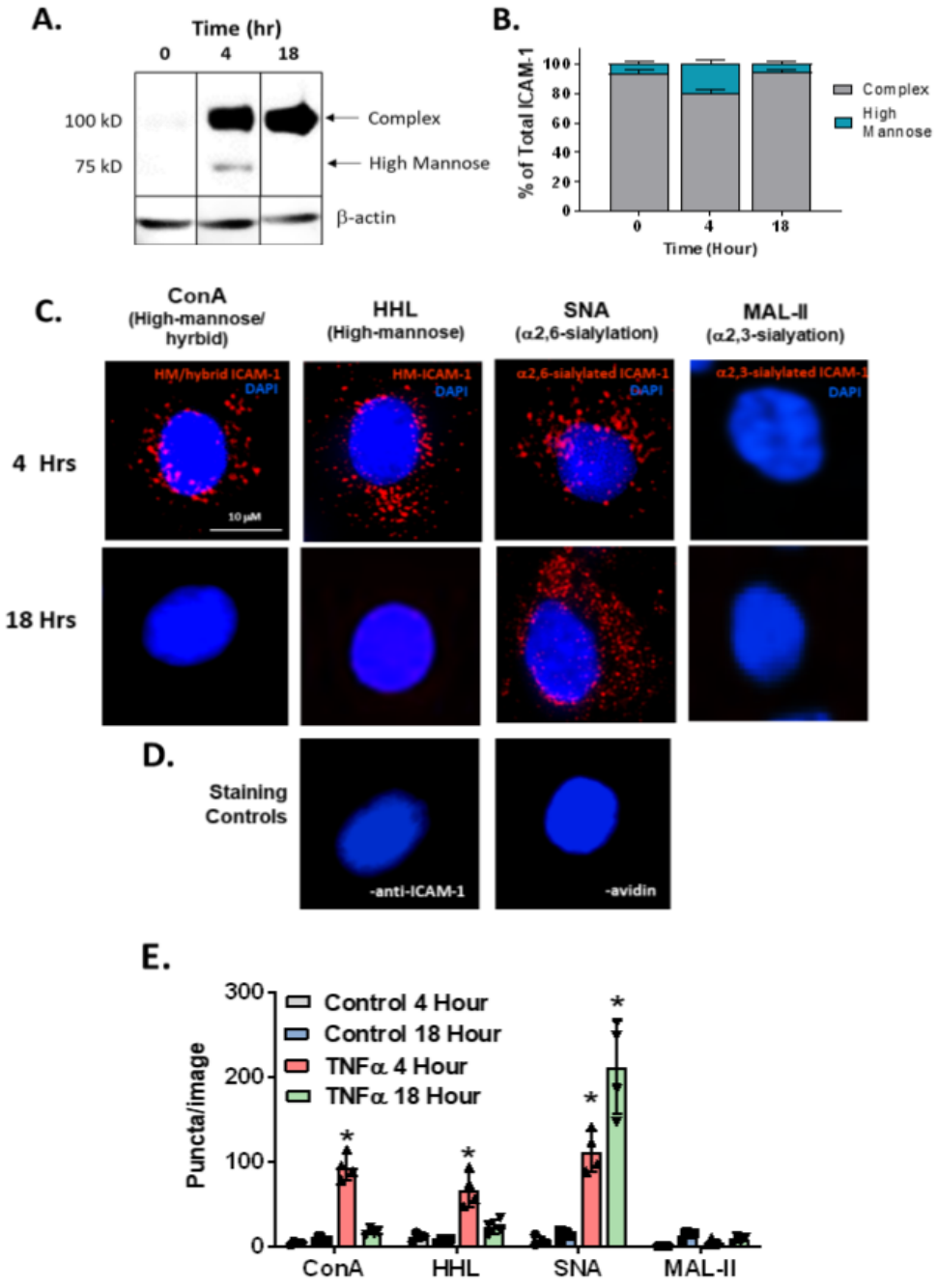


**Figure 2. TNFα forms endothelial HM-ICAM-1 in a time-dependent manner.** HUVECs were treated with 10 ng/mL TNFα for 0, 4, or 18 hours and either lysates were collected for western blot analyses or cells processed for PLA. **A.** Representative Western blot for ICAM-1 expression. The 100 kD band represents the fully glycosylated, complex ICAM-1 and the 75 kD band represents the hypoglycosylated, high-mannose ICAM-1. **B.** Quantification of HM-ICAM-1 as a percentage of total ICAM-1. Data are mean ± SEM, n=3. **C.** HUVECs were treated as above and subject

to a proximity ligation assay (PLA) for HM / hybrid, HM, α2,6-sialylated, and α2,3-sialylated ICAM-1. Shown are representative images from each time point. Red puncta represents positive PLA signal, blue staining is DAPI nuclear stain. **D.** PLA staining controls where one PLA reagent was left out (left, no anti-ICAM-1; right, no avidin). **E.** Quantification of PLA puncta. For each replicate, puncta were counted in three fields and averaged. Each symbol represents an independent replicate. Data are mean ± SEM, n=4. *=$p \leq 0.05$ compared to respective time control by one-way ANOVA with Tukey's posttest.

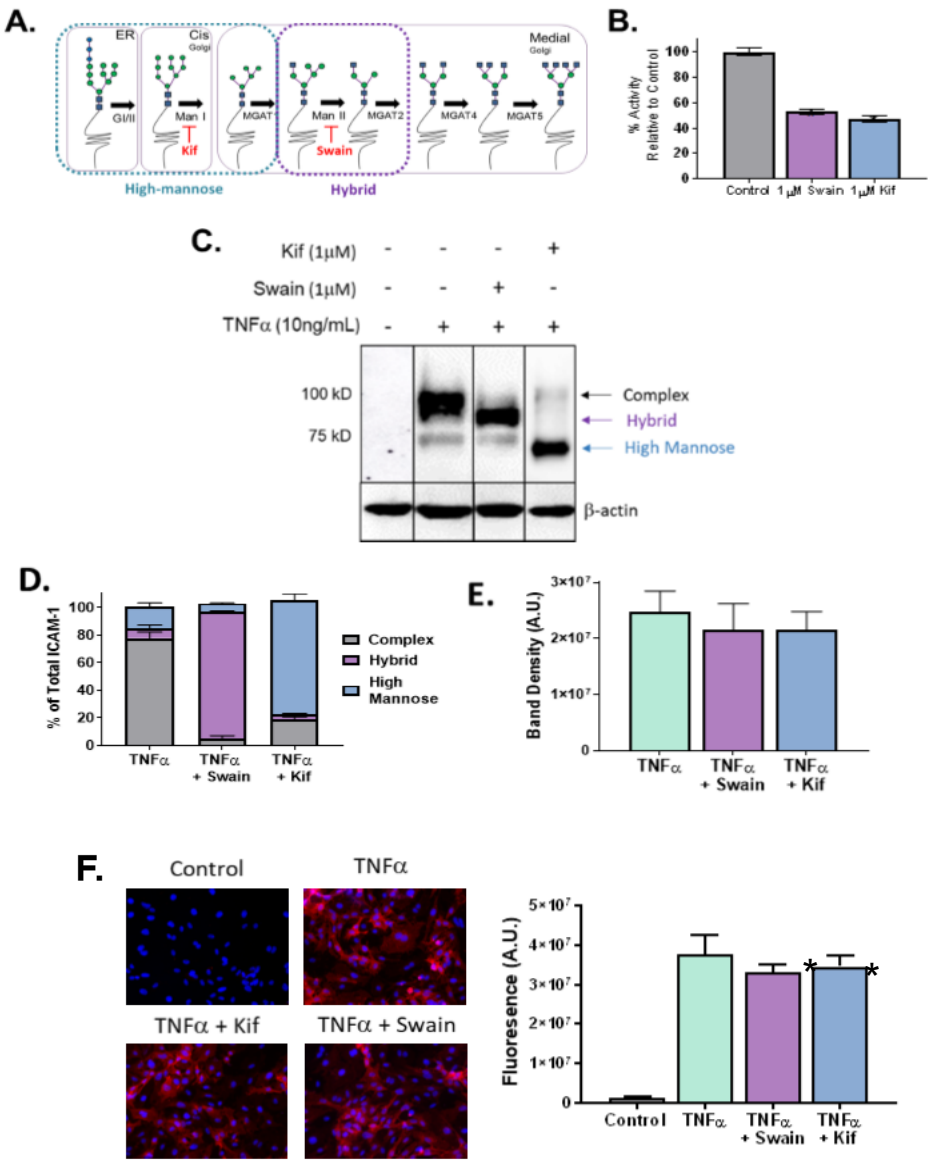


**Figure 3. Kifunensine and Swainsonine selectively form HM and hybrid N-glycans on the activated endothelium. A.** Scheme showing early and sequential processing of N-glycans from HM to hybrid and complex N-glycans. Also shown are sites where Kifunensine (Kif) and Swainsonine (Swain) inhibit class I and II α-mannosidases, respectively. **B.** α-mannosidase activity in HUVECs exposed to 1μM Kif or 1μM Swain. Data show activity relative to control. *=p≤0.05 compared to control by one-way ANOVA with Tukey post-test. **C.** Western blot and **D.** analysis of ICAM-1 glycoforms in HUVECs when exposed to TNFα and/or 1μM Kif or Swain. The 100 kD band represents the fully glycosylated, complex ICAM-1 and the 75 kD band represents the hypoglycosylated, high-mannose ICAM-1. Lane 1, control; lane 2, TNFα only; lane 3, TNFα and Swain; lane 4, TNFα and Kif. **E.** Total band density of ICAM-1 from (C). **F.** ICAM-1 surface stain (left panel) and quantitation (right panel) on HUVECs treated with TNFα and/or 1μM Kif or Swain.

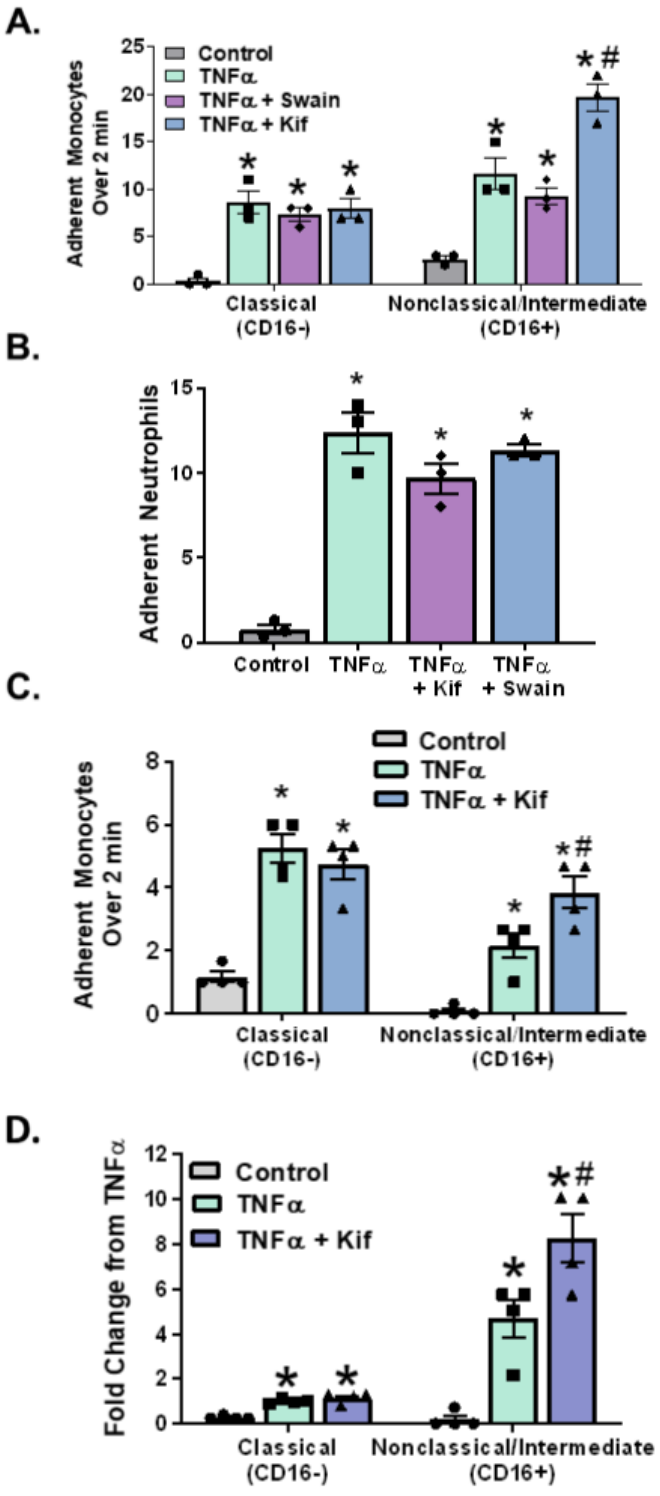


**Figure 4. CD16$^+$ monocyte adhesion is enhanced by endothelial HM epitopes. A.** HUVECs were treated as above and exposed under flow to fluorescently-labeled CD16$^+$ and CD16$^-$ monocytes. Each symbol represents the average of an independent experiment. Data are mean ± SEM, n=3. *=p≤0.05 compared to control or #=p≤0.05 compared to TNFα by one-way ANOVA with Tukey's posttest within monocyte groups. **B.** HUVECs were treated and neutrophils adhesion under flow determined as described. Data are mean ± SEM, n=3. *=p≤0.05 compared to control alone by one-way ANOVA. **C.** Monocyte adhesion under flow to HUVECs at physiological ratios (225,000 cells/mL CD16$^-$ and 25,000 cells/mL CD16$^+$). Each bar represents the average of four independent experiments. Data are mean ± SEM, n=4. *=p ≤ 0.05 compared to control or #=p≤0.05 compared to TNFα by one-way ANOVA with Tukey's posttest within monocyte groups. **D.** Monocyte adhesion from (C) as a fold change compared to CD16$^-$ adhesion to TNFα treated HUVEC. Each symbol represents the average of four independent experiments. Data are mean ± SEM, n=4. *=p≤0.05 compared to control or #=p≤0.05 compared to TNFα by one-way ANOVA with Tukey's posttest within monocyte groups.

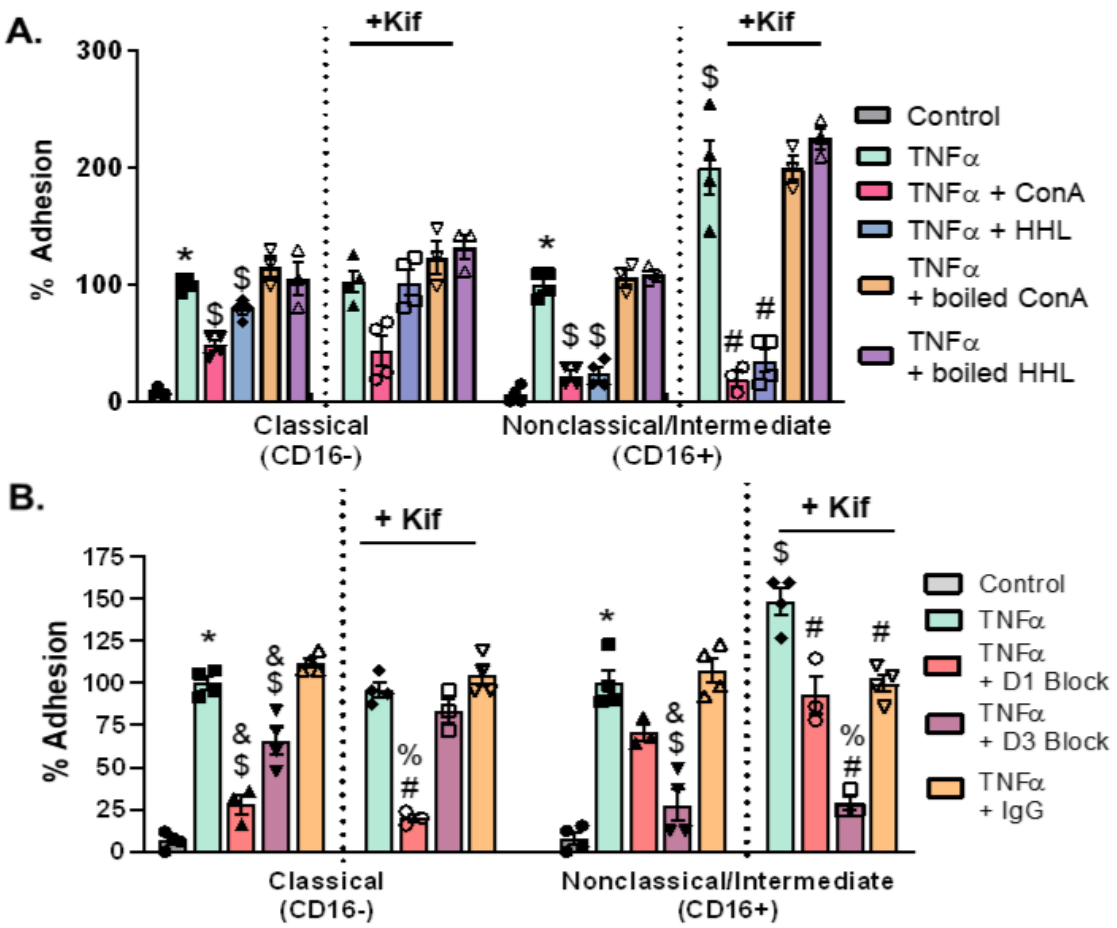


**Figure 5. CD16$^{+}$ monocyte adhesion is dependent on endothelial HM epitopes and ICAM-1. A**. HUVECs were treated with 10 ng/mL TNFα for 4 hours prior to monocyte adhesion assay. Some cells were pretreated with Kif to form HM epitopes on the cell surface and then monocyte adhesion under flow measured. Prior to adhesion assay, some cells were treated with the lectins HHL or ConA to block HM / hybrid N-glycans on the cell surface, or with denatured lectins to assess non-specific binding effects. Each symbol represents the average of an independent experiment. Data are mean ± SEM, n=3 or 4. *=p≤0.05 compared to control; $=p≤0.05 compared to TNFα alone; and #=p≤0.05 compared to TNFα+Kif by one-way ANOVA with Tukey's posttest within monocyte groups. **B.** HUVECs were treated as described and some cells were treated with anti-ICAM-1 blocking antibodies that recognize D1 or D3 of ICAM-1 prior to monocyte adhesion assay. Each symbol represents the average of an independent experiment. Data are mean ± SEM, n=3 or 4. *=p≤0.05 compared to control; $=p≤0.05 compared to TNFα; &=p≤0.05 compared to TNFα + IgG control; #=p≤0.05 compared to TNFα + Kif; %=p≤0.05 compared to TNFα + Kif + IgG control by one-way ANOVA with Tukey's posttest within monocyte and cell treatment groups.

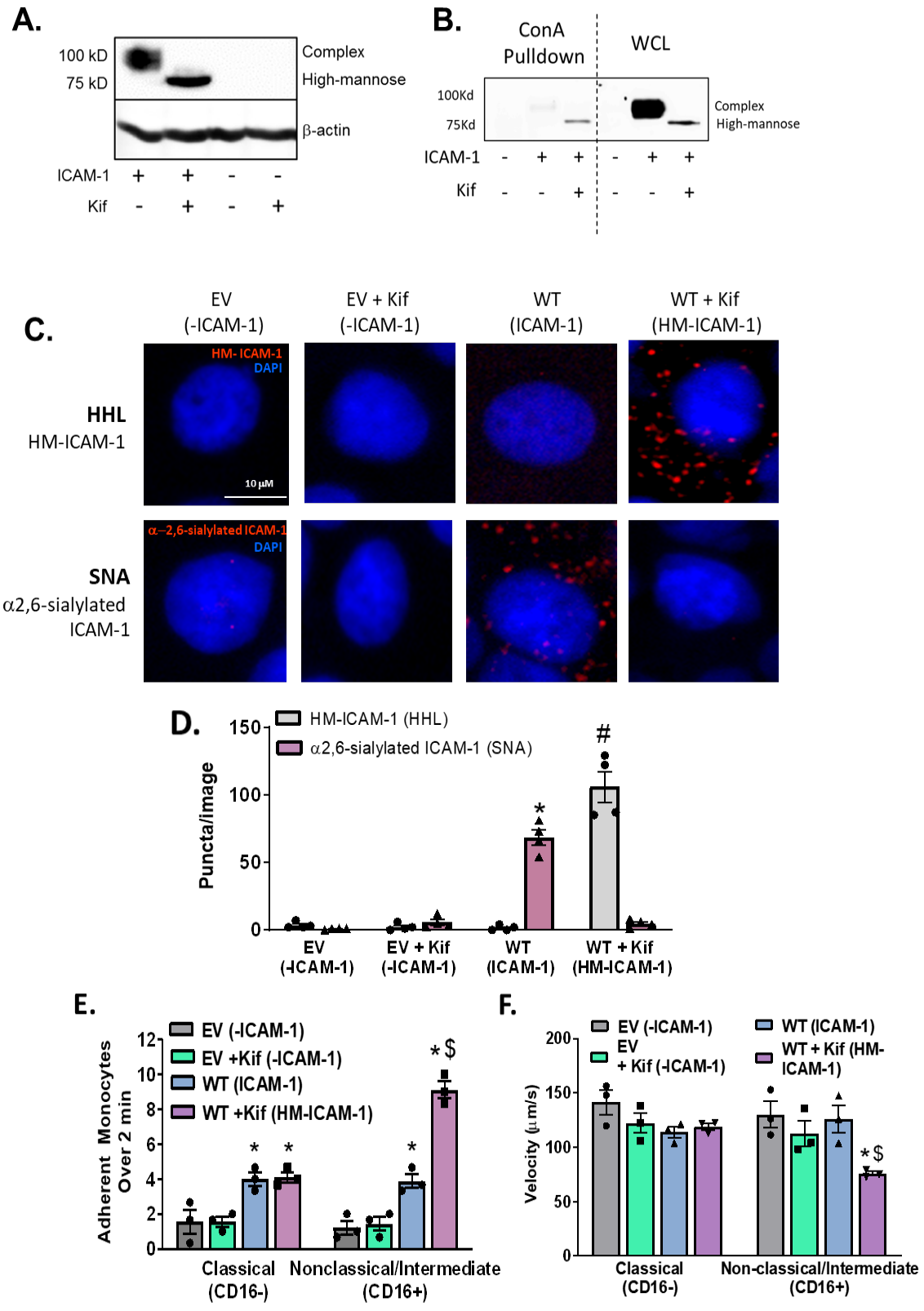
A.
100 kD
75 kD
Complex
High-mannose
β-actin
ICAM-1 + + - -
Kif - + - +
B.
ConA Pulldown
WCL
100Kd
75Kd
Complex
High-mannose
ICAM-1 - + + - + +
Kif - - + - - +
C.
EV (-ICAM-1)
EV + Kif (-ICAM-1)
WT (ICAM-1)
WT + Kif (HM-ICAM-1)
HHL
HM-ICAM-1
HM- ICAM-1
DAPI
10 μM
SNA
α2,6-sialylated ICAM-1
α–2,6-sialylated ICAM-1
DAPI
D.
HM-ICAM-1 (HHL)
α2,6-sialylated ICAM-1 (SNA)
Puncta/image
150
100
50
0
*
#
EV (-ICAM-1)
EV + Kif (-ICAM-1)
WT (ICAM-1)
WT + Kif (HM-ICAM-1)
E.
EV (-ICAM-1)
EV +Kif (-ICAM-1)
WT (ICAM-1)
WT +Kif (HM-ICAM-1)
Adherent Monocytes Over 2 min
12
10
8
6
4
2
0
* *
* *$
Classical (CD16-)
Nonclassical/Intermediate (CD16+)
F.
EV (-ICAM-1)
EV + Kif (-ICAM-1)
WT (ICAM-1)
WT + Kif (HM-ICAM-1)
Velocity (μm/s)
200
150
100
50
0
*$
Classical (CD16-)
Non-classical/Intermediate (CD16+)

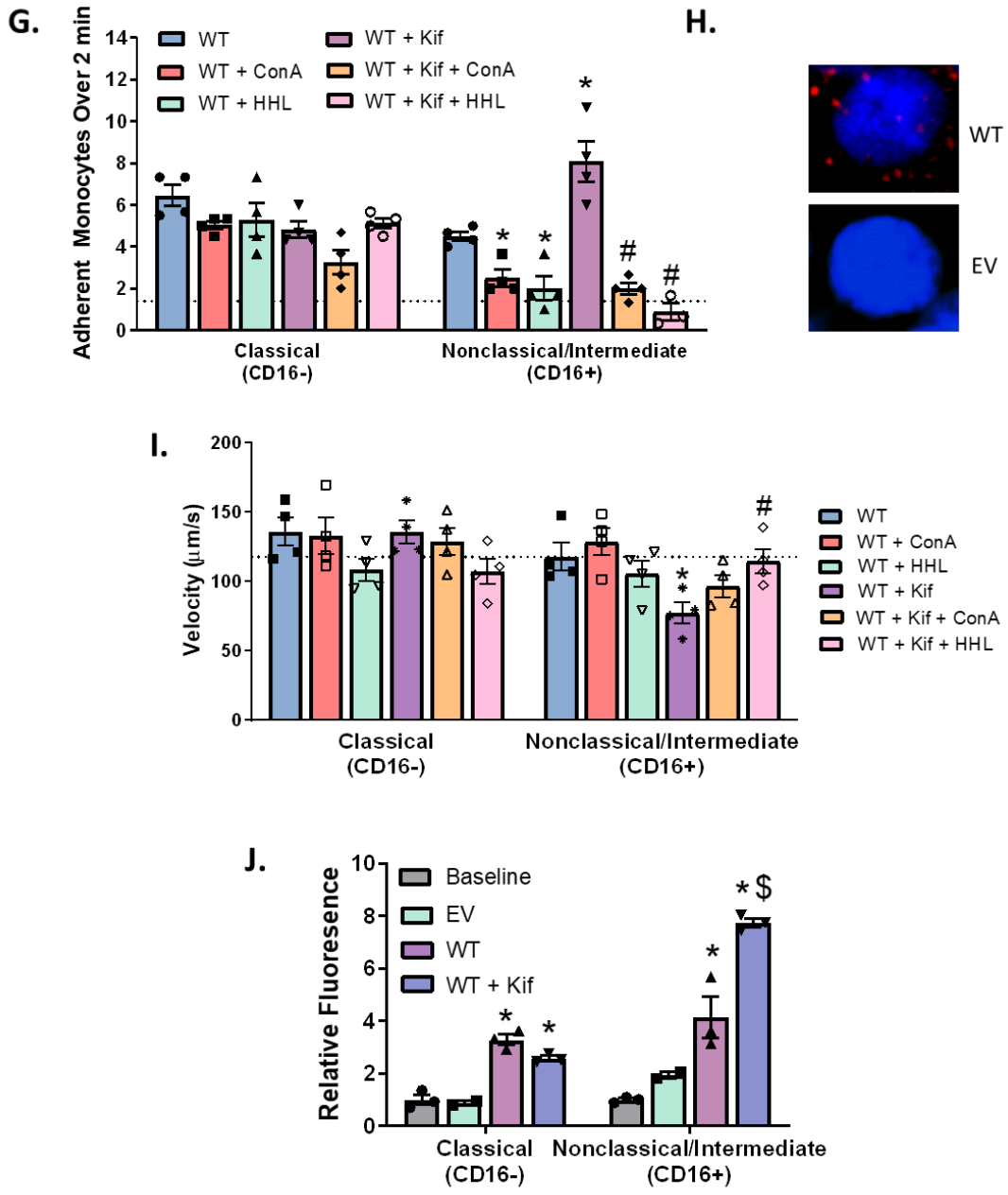


**Figure 6. HM-ICAM-1 enhances CD16$^+$ monocyte adhesion under flow. A**. Western blot of ICAM-1 from Cos-1 cells transfected with or without human ICAM-1 and grown in the presence or absence of Kif. **B.** Surface ConA reactive epitopes were immunoprecipitated from Cos-1 cells grown in the presence or absence of Kif and ICAM-1 levels determined by western blotting. **C.** Cos-1 cells transfected with or without human ICAM-1 and grown in the presence or absence of Kif were subject to a proximity ligation assay (PLA) for HM- and α-2,6-sialylated ICAM-1. Shown are representative images from each time point. Red puncta represents positive PLA signal, blue staining is DAPI nuclear stain. **D.** Quantification of PLA signal from Cos-1 cells. *=p≤0.05 compared to WT-HHL signal; #=p≤0.05 compared to WT+Kif SNA signal. Data are mean ± SEM, n=3 with an average of 2 fields per n. **E.** Cos-1 cells treated as above were exposed to

isolated $C16^+$ and $CD16^-$ monocytes under flow and adhesion measured over 2 minutes. Data are mean ± SEM, n=3, each symbol represents a single experiment with two replicates per experiment. *=p≤0.05 compared to EV; $=p≤0.05 compared to WT alone by one-way ANOVA with Tukey's post-test within monocyte groups. **F.** Monocyte rolling velocities from (E) were calculated as described above. Data are mean ± SEM, n=3 or 4. *=p≤0.05 compared to EV; $=p≤0.05 compared to WT alone by one-way ANOVA with Tukey's post-test within monocyte groups. **G**. Cos-1 cells were subjected to monocyte adhesion under flow as described above. Prior to adhesion assay, some cells were treated with the lectins HHL or ConA to block HM / hybrid N-glycans on the cell surface. Data are mean ± SEM, n=3 or 4 with two replicates per experiment. *=p≤0.05 compared to WT alone; #=p≤0.05 compared to WT + Kif by one-way ANOVA with Tukey's post-test within monocyte groups**.** Dotted line represents average of non-transfected cells. **H.** PLA images from WT and EV Cos-1 cells subject to PLA for ICAM-1 and HHL from (C) collected with longer exposure times. **I.** Velocities calculated from (G). Data are mean ± SEM, n=4. *=p≤0.05 compared to WT; #=p≤0.05 compared to WT + Kif by one-way ANOVA and Tukey's posttest within monocyte groups. Dotted lines represent average of non-transfected cells. **J.** Following native monocyte adhesion to Cos-1 cells under flow, cells were fixed and stained for $CD16^+$ and $CD16^-$ markers. Data are mean ± SEM, n=3. *=p≤0.05 compared to baseline; $=p≤0.05 compared to WT by one-way ANOVA with Tukey's posttest within monocyte groups. .

# ASSESSMENT OF ICAM-1 N-GLYCOFORMS IN MOUSE AND HUMAN MODELS OF ENDOTHELIAL DYSFUNCTION

by

KELLIE REGAL MCDONALD, MAHESHIKA SOMARATHNA, TIMMY LEE, SILVIO H. LITOVSKY, JARROD BARNES, J.M.PERETIK, J.G. TRAYLOR JR., A. WAYNE ORR, AND RAKESH P. PATEL

In revision for PLoS One

Format adapted for dissertation

Abstract

Endothelial dysfunction is a critical event in vascular inflammation characterized, in part, by elevated surface expression of adhesion molecules such as intercellular adhesion molecule-1 (ICAM-1). ICAM-1 is heavily N-glycosylated, and like other surface proteins, it is largely presumed that fully processed, complex N-glycoforms are dominant. However, our recent studies suggest that hypoglycosylated or high mannose (HM)-ICAM-1 N-glycoforms are also expressed on the cell surface during endothelial dysfunction, and have higher affinity for monocyte adhesion and regulate outside-in endothelial signaling by different mechanisms. Whether different ICAM-1 N-glycoforms are expressed *in vivo* during disease is unknown. In this study, using the proximity ligation assay, we assessed the relative formation of high mannose, hybrid and complex α-2,6-sialyated N-glycoforms of ICAM-1 in human and mouse models of atherosclerosis, as well as in arteriovenous fistulas (AVF) of patients on hemodialysis. Our data demonstrates that ICAM-1 harboring HM or hybrid epitopes as well as ICAM-1 bearing α-2,6-sialylated epitopes are present in human and mouse atherosclerotic lesions. Further, HM-ICAM-1 positively associated with increased macrophage burden in lesions as assessed by CD68 staining, whereas α-2,6-sialylated ICAM-1 did not. Finally, both HM and α-2,6-sialylated ICAM-1 N-glycoforms were present in hemodialysis patients who had AVF maturation failure compared to successful AVF maturation. Collectively, these data provide evidence that HM- ICAM-1 N-glycoforms are present *in vivo*, and at levels similar to complex α-2,6-sialylated ICAM-1 underscoring the need to better understand their roles in modulating vascular inflammation.

## Introduction

Inflammation is a carefully orchestrated response involving the release of pro-inflammatory factors and homing of immune cells to injured tissue. The vascular endothelium is a key player in the inflammatory process, responding to stressors such as oscillatory blood flow (that occurs at bifurcations in the vessel) and increased pro-inflammatory factors(2-4). The resulting activated endothelium provides a pro-adhesive surface that allows circulating immune cells to adhere and migrate into the inflamed tissue in a multi-step process of capture, rolling, firm adhesion, and transmigration. These steps are mediated by multiple endothelial surface adhesion molecules (5-10).

Many surface and secreted proteins, including adhesion molecules, are N-glycosylated. While this post (or co-)-translational modification regulates protein stability and transport to the cell surface, these glycan structures are also important in mediating binding between cognate receptors, which is exemplified by binding between selectins and their sialyl Lewis$^X$ ligands (11, 12). Relatively little is known, however, about how N-glycosylation of endothelial adhesion molecules may be regulated during inflammation (13). Protein N-glycosylation occurs in the endoplasmic reticulum-Golgi network via a multi-step process involving initial attachment of a core oligosaccharide, comprised of $Glu_3Man_9GlcNAc_2$, onto the amide residue of asparagine within the consensus sequence N-X-S/T (where X cannot be proline). Sugars from this core are temporally and sequentially cleaved by ER/Golgi resident glycosidases, leading to high mannose structures, followed by partial rebuilding to hybrid N-glycan structures (collectively referred herein as hypoglycosylated N-glycans) by glycosyltransferases; after which multiple fucose, GlcNAc, and sialic acid residues are added to form complex N-glycoproteins (14). While it is

assumed that most glycoproteins require complete processing to the complex form for cell-surface expression, we and others have demonstrated that during atherogenic inflammation, the endothelial surface is characterized by decreased N-glycan complexity, or an increase in hypoglycosylated N-glycans (12, 15-17). However, the exact endothelial proteins that harbor these hypoglycosylated N-glycans and their presence *in vivo* remains unclear.

Intercellular adhesion molecule-1 (ICAM-1) is an adhesion molecule that mediates leukocyte adhesion and whose expression is induced by pro-inflammatory stimuli. ICAM-1 has 8 putative N-glycosylation sites and we have previously shown that, in activated cultured endothelial cells, both high mannose/hybrid and complex (specifically α2,6-sialylated) ICAM-1 can be expressed on the cell-surface (16). Interestingly, we observed that hypoglycosylated ICAM-1 N-glycoforms bound monocytes with higher affinity and regulated "outside-in" signaling via different mechanisms compared to ICAM-1 glycoforms containing complex, α-2,6-sialylated N-glycans (16, 18). Further, we recently demonstrated that a hypoglycosylated, high-mannose (HM), form of ICAM-1 specifically enhances adhesion of pro-inflammatory monocyte subsets (19). These findings suggest unique and distinctive functions for the different ICAM-1 N-glycoforms, however, whether these distinct ICAM-1 N-glycoforms are present *in vivo* is not yet known.

Herein, we tested whether different ICAM-1 N-glycoforms are present *in vivo* by modifying the DuoLink® proximity ligation assay (PLA) to detect co-localization of specific N-glycan structures and ICAM-1 in two disease states where endothelial dysfunction has been demonstrated to play a prominent role (see **Figure 1** for assay schematic

and lectin specificity). Both human and mouse atherosclerotic tissue, as well as arteriovenous fistulas (AVF) of advanced chronic kidney disease patients, were evaluated for the presence of ICAM-1 N-glycoforms. Our data demonstrate that hypoglycosylated ICAM-1 N-glycoforms are present in advanced disease states in all models observed at similar, if not higher, levels of α-2,6-sialylated N-glycoforms. Importantly, HM-ICAM-1, but not α-2,6-sialylated ICAM-1 positively correlated with macrophage burden as assessed by CD68 staining indicating a significant role for hypoglycosylated N-glycans in vascular inflammation.

## Experimental procedures

### *Materials*

DuoLink® proximity ligation assay kit was purchased from ThermoFisher (Waltham, MA). HistoPrep™ was purchased from Fisher Scientific (Hampton, NH). Anti-human ICAM-1 antibody was purchased from ThermoFisher (BMS108), and anti-mouse ICAM-1 antibody was purchased from Abcam (25375) (Cambridge, UK). *Concanavalin A* (ConA), *Sambucus Nigra* (SNA), *Hippeastrum Hybrid Amaryllis* (HHL), and *Maackia Amurensis Lectin II* (MAL-II) lectins were purchased from Vector laboratories (Birlingame, CA). Anti-ICAM-1 and avidin were conjugated to oligomer probes using the DuoLink Probemaker kits (Sigma) per manufacturer provided protocols. All other reagents were purchased from Sigma-Aldrich (St. Louis, MO) unless otherwise noted.

*Human vessel collection and processing*

Human arteries were obtained post-mortem, after authorization of autopsy that includes permission to remove tissues for research purposes, from the Department of Pathology at the University of Alabama at Birmingham and Louisiana State University Health Sciences Center. Vessel segments were fixed using formalin (10%) for 24h and then embedded in paraffin. Lesion type was determined according to the Stary scale from 1-5 by a cardiovascular pathologist (20). All procedures were performed per Institutional Review Board approved protocols.

In addition, human vein samples were collected from subjects at the time of 1$^{st}$ and 2$^{nd}$ stage basilic vein transposition surgery. At the time of both surgeries, a circumferential piece of vein (~10-15 mm and adjacent to site of anastomosis creation) was excised and immediately stored in formalin for histology and immunohistochemistry (IHC) studies. Each venous tissue sample was embedded in paraffin as previously described(21). Following paraffin embedding, each piece was sliced into 5μM sections for histological studies. These vein samples were collected under approval by the University of Alabama at Birmingham Institutional Review Board. Donor specimens from cadaveric donors at the time of organ harvesting were obtained using services from the National Disease Research Interchange, Philadelphia, PA, and fixed in formalin, as previously described(22).

*Mouse vessel collection and processing*

8-10 week old male ApoE-/- mice were fed a high fat, Western-type diet (21% fat by weight, 0.15% cholesterol, and 19.5% casein without sodium cholate) for 12 weeks,

and the innominate artery (i.e. brachiocephalic) collected for histological analysis. Both lesion and non-lesion areas of the same segment were analyzed. Carotid arteries were also collected from male ApoE-/- mice fed a control diet. In the second model, 8-10 week old, male ApoE-/- mice underwent partial ligation of the left carotid artery to induce disturbed flow as described previously(23, 24). After induction of anesthesia (5% isoflurane, followed by 2% isoflurane for maintenance of anesthesia), the external, internal, and occipital arteries were ligated with a 7-0 silk suture leaving the superior thyroid artery patent, and the resulting disturbed flow pattern was verified by ultrasound measurements using a VisualSonics VEVO3100 system. When this model is performed in atherosclerosis-prone ApoE-/- mice, accelerated atherosclerosis develops in the left carotid artery due to disturbed flow compared to the paired right carotid artery(25). Mice were euthanized by pneumothorax under isoflurane anesthesia, and then ex-sanguinated followed by vessel collection. For all samples, the adventitia was carefully removed and vessel segments fixed in formalin (10%) for 24h and then embedded in paraffin blocks for mounting to slides. Male mice were used due to their susceptibility to atherosclerosis development compared to female mice. All procedures were performed according to LSU Health Sciences Center-Shreveport and University of Alabama at Birmingham IACUC approved protocols.

*Tissue immunofluorescence*

Paraffin-embedded tissue sections were rehydrated using standard protocols. Briefly, slides were treated with xylene followed by decreasing Histoprep concentrations

(100%, 95%, 85%, 75%) before immersion in 1x PBS. Antigen retrieval was accomplished using 10mM sodium citrate buffer (pH 6.0) and heated for 12 minutes in the microwave. Following antigen retrieval, tissues were washed in PBS and proximity-ligation or total ICAM-1 staining performed as outlined below.

*Proximity-ligation assay*

Briefly, 20 μg of the following biotinylated lectins: HM and hybrid N-glycan-specific lectin *Concanavalin A* (ConA), the α2,6-sialyation specific lectin *Sambucus nigra* (SNA), the HM-specific lectin *Hippeastrum hybrid* (HHL), or the α2,3-sialylation specific lectin *Maackia amurensis* (MAL-II) were added for 30 minutes at 4°C (see **table I**). These lectins were chosen to provide broad coverage of different N-glcyan structures. After washing twice with PBS, samples were blocked with 1X Carbo-Free blocking solution (Vector Labs) for 30 min at 20-25°C. Immediately following blocking, samples were incubated with oligo-tagged avidin or anti-ICAM-1 (10 μg/mL) for one hour at 37°C followed by ligation and amplification steps as per the protocol. Both anti-mouse and human ICAM-1 antibodies recognize extracellular (domain 1) epitopes on ICAM-1. Slides were left to dry and mounted using the DuoLink® mounting medium containing DAPI.

*Total ICAM-1 Immunofluorescence*

Slides were process as described above. After blocking, slides were incubated with mouse or human anti-ICAM-1 for 1 hour at 20-25°C, followed by a 1 hour incubation at 20-25°C with the species-appropriate secondary antibody conjugated to Alexa

Fluor 594. After washing, slides were left to dry and mounted using DuoLink® mounting medium containing DAPI.

*Image acquisition and analysis*

Images were acquired on a BioTek Lionheart live cell imager using DAPI (377/447), GFP (469/525), and Texas Red (586/647) filters. LED intensity, camera gain, and integration time for each channel was uniform across all samples. Images at three random locations within lesion and non-lesion areas were recorded per section. Images were collected at 4x and 60x magnification. Image quantification was performed using either Gen5 (Biotek) or ImageJ software (NIH). To quantify PLA images, 3 random fields per group, per experiment were selected and number of puncta counted using ImageJ particle analysis software (NIH).

*Statistics*

All statistical analysis was performed using GraphPad Prism software. Paired student t-tests were utilized in comparing the same areas of the vessels, as well as lesion vs. non-lesion sites of the same vessel, unless otherwise stated. A p-value less than 0.05 was considered significant.

## Results

*Hypoglycosylated ICAM-1 is present in mouse atherosclerotic lesions*

Vessels from ApoE-/- mice were collected after 12 weeks feeding of a control or high fat diet, with the latter being an established method to reproducibly promote atherosclerosis(8, 26, 27). Total ICAM-1 levels (measured using an anti-ICAM-1 antibody that binds to epitopes on the N-glycan-devoid domain 1 of the protein) were detected on the luminal surface of lesions, consistent with prior reports of up-regulation of this adhesion molecule on the endothelium (28-30) (**Figure 2A**). No ICAM-1 was detected on areas of the vessel devoid of lesions, nor on vessels collected from mice fed a normal chow diet. To determine which N-glycoforms of ICAM-1 were present, we used the PLA assay (**Figure 1**), where red puncta indicate positive staining that the two epitopes are within 40nm of each other. To measure HM and hybrid ICAM-1, samples were labeled with biotinylated ConA, a lectin that binds both of these sugar structures, followed by treatment with avidin and an anti-ICAM-1 antibody both tagged with complementary oligonucleotides. High mannose N-glycans, α-2,6-sialylation, and α-2,3-sialylation on ICAM-1 were measured using the same method with HHL, SNA and MAL-II lectins, respectively. **Figure 2A** shows red puncta for the ICAM-1 N-glycoforms in lesion areas only; no PLA staining was observed in non-lesion areas of the same vessels nor in vessels from ApoE-/- mice fed normal chow. As an immunostaining control, the antibody against ICAM-1 or avidin were excluded (**Figs 2B-C** respectively) and showed no PLA-positive staining associated with lesions. **Figures 2D-E** show that total ICAM-1, HM / hybrid, and α-2,6-sialyated N-glycoforms of ICAM-1 were significantly increased in lesion vs. non-lesion regions. No difference in α-2,3-sialyated ICAM-1 was detected between lesion and non-

lesion areas. Further, macrophage burden was assessed by CD68 staining in lesion and non-lesion samples. As shown in **Figs. 2F-G**, CD68 staining was significantly higher in lesion compared to non-lesion areas.

We also collected vessels from ApoE-/- mice that underwent partial carotid ligation, which creates oscillatory flow in the left carotid artery while leaving the right carotid artery as an internal control. This model rapidly causes endothelial dysfunction and atherosclerosis (23). Both the left and right carotid arteries from mice that underwent partial ligation were collected 7 days post-ligation and stained for total ICAM-1 and ICAM-1 N-glycoforms. **Figures 3A-C** show representative images and quantification of ICAM-1 staining. Total ICAM-1, HM / hybrid N-glycoforms were increased in the ligated left carotid artery (LC) compared to the control right carotid artery (RC). CD68 staining was significantly higher in areas of lesion (**Figs 3D-E**).

Finally, **Figs. 4A-F** show correlations between CD68 staining intensity and the ICAM-1 N-glycoforms tested by PLA in both animal models. Closed symbols (**Figs. 4A, C, & E**) represent HFD ApoE-/- mice, and open symbols (**Figs. 4B, D, & E**) represent partial carotid ligation mice. Correlation was determined via Pearson's correlation test between number of PLA puncta per vessel and CD68 staining intensity of the same vessels. CD68 significantly positively correlated with HM / hybrid (ConA) and HM (HHL) ICAM-1 in both animal models (**Figs. 4A-D**). α-2,6-sialylated (SNA) ICAM-1 significantly correlated with CD68 in the ApoE-/- mice, although to a lesser extent than the HM and hybrid lectins ($r=0.85$ vs $>0.9$; **Fig. 4E**). There was no correlation between α-2,6-sialylated ICAM-1 and CD68 in the partial carotid ligation model (**Fig. 4F**).

*HM / hybrid and α-2,6-sialylated ICAM-1 are present in advanced human atherosclerotic lesions*

To determine whether distinct ICAM-1 N-glycoforms are present in human atherosclerosis and whether they were dependent on disease severity, human vessels were collected at autopsy and luminal surface total ICAM-1 and HM / hybrid, α-2,3-sialylated, and α-2,6-sialylated ICAM-1 were measured via PLA. **Table 1** summarizes patient demographics, vessel location, and lesion type. ICAM-1 N-glycoforms were only seen in advanced lesions (**Figure 5A**). Very little ICAM-1 was detected in the less advanced lesions (types 1 and 2), while higher amounts were observed in more advanced lesions (types 3-5) (**Figs 5A, D**). HM-ICAM-1 levels were significantly higher than α-2,6- or α-2,3- sialylated-ICAM-1 (**Figure 5E**). **Figures 5B** and **5C** show specificity for HM / hybrid and sialylated-ICAM-1 staining; no PLA-positive staining was observed when individual PLA reagents were omitted.

Finally, CD68 staining was significantly higher in advanced lesions compared to earlier stage lesions (**Figs 6A-B**). Further, CD68 staining had a significant positive correlation with HM-ICAM-1 levels. There was no significant correlation with α-2,6-sialyated ICAM-1 and CD68 levels. (**Figs 6 C-E**).

*HM / hybrid and α-2,6-sialylated ICAM-1 are present in patients on hemodialysis with failed AVFs*

Advanced chronic kidney disease (CKD) patients that reach end-stage renal disease require hemodialysis. A common limitation with this therapy is failure of the AVF to successfully mature due to endothelial dysfunction and inflammation mediated in part

by oscillatory flow (31, 32). To determine if ICAM-1 N-glycoforms are also present in AVF failure models, basilic vein samples from CKD patients that had undergone surgical AVF creation were obtained and subjected to PLA for HM/hybrid, α-2,3-sialylated, and α-2,6-sialylated ICAM-1. **Table 2** shows patient demographics, and the success vs. failure status of AVF. **Figure 7A** show representative images indicating that total ICAM-1, HM / hybrid, α-2,6-sialylated, and α-2,3-sialylated ICAM-1 were present in the failed AVFs. Little to no ICAM-1 was detected in successful AVFs (**Figure 7A and B)**. HM / hybrid and α-2,6-sialylated ICAM-1 levels were significantly higher in failed AVFs compared to successful AVFs (**Figure 7C**).

## Discussion

Inflammation is a carefully orchestrated process involving the homing of immune cells to inflamed tissues, a process mediated by adhesion molecules on the endothelial cell surface (6). Surface adhesion molecules are heavily N-glycosylated with ~20-50% of their observed molecular weights attributed to N-glycans. While insights into the role of protein N-glycosylation in regulating inflammation have primarily focused on circulating immune cells (e.g. CD44 and other selectin ligands on neutrophils and T-cells (11, 25), (33)), relatively little attention has been paid to the impact N-glycans may have on the function of endothelial adhesion molecules in diseases mediated by endothelial dysfunction.

ICAM-1 is a well-established mediator of increased monocyte-endothelial interactions and interestingly, compared to the related adhesion molecule, VCAM-1, contains more N-glycans as a proportion of its overall molecular weight (~50% in ICAM-1 vs.

~25% in VCAM-1) (34). Numerous studies have shown that deletion of ICAM-1 or blocking its ability to engage Mac-1 or LFA-1 on leukocytes prevents inflammation (35-38). It is also known that N-glycosylation can modulate ICAM-1 function. For example, Mac-1 binding is higher to ICAM-1 bearing HM structures(39). Moreover, different ICAM-1 N-glycoforms may regulate tumor burden and inflammatory signaling, and that the degree of ICAM-1 N-glycosylation can change depending on the cell in which it is expressed (40-44). In our previous work, we showed that HM / hybrid ICAM-1 was formed in activated endothelial cells, and this hypoglycosylated ICAM-1 N-glycoform mediated higher affinity binding to monocytes compared to fully processed, sialylated ICAM-1 N-glycoforms. In addition, ligation dependent interactions between ICAM-1 and the actin cytoskeleton was also distinctly regulated between HM / hybrid ICAM-1 and complex-ICAM-1(16, 34).

While the aforementioned studies suggest altered functions for hypoglycosylated vs. complex sialyated ICAM-1, whether these N-glycoforms are expressed in disease is not known and important to establish translational significance. By using vessels from patients with varying stages of atherosclerotic lesions, from CKD patients with successful or failed AVFs, and from two atherosclerotic mouse models (ApoE -/- mice fed high-fat diet and ApoE -/- mice post-partial carotid ligation), we show that HM / hybrid and complex ICAM-1 N-glycoforms are found in vascular lesions and areas of endothelial dysfunction, but not in non-lesion areas. For complex, sialylated N-glycans, our data suggest a prevalence of α-2,6-sialylated ICAM-1 relative to α-2,3-sialyated ICAM-1 in human and mouse samples, with the latter only being observed in AVF failures. Interestingly,

HM / hybrid ICAM-1 was present at similar or even greater levels compared to α-2,6-sialylated ICAM-1. However, only HM / hybrid ICAM-1 levels correlated with CD68 macrophage staining in human and some mouse models, suggesting that hypoglycosylated ICAM-1 may play a more prominent role in mediating monocyte recruitment compared to α-2,6-sialyated ICAM-1. Even in the ApoE-/- model where α-2,6-sialylation positively correlated with CD68 staining, the correlation coefficient was less than that of HM / hybrid ICAM-1. Consistent with this hypothesis, our previous data showed that the affinity of pro-inflammatory monocyte adhesion to HM / hybrid ICAM-1 was greater compared to α-2,6-sialyated ICAM-1 (19).

To date, very few studies have focused on N-glycosylation of endothelial cells and their role in disease. The complexity of studying surface adhesion proteins and their N-glycan patterns may be a contributing factor to the lack of studies in this area. For example, ICAM-1 contains 8 putative N-glycosylation sites. This, coupled with the different possible combination of N-linked sugars ranging from HM- to complex N-glycans, means that ICAM-1 may exist in >200,000 possible N-glycoforms (calculated from data in Lau et al(45)). This complexity clearly makes identification of specific N-glycoforms challenging (18, 46). It is for this reason we employed 4 different lectins in this study to identify different ICAM-1 N-glycoforms. By using lectins that recognize high-mannose, hybrid, and two different types of sialic acid linkages, we detected ICAM-1 decorated with at least 4 different types of N-glycans *in vivo* (note: ConA and HHL have some overlapping N-glycan binding specificities). To our knowledge, this data represents the first study demonstrating distinct N-glycoforms on ICAM-1 *in vivo*. We do note limitations of our study, namely the sole reliance on the PLA assay to discern HM, hybrid, and

sialylated-ICAM-1 and that this assay only informs on spatial proximity; it is possible that HM-epitopes on other proteins and ICAM-1 are co-expressed. However, previous data with cultured endothelial cells and the fact that ICAM-1 immunoprecipitated from human atherosclerotic lesion lysates has a similar molecular weights to HM/hybrid ICAM-1 supports PLA data reported here (16). An additional limitation is quantitation of PLA-positive puncta. Differential affinities for binding between specific N-glycan structures and the different lectins could lead to different staining intensities. For this reason, we quantified data based only on the number of positive puncta and not on staining intensity. However, we recognize that relative differences in lectin binding may have affected sensitivity for detecting discreet PLA-positive puncta.

Further studies using more specific and selective approaches for N-glycan analyses are required to determine the exact N-glycoforms of ICAM-1 present in vascular inflammation and their function. Little is known about the regulation and control of different N-glycoforms, and if the regulation may be disease specific. For example, while our data showed little α-2,3-sialylated ICAM-1 in human atherosclerosis, it was present in failed AVFs from humans. This observation perhaps indicates that regulation of N-glycoforms depends on the disease state. Future studies in the lab will focus on the regulation of N-glycans during inflammation; specifically by looking at the enzymes responsible for N-glycosylation, such as α-mannosidases and glycosyltransferases.

Distinct biological functions of ICAM-1 N-glycoforms may also have therapeutic implications. Attempts to therapeutically target ICAM-1 to abrogate atherosclerosis *in vivo* have been successful in animal models; for example ICAM-1 deficiency and anti-ICAM-1 antibody treatment protects against atherosclerosis in ApoE-deficient mice (38,

47). However, anti-ICAM-1 therapies have not translated into humans. Treatment with functional blocking anti-ICAM-1 antibodies have had no effect in improving kidney allograft rejection rates nor mortality rates in stroke patients, and in fact induced a neutrophil-dependent pro-inflammatory response in stroke patients (48-50). Moreover, a general concern with a long-term anti ICAM-1 therapeutic strategy is the potential for inhibiting innate immunity(51). ICAM-1 is a diverse protein with functions spanning mitogenic signaling, leukocyte adhesion, and cell survival mechanisms (52-54), and therefore global targeting can result in a potentially detrimental disruption of normal responses. Our findings that different N-glycoforms of ICAM-1 are expressed, coupled with these having distinct functions, may offer new therapeutic strategies that involve targeting hypoglycosylated HM-ICAM1 specifically. We posit that blocking HM / hybrid ICAM-1 may lead to selective attenuation of pro-inflammatory monocyte ingress into atheroprone endothelial beds. A better understanding of the glycosylation patterns of the activated endothelium throughout the course of disease may yield more selective therapeutics that target endothelial inflammation in a disease and vascular bed-specific manner.

# References

1. Stanley P, Cummings RD. Structures Common to Different Glycans. In: nd, Varki A, Cummings RD, Esko JD, Freeze HH, Stanley P, et al., editors. Essentials of Glycobiology. Cold Spring Harbor (NY)2009.

2. Libby P. Inflammation in atherosclerosis. Nature. 2002;420(6917):868-74.

3. Hansson GK, Libby P. The immune response in atherosclerosis: a double-edged sword. Nat Rev Immunol. 2006;6(7):508-19.

4. Libby P. History of Discovery: Inflammation in Atherosclerosis. Arterioscler Thromb Vasc Biol. 2012;32(9):2045-51.

5. Springer TA. Adhesion receptors of the immune system. Nature. 1990;346(6283):425-34.

6. Chi Z, Melendez AJ. Role of cell adhesion molecules and immune-cell migration in the initiation, onset and development of atherosclerosis. Cell Adh Migr. 2007;1(4):171-5.

7. Galkina E, Ley K. Vascular adhesion molecules in atherosclerosis. Arterioscler Thromb Vasc Biol. 2007;27(11):2292-301.

8. Galkina E, Ley K. Immune and inflammatory mechanisms of atherosclerosis (*). Annu Rev Immunol. 2009;27:165-97.

9. Gerhardt T, Ley K. Monocyte trafficking across the vessel wall. Cardiovasc Res. 2015;107(3):321-30.

10. Li J, Ley K. Lymphocyte migration into atherosclerotic plaque. Arterioscler Thromb Vasc Biol. 2015;35(1):40-9.

11. Katayama Y, Hidalgo A, Chang J, Peired A, Frenette PS. CD44 is a physiological E-selectin ligand on neutrophils. J Exp Med. 2005;201(8):1183-9.

12. Asano M, Nakae S, Kotani N, Shirafuji N, Nambu A, Hashimoto N, et al. Impaired selectin-ligand biosynthesis and reduced inflammatory responses in beta-1,4-galactosyltransferase-I-deficient mice. Blood. 2003;102(5):1678-85.

13. Scott DW, Patel RP. Endothelial heterogeneity and adhesion molecules N-glycosylation: implications in leukocyte trafficking in inflammation. Glycobiology. 2013;23(6):622-33.

14. Stanley P, Schachter H, Taniguchi N. N. Glycans. In: Varki A, Cummings R, Esko J, Freeze H, Stanley P, Bertozzi C, et al., editors. Essentials of Glycobiology. New York: Cole Sping Harbor; 2009.

15. Kobata A, Amano J. Altered glycosylation of proteins produced by malignant cells, and application for the diagnosis and immunotherapy of tumours. Immunol Cell Biol. 2005;83(4):429-39.

16. Scott D, Dunn T, Ballestas M, Litovsky S, Patel RP. Identification of a high-mannose ICAM-1 glycoform: effects of ICAM-1 hypoglycosylation on monocyte adhesion and outside in signaling. Am J Physiol Cell Physiol. 2013;305(2):C228-37.

17. Garcia-Vallejo JJ, Van Dijk W, Van Het Hof B, Van Die I, Engelse MA, Van Hinsbergh VW, et al. Activation of human endothelial cells by tumor necrosis factor-alpha results in profound changes in the expression of glycosylation-related genes. J Cell Physiol. 2006;206(1):203-10.

18. Ramos TN, Bullard DC, Barnum SR. ICAM-1: Isoforms and Phenotypes. J Immunol. 2014;192(10):4469-74.

19. Regal-McDonald K, Xu B, Barnes JW, Patel RP. High-mannose intercellular adhesion molecule-1 (ICAM-1) enhances CD16+ monocyte adhesion to the endothelium. Am J Physiol Heart Circ Physiol. 2019.

20. Stary HC. Composition and classification of human atherosclerotic lesions. Virchows Archiv A. 1992;421(4):277-90.

21. Lee T, Chauhan V, Krishnamoorthy M, Wang Y, Arend L, Mistry MJ, et al. Severe venous neointimal hyperplasia prior to dialysis access surgery. Nephrol Dial Transplant. 2011;26(7):2264-70.

22. Lee T, Somarathna M, Hura A, Wang Y, Campos B, Arend L, et al. Natural history of venous morphologic changes in dialysis access stenosis. J Vasc Access. 2014;15(4):298-305.

23. Nam D, Chih-Wen N, Rezvan A, Suo J, Budzyn K, Llanos A, et al. Partial carotid ligation is a model of acutely induced disturbed flow, leading to the radpi endothelial dysfunction and atherosclerosis. Am J Physiol Heart Circ Physiol. 2009;297:1535-43.

24. Kumar S, Kang DW, Rezvan A, Jo H. Accelerated atherosclerosis development in C57Bl6 mice by overexpressing AAV-mediated PCSK9 and partial carotid ligation. Lab Invest. 2017;97(8):935-45.

25. Hidalgo A, Peired AJ, Wild MK, Vestweber D, Frenette PS. Complete identification of E-selectin ligands on neutrophils reveals distinct functions of PSGL-1, ESL-1, and CD44. Immunity. 2007;26(4):477-89.

26. Getz G, Reardon C. Animal Models of Atherosclerosis. Arterioscler Thromb Vasc Biol. 2012(32):1104-15.

27. Zadelaar S, Kleemann R, Verschuren L, Van der Weij J, van der Hoorn J, Princen H, et al. Mouse Models for Atherosclerosis and Pharmaceutical Modifiers. Arterioscler Thromb Vasc Biol. 2007;27:1706-21.

28. Chen P-Y, Quin L, Baeyens N, Li G, Afolabi T, Budatha M, et al. Endothelial-to-mesenchymal transition drives atherosclerosis progression. J Clin Invest. 2015;125(12):4514-28.

29. Iiyama K, Hajra L, Iiyama M, Li H, DiChiara M, Medoff BD, et al. Patterns of vascular cell adhesion molecule-1 and intercellular adhesion molecule-1 expression in rabbit and mouse atherosclerotic lesions and at sites predisposed to lesion formation. Circ Res. 1999;85(2):199-207.

30. Hou H-F, Yuan N, Guo Q, Sun T, Li C, Liu J-B, et al. Citreoviridin enhances atherogenesis in hypercholesterolemic ApoE-deficient mice via upregulating inflammation and endothelial dysfunction. PLoS One. 2015;10(5).

31. Asif A, Roy-Chaudhury P, Beathard GA. Early arteriovenous fistula failure: a logical proposal for when and how to intervene. Clin J American Soc Neph. 2006;2(1):332-9.

32. Fitts MK, Pike DB, Anderson K, Shie Y. Hemodynamic shear stress and endothelial dysfunction in hemodialysis access. Open Urol Nephrol J. 2014;7:33-44.

33. Sellak H, Franzini E, Hakin J, Pasquier C. Reactive oxygen species rapidly increase endothelial ICAM-1 ability to bind neutrophils without detectabel upregulation. Blood. 1994;83:2669-77.

34. Scott DW, Chen J, Chacko BK, Traylor JG, Orr AW, Patel RP. Role for endothelial N-glycan mannose residues in monocyte recruitment during atherogenesis. Arterioscler Thromb Vasc Biol. 2012;32(8).

35. Sumagin R, Sarelius IH. A role for ICAM-1 in maintenance of leukocyte-endothelial cell rolling interactions in inflamed arterioles. Am J Physiol Heart Circ Physiol. 2007;293(5):2786-98.

36. Whitcup SN, Chan C-C, Kozhich AT, Magone MT. Blocking ICAM-1 (CD54) and LFA-1 (CD11a) inhibits experimental allergic conjuctivitis. Clinical Immunology. 1999;93(2):107-13.

37. Bendjelloul F, Maly P, Mandys V, Jirkovska M, Prokesova L, Tuckova L, et al. Intercellular adhesion molecule 1 (ICAM-1 deficiency protects mice against severe forms of colitis. Clin Exp Immunol. 2000;119(1):57-63

38. Bourdillon MC, Poston RN, Covacho C, Chignier E, Bricca G, McGregor JL. ICAM-1 deficiency reduces atherosclerotic lesions in double-knockout mice (ApoE(-/-)/ICAM-1(-/-)) fed a fat or chow diet. Arterioscler Thromb Vasc Biol. 2000;20(12):2630-5.

39. Diamond MS, Staunton DE, Marlin SD, Springer TA. Binding of the integrin Mac-1 (CD11b/CD18) to the third immunoglobulin-like domain of ICAM-1 (CD54) and its regulation by glycosylation. Cell. 1991;65:961-71.

40. Otto VI, Schurpf T, Folkers G, Cummings RD. Sialylated complex-type N-glycans enhance the signaling activity of soluble intercellular adhesion molecule-1 in mouse astrocytes. J Biol Chem. 2004;279(34):35201-9.

41. Yuan K, Kucik D, Singh RK, Listinsky CM, Listinsky JJ, Siegal GP. Alterations in human breast cancer adhesion -motility in response to changes in cell surface glycoproteins displaying alpha-L-fucose moieties. Int J Oncol. 2008;32(4):797-807.

42. Saldova R, Fan Y, Fitzpatrick JM, Watson RW, Rudd PM. Core fucosylation and {alpha}2-3 sialylation in serum N-glycome is significantly increased in prostate cancer comparing to benign prostate hyperplasia. Glycobiology.

43. Hubbard AK, Rothlein R. Intercellular adhesion molecule 1 (ICAM-1) expression and cell signaling cascades. Free Radic Biol Med. 2000;28(9):1379-86.

44. Bloom JW, Madanat MS, Ray MK. Cell line and site-specific comparative analysis of the N-linked oligosaccharides on human ICAM-1des454-532 by electrospray ionization mass spectrometry. Biochemistry. 1996;35(6):1856-64.

45. Lau KS, Partridge EA, Grigorian A, Silvescu CI, Reinhold VN, Demetriou M, et al. Complex N-glycan number and degree of branching cooperate to regulate cell proliferation and differentiation. Cell. 2007;129(1):123-34.

46. Jimenez D, Roda-Navarro P, Springer TA, Casanovas JM. Contribution of N-linked glycans to the conformation and function of intercellular adhesion molecules (ICAMs). J Biol Chem. 2005;280(17):5854-61.

47. Patel SS, Thiarajan R, Willerson JT, Yeh ETH. Inhibition of alpha-4 integrin and ICAM-1 markedly attenuate macrophage homing to atherosclerotic plaques in ApoE-deficient mice. Circulation. 1998;97:75-81.

48. Investigators EAST. Use of Anti-ICAM-1 therapy in ischemic stroke: results of the Enlimomab Acute Stroke Trial. Neurology. 2001;57(8):1428-34.

49. Vuorte J, Lindsberg PJ, Kaste M, Meri S, Jansoon S-E, Rothlein R, et al. Anti-ICAM-1 monoclonal antibody R6.5 (Enlimomab) promotes activation of neutrophils in whole blood. J Immunol. 1999;162(4):2353-57.

50. Salmela K, Wramner L, Ekberg H, Hauser I, Bentdal O, Lins LE, et al. A randomized multicenter trial of the anti-ICAM-1 monoclonal antibody (enlimomab) for the prevention of acute rejection and delayed onset of graft function in cadaveric renal transplantation: a report of the European Anti-ICAM-1 Renal Transplant Study Group. Transplantation. 1999;67(5):729-36.

51. Haverslag R, Pasterkamp G, Hoefer I. Targeting adhesion molecules in cardiovascular disorders. Cardiovasc Hematol Disord Drug Targets. 2008;8(4):252-60.

52. Dougherty GJ, Murdoch S, Hogg N. The function of human intercellular adhesion molecule-1 (ICAM-1) in the generation of an immune response. Eur J Immunol. 1988;18(1):35-9.

53. Etienne S, Adamson P, Greenwood J, Strosberg AD, Cazaubon S, Couraud PO. ICAM-1 signaling pathways associated with Rho activation in microvascular brain endothelial cells. J Immunol. 1998;161(10):5755-61.

54. Lawson C, Wolf S. ICAM-1 signaling in endothelial cells. Pharmacol Rep. 2009;61(1):22-32.

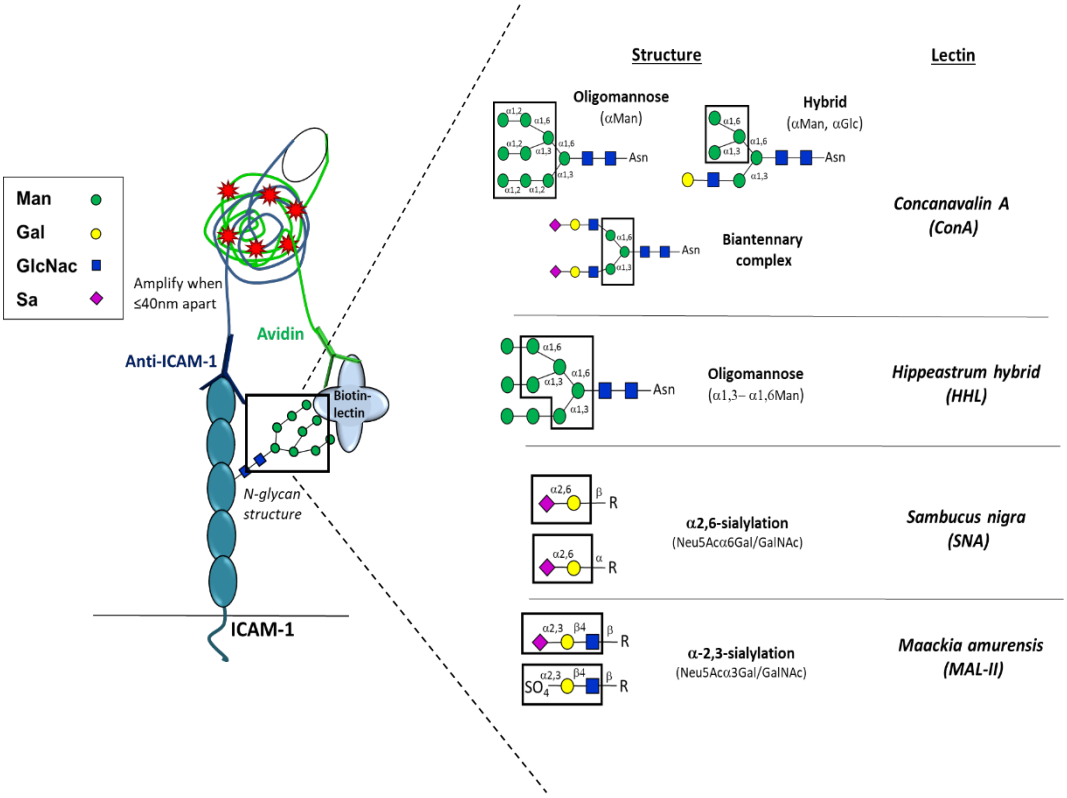


**Figure 1. Proximity-Ligation assay (PLA) schematic and lectin specificity.** Biotinylated lectins with indicated specificties, were added first to label specific sugars. Anti- ICAM-1 antibody and avidin, conjugated to complementary oligos, were then added. When lectin-recognized sugar epitopes are less than 40 nm from anti-ICAM-1, the complementary oligos hybridize and amplify, producing red fluorescent puncta. Right panel shows N-glycan structures recognized by different lectins used (adapted from(1)). Man= Mannose; Gal = Galactose; GlcNac = N-acetylglucosamine; Sa = Sialic acid; R= varying N-glycan structures.

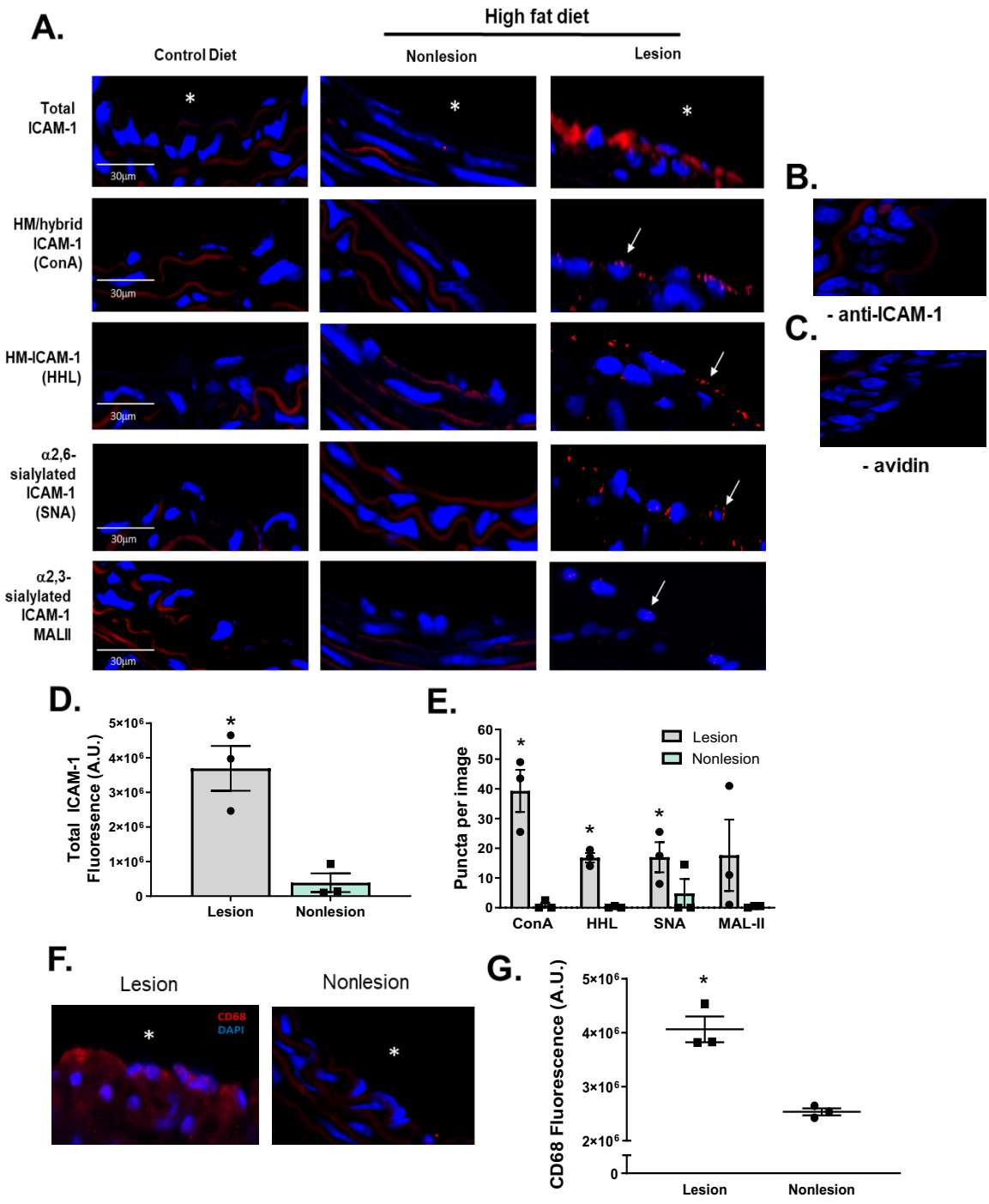


**Figure 2. HM epitopes co-localize with ICAM-1 in high fat-induced mouse atherosclerosis**. **A**) Total, HM / hybrid, α-2,6-sialylated, and α-2,3-sialylated ICAM-1 were measured in the innominate arteries of ApoE-/- mice fed a normal or high fat diet. Shown are representative images from vessels from control or high-fat diet fed mice. In the latter, paired lesion and non-lesion areas of the same vessel section are shown. Red

staining represents total ICAM-1, red puncta represent positive PLA staining for specific ICAM-1 N-glycoforms (indicated by arrows), blue staining represents DAPI. Asterisks indicate the lumen of each vessel. Panels **B** and **C** show PLA staining of lesion areas when the anti-ICAM-1 antibody or avidin were excluded. Panel **D** shows total ICAM-1 staining in lesion versus non-lesion areas. Panel **E** shows number of puncta for HM / hybrid, HM, α-2,6-sialylated, and α-2,3-sialylated ICAM-1 in lesion versus non-lesion areas. Data are mean ± SEM, n=3. * = $p<0.05$ compared to non-lesion via t-test. **F**. Representative images of CD68 staining (red) in lesion vs. nonlesion areas in mice. **G**. Quantitation of CD68 staining in lesion and nonlesion areas. Data are mean ± SEM, n=3 for each group. * = $p<0.05$ compared to nonlesion via t-test.

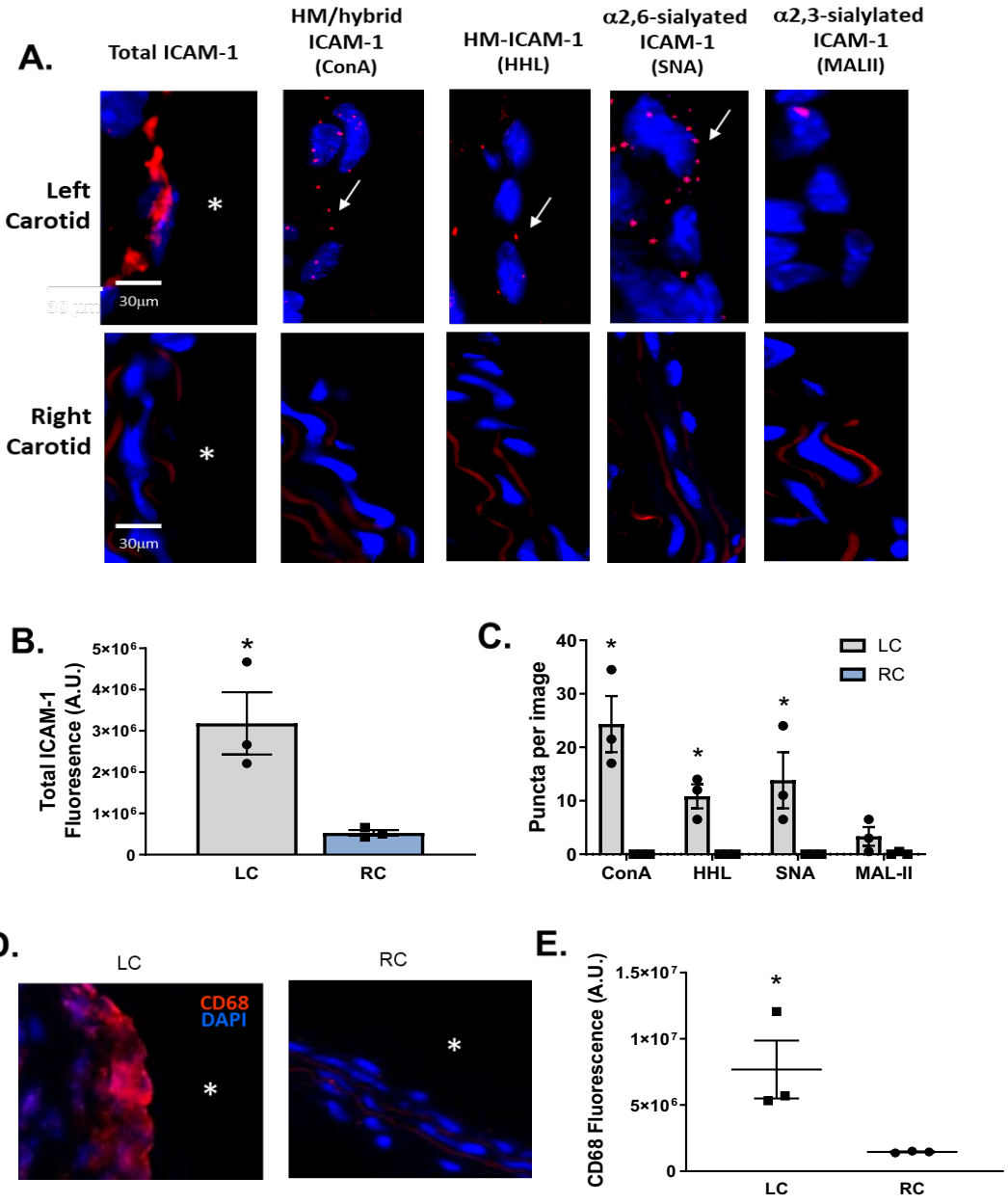


**Figure 3. HM / hybrid, HM, and α-2,6-sialylated ICAM-1 are increased in mouse atherosclerosis after induction of disturbed flow *in vivo*. Panel A** shows representative images of total ICAM-1 HM / hybrid, HM, α-2,6-sialylated, and α-2,3-sialylated ICAM-1 in the left carotid artery (after partial ligation) and right carotid artery (control). Positive PLA puncta are indicated by arrows. **Panels B & C** show total ICAM-1 staining in left versus right carotid artery and ICAM-1 N-glycoforms puncta, respectively. Data are mean ± SEM, n=3. * = $p<0.05$ compared to RC via t-test. **D.** Representative images of CD68 staining (red) in LC vs. RC areas in mice. **E.** Quantitation of CD68 staining in LC and RC areas. Data are mean ± SEM, n=3 for each group. * = $p<0.05$ compared to RC via t-test.

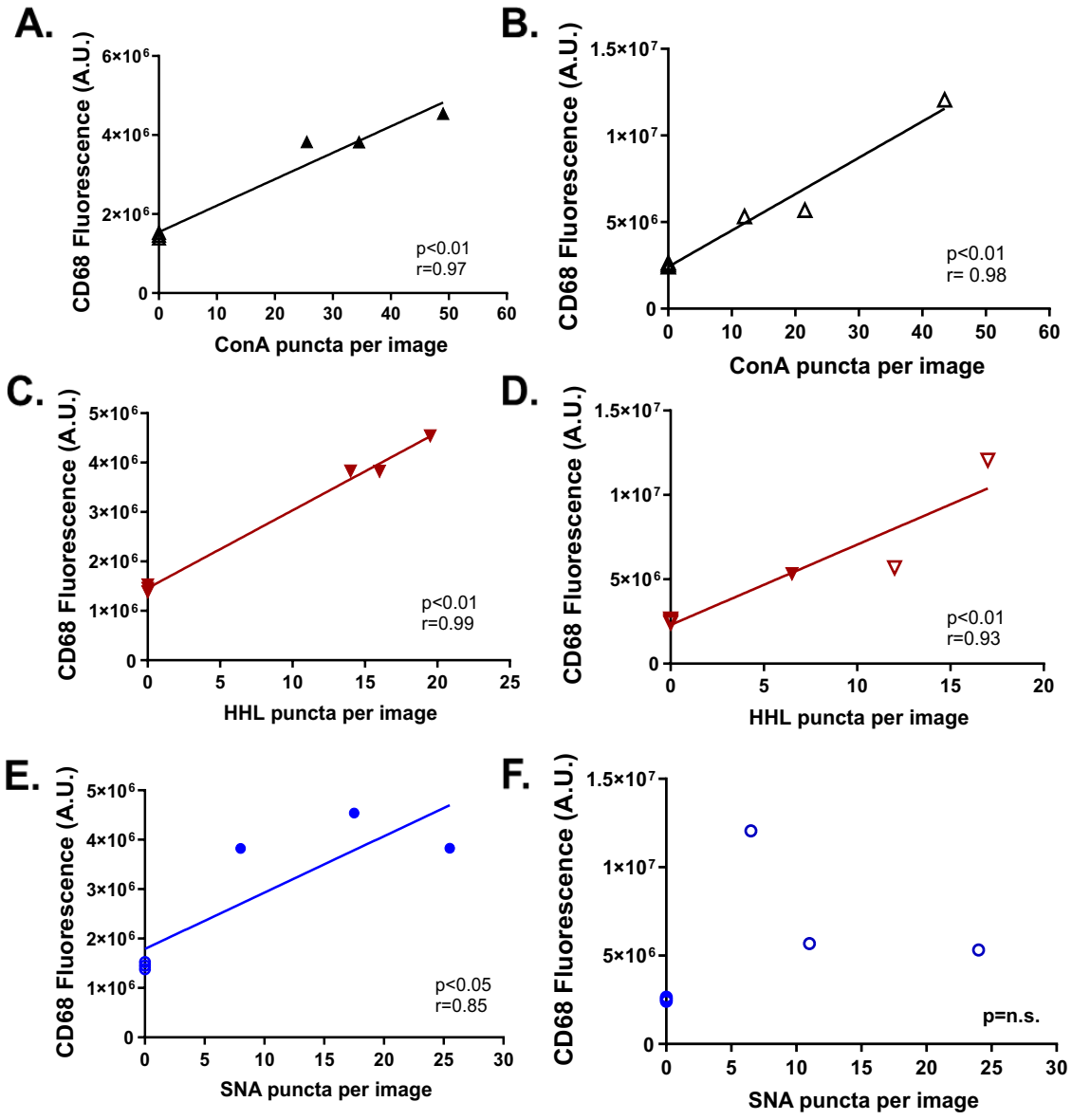


**Figure 4. CD68 macrophage staining positively correlates with HM-ICAM-1 in mouse models of atherosclerosis. A-F**. CD68 signal as a function of ConA, HHL, and SNA puncta for both animal models. n=6 vessels for each graph. Closed symbols represent vessels from the high-fat diet model (**A, C, E**) and open symbols represent vessels from the partial carotid ligation model (**B, D, F**). Best fit lines determined by Pearson correlation analyses with indicated p- and r-values.

| Patient # | Age | Sex and Race | Atherosclerotic Lesion Type | Vessel Sample(s) |
|---|---|---|---|---|
| 1 | 28 | Female, White | 1 | Right coronary Circumflex |
| 2 | 47 | Male, White | 2 | Right coronary |
| 3 | 22 | Male, N.D. | 3 | Left anterior descending artery |
| 4 | 22 | Male, African American | 3 | Right coronary |
| 5 | 66 | Male, African American | 4<br>5<br><br>5 | Circumflex<br>Left anterior descending<br>Right coronary |
| 6 | 58 | Male, White | 2 | Thoracic Aorta |
| 7 | 31 | Male, White | 1 | Thoracic Aorta |

**Table 1.** Atherosclerosis patient demographics.

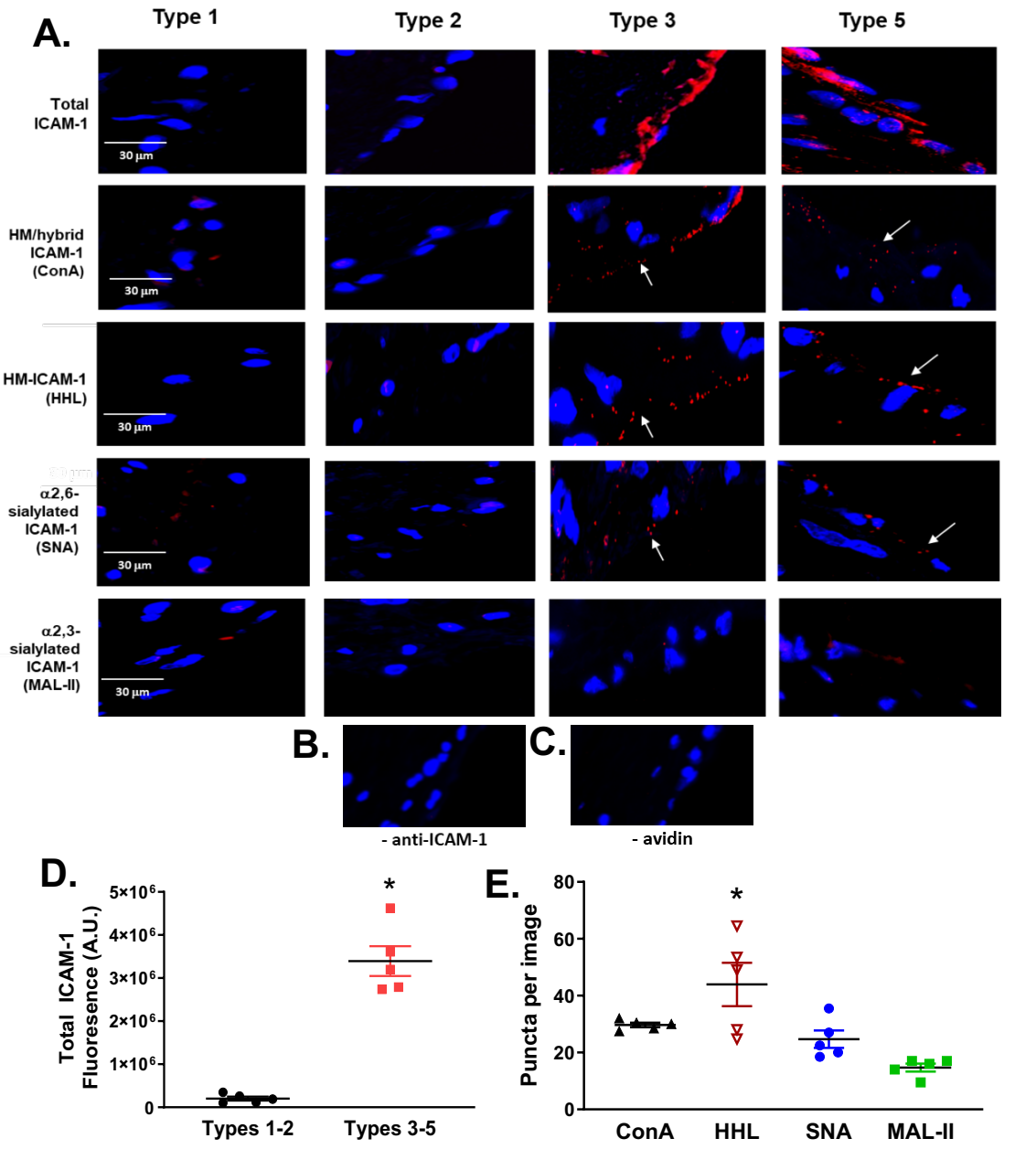


**Figure 5. HM / hybrid ICAM-1 is increased in human atherosclerosis. Panel A** shows representative images of total ICAM-1 and specified N-glycoforms in human vessels with lesions spanning types 1-5. Images represent n=10 vessel samples total from 7 separate patients. Inserts show magnified images. Red puncta represent positive PLA staining (as indicated by arrows). **Panels B** and **C** show staining of lesion areas when the anti-ICAM-1 antibody or avidin were excluded**. Panel D** shows the quantification of total ICAM-1 in early (1-2) and late (3-5) disease stages. Data are mean ± SEM, n=5. * = $p<0.05$ compared to types 1-2 via unpaired t-test. **Panel** E shows the quantification of HM / hybrid, HM, α-2,6-sialylated, and α-2,3-sialylated ICAM-1 puncta from advanced lesions. * = $p<0.05$ compared to α-2,6-sialylated, and α-2,3-sialylated ICAM-1 by 1-was ANOVA with Tukey post-test. Error bars are mean ± SEM.

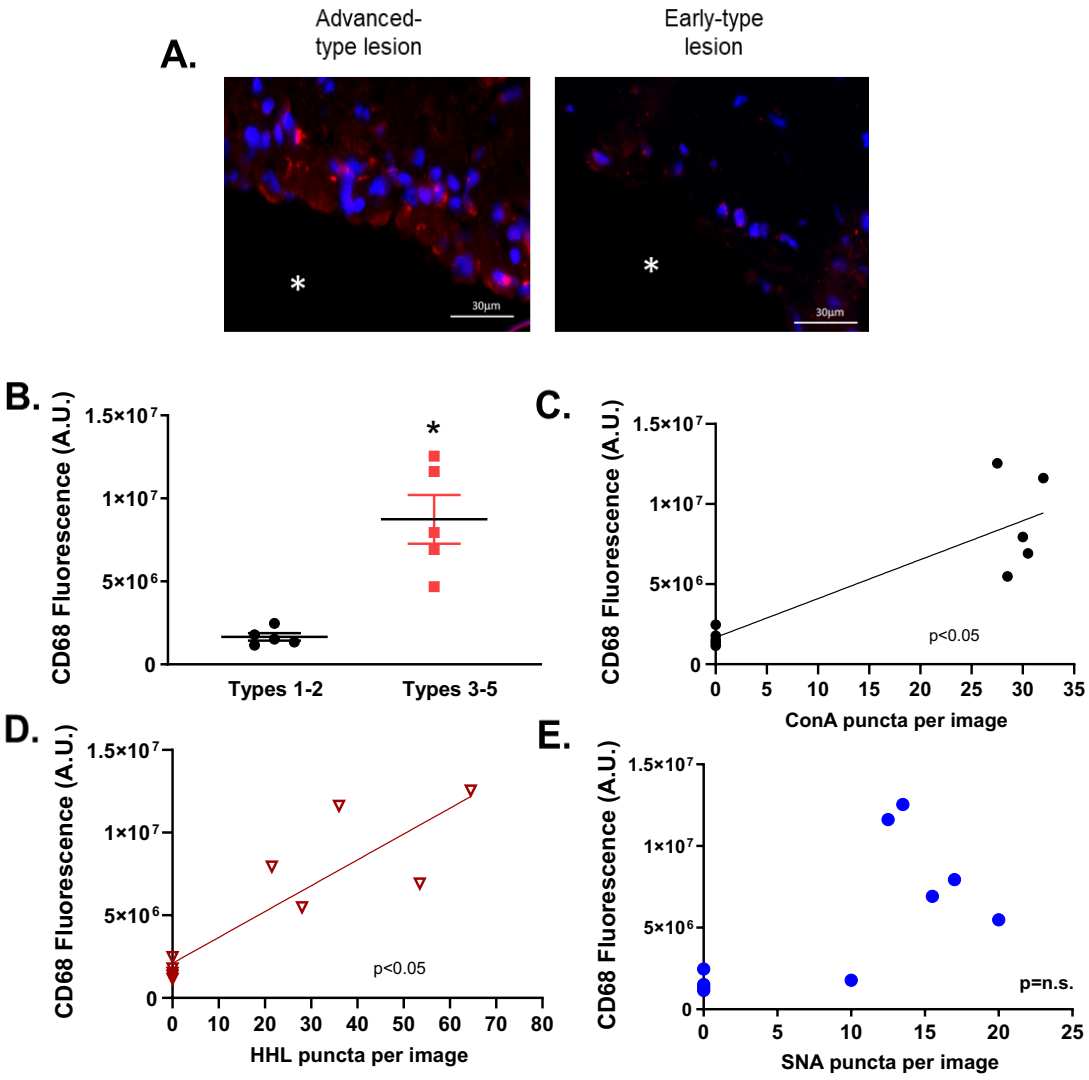


**Figure 6. CD68 macrophage staining positively correlates with HM / hybrid ICAM-1. Panels A** and **B** show representative images and quantitation, respectively, of CD68 staining in advanced and early type lesions. Data are mean ± SEM, n=10. * = $p<0.05$ compared to types 1-2 via t-test. **C-E.** ConA, HHL, and SNA puncta plotted against CD68 staining. Data are from n = 5 for each group. Best fit lines were determined by Pearson correlation analyses with indicated p-values.

| Patient # | AVF Status | Age | Sex and Race | Vessel Sample(s) |
|---|---|---|---|---|
| 8 | Successful | 55 | Male, White | Basillic |
| 9 | Successful | 77 | Female, African American | Basillic |
| 10 | Successful | 54 | Male, White | Basillic |
| 11 | Successful | 72 | Female, African American | Basillic |
| 12 | Failed | 73 | Female, African American | Basillic |
| 13 | Failed | 63 | Female, African American | Basillic |
| 14 | Control – no AVF | 58 | Female, White | Basillic |
| 15 | Control – no AVF | 69 | Female, White | Basillic |
| 16 | Control – no AVF | 56 | Female, White | Basillic |
| 17 | Failed | 58 | Female, African American | Basillic |
| 18 | Failed | 36 | Male, African American | Basillic |

**Table 2**. AVF patient demographics.

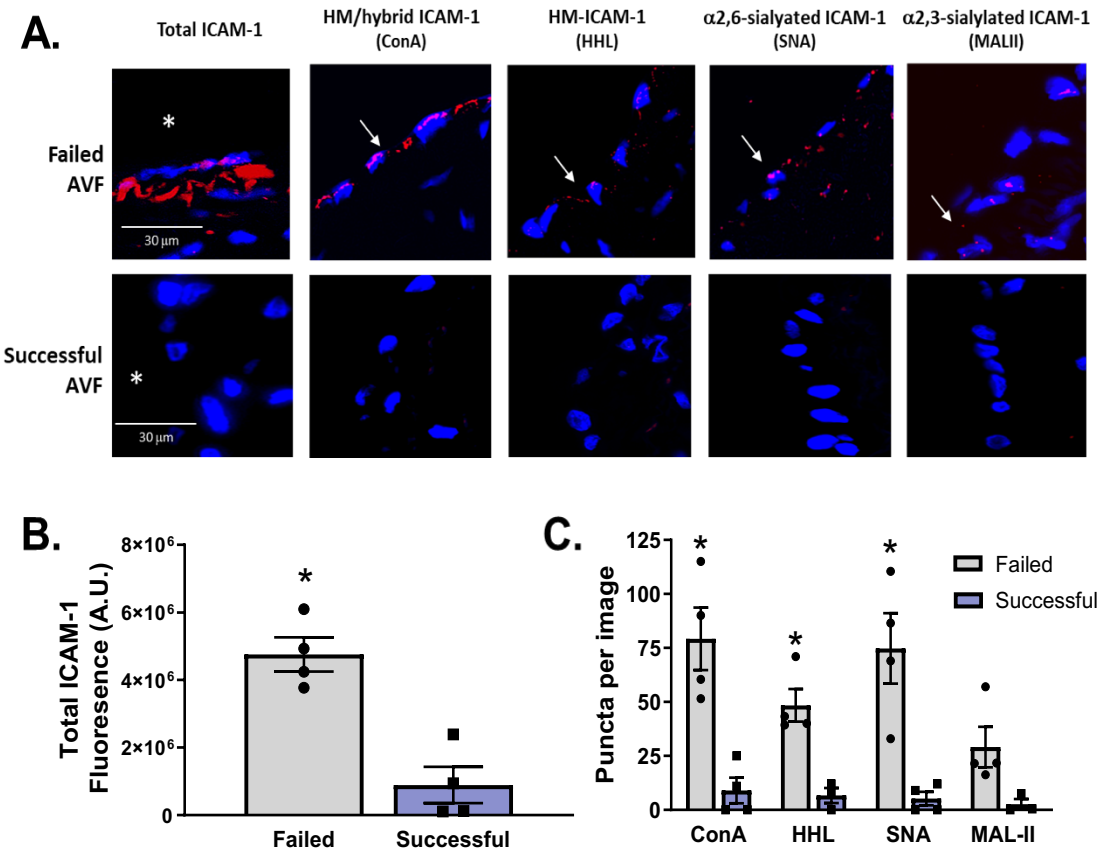


**Figure 7. HM / hybrid, HM, α-2,6-sialylated, ICAM-1 are increased CKD patients with failed arteriovenous fistulas. Panel A** shows total ICAM-1 and specified N-glycoforms in vessels from CKD patients with failed or successful AVF creation. Red puncta represent positive PLA staining (as indicated by arrows). **B)** Quantification of total ICAM-1 signal in failed and successful AVF samples (n=4 each). Error bars are mean ± SEM; * = $p<0.05$ compared to successful AVF samples by t-test. **C)** Quantification of HM / hybrid, HM, α-2,6-sialylated, and α-2,3-sialylated ICAM-1 as puncta per total ICAM-1 signal. Error bars are mean ± SEM; * = $p<0.05$ compared to successful AVF samples by unpaired t-test.

# TNFα-INDUCED HYDROGEN PEROXIDE INHIBITS ENDOTHELIAL α-MANNOSIDASE ACTIVITY AND INCREASES SURFACE HIGH-MANNOSE N-GLYCANS

by

KELLIE REGAL MCDONALD, ALEXANDRIA L. HERNANDEZ-NICHOLS, AND RAKESH P. PATEL

*In preparation for submission*

Format adapted for dissertation

## Abstract

N-glycosylation is a co- and post-translational modification that adds sugar molecules to surface and secreted proteins and is important for cell function and cell-to-cell communication. While it has been thought that proteins undergoing N-glycosylation will not be expressed unless fully processed to a complex N-glycoform, emerging data has suggested that hypoglycosylated N-glycoforms can exist on the cell surface during disease. Previous data from our lab has shown that endothelial inflammation produces a hypoglycosylated, or high-mannose (HM), intercellular adhesion molecule-1 (ICAM-1) which selectively enhances the adhesion of pro-inflammatory monocytes associated with more severe vascular inflammation and disease. The mechanisms regulating HM-ICAM-1 formation remains unclear, however. Here, we aimed to understand how inflammation may be mediating HM-ICAM-1 formation by measuring α-mannosidase activity. We show that α-mannosidase activity is inhibited in endothelial cells after 4 hours of TNFα treatment, and HM N-glycans are formed on the cell surface at the same time. Further, we demonstrate that α-mannosidase activity inhibition by TNFα is class I-dependent, and is independent of NF-κB upregulation of adhesion molecules. We then show that hydrogen peroxide ($H_2O_2$) inhibited α-mannosidase activity at doses as low at 1μM and as early as 15 minutes. Corroborating those results, we also showed that cell-permeable PEG-catalase prevented TNFα-induced activity inhibition. Finally, TNFα-induced $H_2O_2$ that inhibits α-mannosidase activity is generated in part by endoplasmic reticulum oxidoreductase 1-α (ERO1α). These data together present insights into the regulation of surface N-glycans during inflammation and demonstrate a novel role for reactive species in regulating N-glycans.

## Introduction

N-glycosylation is a co- and post-translational modification that occurs on surface and secreted proteins to ensure proper protein folding and function. While in the endoplasmic reticulum (ER), a tetradecasaccharide ($Glc_3Man_9GlcNac_2$) is added to the Asn residue of proteins with the appropriate consensus sequence (Asn-X-Ser/Thr, where X≠Pro) via oligosaccharyltransferase (OST) (1). As the protein is processed through the ER and Golgi, the tetradecasaccharide undergoes a series of enzymatic processing steps to trim and add sugars, eventually resulting in a fully processed, or complex, N-glycoform; often capped with sialic acids and galactose. These fully processed proteins are then trafficked to the cell membrane where they participate in cell-to-cell communications (1-4).

Endothelial adhesion molecules on the cell surface responsible for immune cell trafficking are heavily N-glycosylated, with proteins such as intercellular adhesion molecule 1 (ICAM-1) having up to 50% of its observed molecular weight attributed to N-glycans (5, 6). Despite the thought that these proteins must be fully processed to the complex N-glycoform for expression on the cell surface, we and others have identified underprocessed, or hypoglycosylated, surface N-glycan structures on these proteins that are associated with pathogenesis of inflammatory diseases such as atherosclerosis (6-13). For example, during inflammation we have shown that an increase in high-mannose (HM), ICAM-1 selectively enhances adhesion of pro-inflammatory monocytes (14). While mechanisms regulating ICAM-1 expression via NF-κB-dependent transcriptional activation is established (15), how N-glycosylation of ICAM-1 is regulated remains unclear.

N-glycosylation is a linear process, progressing from HM to hybrid to complex N-glycan structures through the ER and Golgi. It has been widely thought that cell surface and secreted proteins undergoing N-glycosylation will only be expressed after being fully processed to the complex N-glycoform. If proteins are not fully processed, they will be degraded (16, 17). However, emerging evidence has shown that HM N-glycans can be expressed on cell surfaces during endothelial inflammation, cancer, and autoimmune diseases like lupus (6, 12-14, 18). Novel mechanisms of regulating surface and secreted N-glycans have also recently been demonstrated (19). For example, it was recently shown that the stress-independent activation of the transcription factor XBP1s, a marker of the unfolded protein response (UPR), increases surface HM N-glycans in HEK293 and HeLa cells by altering the transcript levels of key N-glycan processing genes (19), demonstrating a mechanism in which transcription factor activation alters the N-glycome. Therefore, there may in fact be a controlled mechanism during inflammation by which these proteins in endothelial cells are expressed in hypoglycosylated forms to serve a specific purpose, e.g., monocyte adhesion. Yet what these regulatory mechanisms may be is not fully understood.

Our previous work has shown that inflammatory stimuli such as TNFα decrease total endothelial α-mannosidase activity, which is associated with increased cell surface HM N-glycans (6, 20). α-mannosidases catalyze the early processing steps of trimming terminal mannose residues from HM- and hybrid N-glycans (1, 16). There are two classes of α-mannosidases; class I and class II, responsible for trimming different linkages of mannose residues. Class I α-mannosidases are expressed in both the ER and Golgi, sequentially cleaving 4 terminal α-1,2 mannose linkages to drive 9-mannose structures

(HM) to 5-mannose hybrid structures (21-25). Class II α-mannosidases exist only in the Golgi, cleaving terminal α-1,3 and α-1,6 mannose linkages to drive 5-mannose hybrid structures to 3-mannose complex structures (21, 24, 26).

Little is known about the regulation of these enzymes and how that may change during inflammation to generate HM N-glycans on the cell surface. In this study, we addressed the mechanisms by which α-mannosidase activity is inhibited during inflammation. We show that inhibition of α-mannosidases by TNFα is class-I dependent, and independent of NF-κB upregulation of adhesion molecules. Further, we provide evidence that reactive species may be altering N-glycans by showing that hydrogen peroxide ($H_2O_2$) produced by endoplasmic reticulum oxidoreductase 1 – alpha (ERO1-α) during inflammation may be responsible for inhibiting α-mannosidase activity leading to formation of HM-N-glycan on the cell surface.

Current knowledge of how reactive species mediate cell function are mostly in the context of regulating transcription factors, such as NF-κB and Nrf2. Most of these actions occur via the MAPK pathway, although the exact mechanisms are not yet understood (27, 28). It is also known that oxidation of cysteine residues in Keap1, the repressor protein that binds Nrf2, will cause Nrf2 translocation to the nucleus to induce transcription of key scavenger proteins and antioxidant mechanisms (27). While Nrf2 is a redox-sensitive transcription factor and has been thought to be anti-atherogenic, emerging evidence suggests that it also possesses pro-atherogenic functions, most of which are still being explored (29). Here, we add another function of redox signaling in the cell aside from transcription factors by demonstrating a role for reactive species in altering enzyme function that directly impacts a post-translational modification.

The data herein provide a new insight into the regulation of surface N-glycans during disease, as well as reveal a novel mechanism for redox signaling in the regulation of protein N-glycoforms.

## Experimental procedures

### *Materials*

Human umbilical vein endothelial cells (HUVEC) were isolated from umbilical veins via collagenase as described (7). Human aortic endothelial cells (HAEC) and pulmonary microvascular endothelial cells (PMVEC) were purchased from ATCC (Manassas, VA). MCDB131, HI-FBS, trypsin, L-glutamine, and Penicillin/Streptomycin were purchased from Invitrogen (Carlsbad, CA). *Concanavalin A* (ConA), *Sambucus Nigra* (SNA), *Hippeastrum Hybrid Amaryllis* (HHL), and *Maackia Amurensis Lectin II* (MAL-II) lectins were purchased from Vector laboratories (Birlingame, CA). Kifunensine (Kif) and Swainsonine (Swain) were purchased form Cayman Chemicals (Ann Arbor, MI). EN460 was purchased from Millipore-Sigma (Burlington, MA). GKT137831 was a generous gift from Dr. Victor Thannickal (University of Alabama at Birmingham). All other reagents were purchased from Sigma-Aldrich (St. Louis, MO) unless otherwise noted.

### *Cell culture and treatment*

HUVEC, HAEC, and PMVEC were cultured in 35mm dishes as previously described (20) and used between passages 3-7 for experiments. Cells were used within one day of reaching confluence and were serum-starved in MCDB-131 media containing 1% FBS for 2 hours prior to treatment. Cells pre-treated with the class I and II α-mannosidase

inhibitors, Kifunensine or Swainsonine, respectively, were treated 2 hours prior to exposure to 10 ng/mL TNFα for 4 hours, unless otherwise stated. Exogenous hydrogen peroxide concentration was measured at 240nm and was diluted immediately prior to cell treatment. ONOO- concentration was measured at 302nm and made fresh immediately prior to cell treatment. HOCl was made fresh prior to cell treatment.

*α-mannosidase activity assay*

Total (class I and II) α-mannosidase activity was determined as described (20) with minor modifications. Cells were washed with PBS before lysis in PBS containing 1% Triton X-100 for 10 min on ice before clarification at 10,000 x g for 10 min. 50 μL cell lysate (corresponding to 30-40 μg protein) was prepared, in a microtiter plate, in 100 mM acetate buffer (pH 6.5) and 200 μM of the α-mannosidase substrate, resorufin-α-d-mannopyranoside added to start the reaction. Plates were read continuously at 550 ex and 595 em in a Biotek Synergy plate reader for 18 h at 37°C.

*Lectin staining*

Cells were grown on gelatin-coated glass coverslips and treated as indicated. Cells were washed with ice cold 1x PBS containing 1mM $MgCl_2$ and $CaCl_2$ before being incubated with 10 μg/mL FITC- or biotin- tagged lectins (HHL, SNA, MAL-II) for 10 min on ice. Cells were then fixed for 15 min at RT in 4% paraformaldehyde before being washed and mounted with DAPI-containing mounting medium. Cells treated with biotin-tagged lectins also underwent a 1 hour incubation at RT with avidin conjugated to AlexaFluor

594 prior to DAPI mounting. Images were acquired on a Biotek Lionheart fluorescent microscope and analyzed as a total fluorescence intensity per nuclei.

*Western blotting*

Cells were treated as described and lysed in RIPA buffer for 10 min on ice. 20 μg protein was loaded onto a 10% SDS-PAGE gel and subject to electrophoresis before being transferred to a 0.2 μm nitrocellulose membrane and probed for the described protein by incubation with primary antibody O/N at 4 degrees C with rocking. Membranes were incubated with HRP-linked, species-appropriate secondary antibodies for 2 hours at RT prior to chemiluminescence measurement. Images were analyzed using ImageQuant software (GE Healthcare Life Sciences).

*Monocyte isolation*

Primary human monocytes and neutrophils were isolated from freshly drawn whole blood collected by venipuncture from healthy volunteers using magnetic beads as described (30). Briefly, after removal of the plasma layer, blood was layered on top of a Histopaque 1119 to 1077 gradient and centrifuged at 700 x g for 20 minutes at RT. Monocytes appear at the interface of media and the 1077 layer while neutrophils appear between the two Histopaque layers. Monocytes were incubated with a CD16 antibody and isolated using positive selection via a magnetic column. The flow-through ($CD16^-$ cells) was then incubated with a CD14 antibody to isolate distinct $CD16^+$ and $CD16^-$ monocyte populations. Neutrophils were incubated with a CD15 antibody and isolated in the same

manner. All cell separations were confirmed via flow cytometry analysis (not shown). All protocols were approved by the UAB Institutional Review Board.

*Monocyte rolling and adhesion assay*

Isolated monocyte populations were incubated with 1μM fluorescent CellTracker™ dyes; $CD16^-$ cells were labeled with CellTracker™ green (CMFDA) and $CD16^+$ cells were labeled with CellTracker™ blue (CMAC) for 30 min at 37°C. Cells were pelleted and supernatant aspirated to remove any unincorporated dye. $CD16^-$ and $CD16^+$ monocytes were then were combined in equal amounts (final cell count 250,000 cells/mL; 125,000 cell/ml of each subtype), unless otherwise stated. Treated HUVEC or Cos-1 cells were exposed to fluorescent monocytes or neutrophils at a flow rate of 100 μL/min, corresponding to 1 dyne/$cm^2$, in a GlycoTech parallel plate flow chamber. Images were captured on a Biotek Lionheart live cell imager over 2 minutes at 30 frames/sec. Any cell that was stationary for ≥ 5 sec was considered firmly adhered as described (30, 31).

*Measurement of reactive species*

HUVECs were plated in 96-well plates and treated with ERO1α and NOX4 inhibitors as described prior to TNFα treatment (35, 36). At end of treatment, cells were washed 2x with 1x PBS and 20μM of DCFDA was added to each well. Plates were read after 1 hour at 485/535 for DCF signal and analyzed as a change from control values.

*Statistics*

All statistical analysis was performed using GraphPad Prism software. Paired t-test or one-way ANOVA followed by Tukey's post hoc test were performed as indicated in the figure legends. A minimum of three independent experiments were performed for each replicate.

## Results

### *TNFα decreases α-mannosidase activity and increases hypoglycosylation in ECs in a time-dependent manner*

Early-stage N-glycan processing occurs in the ER and cis/medial Golgi, where α-mannosidases class I and II are involved in trimming mannose residues from HM and hybrid N-glycan structures (**Fig. 1A**). Since our previous data has shown that TNFα decreases total α-mannosidase activity, we first further characterized the effect of TNFα on activity and N-glycan formation in various ECs. HUVECs, HAECs, and PMVECs were exposed to 10 ng/mL TNFα for 0-18 hours and α-mannosidase activity measured as described. In HUVECs and HAECs, α-mannosidase activity was significantly decreased early (4 hours), but then rebounded back to control levels by 18 hours (**Figure 1B**). In PMVECs, TNFα had no significant effect on α-mannosidase activity at any time tested **(Figure 1B)**. Likewise, staining for high-mannose (HM), hybrid, α-2,6- and α-2,3- sialylated N-glycans using the lectins HHL, ConA, SNA, and MAL-II, respectively, showed an increase in HM structures in HUVECs and HAECs at 4 hours compared to untreated controls while decreased again at 18 hours (**Figs. 1C, D, & F)** paralleling changes in α-mannosidase activity. PMVECs showed a decrease in HM lectin staining compared

to controls at 4 hours, but had an increase in α2,3-sialyation staining at 18 hours, also consistent with α-mannosidase activity results (**Figs. 1E & F**).

*TNFα inhibition of α-mannosidase activity is class-I dependent*

There is currently no class-specific α-mannosidase activity assay; the assays available and used here measure total α-mannosidase activity. In order to elucidate the distribution of class I and II α-mannosidases in HUVECs and HAECs, cells were treated with increasing doses of the α-mannosidase class I and II inhibitors, Kifunensine (Kif) and Swainsonine (Swain), respectively, and α-mannosidase activity measured. Refer to **figure 1A** for Kif and Swain inhibition sites. As shown in **figures 2A & B**, in HUVECs and HAECs, Kif (**Fig. 2A**) and Swain (**Fig. 2B**) each inhibited α-mannosidase activity in dose-dependent manner, with maximal inhibition of ~50-60% for class I and maximum of ~40-50% inhibition of class II, suggesting approximately equal distribution of a-mannosidase type in ECs.

After determining a relative distribution of class I and II α-mannosidases in ECs, we wanted to determine if TNFα was inhibiting one of these classes. HUVECs were treated with Kif and Swain prior to exposure to TNFα and α-mannosidase activity measured. **Figure 2C** shows that Kif, Swain, and TNFα alone inhibit α-mannosidase by ~25% each. When added together, TNFα with Swain inhibited ~50% inhibition of activity, while TNFα with Kif pretreatment showed no additive inhibition (~25%). Because inhibition of class II α-mannosidases with Swain resulted in an additive effect with TNFα treatment while class I inhibition did not, these data suggest that TNFα is inhibiting class I α-mannosidases.

To further elucidate the mechanism of α-mannosidase activity inhibition via TNFα, we wanted to determine if α-mannosidases were acting in conjunction with protein transcription via NF-κB that is activated during TNFα exposure. The NF-κB inhibitor, Parthenolide (Parth), was used to decrease ICAM-1 transcription in ECs during TNFα treatment. α-mannosidase activity was measured in ECs treated with Parth and TNFα; **figure 2D** shows that α-mannosidase activity remains decreased, even in the presence of Parth, suggesting that α-mannosidase activity is being inhibited in a parallel but independent mechanism of NF-κB-dependent protein upregulation. Supporting this is data showing that even though ICAM-1 transcription levels were decreased (~70%) with Parth treatment, HM-ICAM-1 is still formed in the ICAM-1 still transcribed (**Figs. 2E & F**). Interestingly, the ratio of HM-ICAM-1 to complex ICAM-1 is even higher in Parth-treated cells compared to TNFα alone (**Figure 2G**), consistent with the α-mannosidase activity data; if there is less ICAM-1 transcription, but the same degree of α-mannosidase inhibition, the ratio of HM to complex ICAM-1 will be greater.

*$H_2O_2$ inhibits class-I α-mannosidase activity*

One of the major mechanisms by which TNFα affects endothelial function is by generating reactive species, including $H_2O_2$ (32-34). To test if $H_2O_2$ alters α-mannosidase activity, exogenous $H_2O_2$ was added to ECs and α-mannosidase activity measured. As shown in **figure 3A**, $H_2O_2$ inhibits α-mannosidase activity in a dose-dependent manner, with inhibition seen with doses as low as 1μM. Maximal inhibition was around ~50%. To then understand how quickly $H_2O_2$ inhibits α-mannosidase activity, 100 μM $H_2O_2$ was

added to ECs for 5 min up to 3 hours. Interestingly, $H_2O_2$ causes maximal inhibition in ECs by 15min and activity does not recover over time (**Fig. 3B**).

Further, to determine which class of α-mannosidases $H_2O_2$ was inhibiting, we pre-treated ECs with Kif or Swain prior to $H_2O_2$ exposure. Consistent with results seen with TNFα treatment, $H_2O_2$ inhibited class I activity, as demonstrated by the additive inhibition seen when pretreated with Swain (~75%, **Fig. 3C**). No additive effect was seen when pretreated with Kif (~50%).

To test if TNFα-dependent inhibition of α-mannosidase activity was mediated by $H_2O_2$, ECs were treated with the cell-permeable polyethylene glycol (PEG)-catalase concurrently with TNFα treatment and α-mannosidase activity measured. As shown in **figure 3D**, treatment with PEG-catalase prevented the TNFα-dependent inhibition of α-mannosidase activity. PEG-catalase alone, interestingly, increased α-mannosidase activity to levels greater than untreated control cells, suggesting that even neutralizing endogenous $H_2O_2$ is sufficient to alter α-mannosidase activity.

After showing the changes in α-mannosidase activity, we wanted to know if $H_2O_2$ and PEG-catalase treatment altered surface N-glycans in accordance with their effects on α-mannosidase activity. **Figure 3E** shows that $H_2O_2$ treatment in ECs significantly increases HM/hybrid N-glycans. This is consistent with the fact that $H_2O_2$ inhibits α-mannosidase activity. Likewise, PEG-catalase treatment in TNFα-treated ECs decreases HM/hybrid N-glycans compared to ECs treated only with TNFα; consistent with the observation that PEG-catalase prevents α-mannosidase activity inhibition by TNFα (**Figure 3E**).

Finally, we wanted to see if PEG-catalase decreasing HM N-glycans had an effect on monocyte adhesion. **Figure 3F** shows that $CD16^+$ monocyte adhesion to TNFα-treated ECs was abrogated when cells were also treated with PEG-catalase. This data is still preliminary and needs to be repeated, but is consistent with our data from **chapter 2** showing that HM N-glycans increase $CD16^+$ monocyte adhesion, and data shown here that PEG-catalase decreases these HM N-glycans on the cell surface.

*Inhibition of ERO1-α rescues TNFα inhibition of α-mannosidase activity*

After establishing that $H_2O_2$ modulates α-mannosidase activity, we then wanted to know where the $H_2O_2$ was originating from during TNFα treatment. Because some of these α-mannosidases reside in the ER, we first looked at prevalent $H_2O_2$-producing enzymes in the ER: NADPH-oxidase 4 (NOX4) and ERO1α. ECs were pretreated with either the dual NOX1/4 inhibitor GKT137831 (35), or the ERO1α inhibitor EN460 (36), and α-mannosidase activity in response to TNFα was measured. As shown in **figure 4A,** NOX4 inhibition was unable to prevent TNFα-induced α-mannosidase activity inhibition while ERO1α inhibition prevented the effect of TNFα, suggesting that the source of $H_2O_2$ via TNFα is from ERO1α. Further corroborating this observation, ERO1α inhibition decreased surface HM N-glycans during TNFα treatment as assessed by lectin staining (**Fig. 4B**). To ensure that these results were not due to decreased surface ICAM-1 levels, we measured surface ICAM-1 via ELISA and showed that inhibition of ERO1α in the presence of TNFα does not alter surface ICAM-1 levels (**Fig. 4C**), therefore the effects seen in lectin staining is due only to changes in surface N-glycans. Finally, we

measured the oxidized and reduced forms of ERO1a in the presence of EN460 via western blot to ensure the compound was working. As shown in **fig. 4D**, TNFα treatment increases the oxidized form of ERO1α, but pretreatment with EN460 decreases the oxidized form and increases the reduced form, preventing ERO1α from generating $H_2O_2$. To ensure that our inhibitors were working to inhibit H2O2 production during TNFα treatment, **Fig. 4E** shows that EN460 does in fact suppress $H_2O_2$ production in the presence of TNFα via DCF assay. Finally, we recognized that inhibiting ER enzymes may inadvertently cause ER stress; at least moreso than is seen with TNFα alone. To determine if our treatments were causing ER stress, we looked at BiP levels, a master regulator of the ER stress pathway, and the preliminary data suggests that our inhibitors are not causing ER stress (**Fig. 4F**). These data will be repeated in ongoing work to confirm this trend.

*Inhibition of α-mannosidase activity is $H_2O_2$ dependent*

To determine if the inhibition of α-mannosidase activity seen by $H_2O_2$ was specific to $H_2O_2$ and not ROS in general, we tested compared effects of HOCl and $ONOO^{-}$. As shown in **Figs. 5A&B,** neither HOCl or $ONOO^{-}$ had an effect on α-mannosidase activity compared to control cells.

## Discussion

N-glycosylation of adhesion molecules play a key role in monocyte adhesion to the endothelium during inflammation, yet little is known how these N-glycans are regulated. Here, we characterized the inhibition of α-mannosidase activity by TNFα, as well as demonstrated a novel role for reactive species in modulating α-mannosidase activity.

Our previous work had showed that TNFα decreases α-mannosidase activity in endothelial cells, and we expanded upon that work here. First, we show that TNFα decreases α-mannosidase activity in HUVECs and HAECs transiently. α-mannosidase activity was decreased in ECs exposed to TNFα for 4 hours, but by 18 hours the activity had returned to control levels. Lectin staining also confirms this pattern so showing increased HM N-glycans at 4, but not 18, hours. This observation highlights an important aspect of the temporal regulation of hypoglycosylated proteins during inflammation; while *in vitro* inflammation induces transient HM epitopes and inhibition of α-mannosidase activity, *in vivo* inflammation in diseases like atherosclerosis is persistent throughout disease, perhaps sustaining the decreased α-mannosidase activity and increased expression of HM epitopes.

Also of note, only HUVECs and HAECs had decreased α-mannosidase activity and increased HM epitopes; PMVECs had an increase only in α-2,3-sialylation, consistent with literature suggesting that α-2,3-sialylation dominates in the lung endothelium (37, 38). These data also support the ongoing model of an endothelial "zip-code" made up of N-glycans (3, 39). When combined with our previous work showing that HM N-glycans enhance pro-inflammatory monocyte adhesion, this work demonstrates that recruitment of these monocytes would only be to vascular beds expressing these HM N-glycans; e.g., HUVECs and HAECs, but not PMVECs (14).

We also interrogated which class of α-mannosidases were inhibited by TNFα. There are two classes of α-mannosidases, class I and class II, which have different cleaving specificities for terminal mannose residues. By utilizing Kif and Swain to inhibit class I and II α-mannosidases, we were able to show that TNFα was acting primarily on class I

α-mannosidases, responsible for the initial steps of N-glycan processing, which is consistent with our previous data and data generated herein that show an accumulation of HM epitopes on the cell surface during inflammation. Narrowing down the class of α-mannosidases being inhibited by inflammation eliminates over half of the potential enzyme isoforms, as class I has four isoforms while class II has five. Ongoing studies in the lab are focusing on exactly which of the four class I isoform(s) is inhibited by TNFα by CRISPR/CAS9 gene deletion in our cells, as well as mRNA transcript analysis of the isoforms during inflammation. To our knowledge, this is the first time a class of α-mannosidases has been identified to be a target of inflammation.

Since TNFα has more than one effect on endothelial cells, we wanted to understand *how* TNFα was working to inhibit α-mannosidase activity. TNFα induces reactive species in endothelial cells, therefore we interrogated the effect of reactive species on α-mannosidase activity and N-glycan formation (32-34). $H_2O_2$ inhibited α-mannosidase activity, and TNFα – induced inhibition could be abrogated by the addition of cell-permeable PEG-catalase. No other reactive species tested had any effect on α-mannosidase activity, suggesting a specific role for $H_2O_2$. To our knowledge, this is the first time a role for reactive species in regulating N-glycosylation has been demonstrated.

Interestingly, our data shows that $H_2O_2$ inhibits α-mannosidase activity within minutes, with maximum inhibition seen by 15 minutes. The quick nature of this inhibition suggests that the effect of $H_2O_2$ on α-mannosidases may be on the activity itself rather than a transcriptional effect of the genes, which as mentioned in the introduction, is where much of our understanding of redox signaling lies. These data present a new role for redox signaling at the level of protein modification rather than transcription. Ongoing

studies in the lab are working to elucidate the mechanism of inhibition. One potential mechanism is oxidation of the enzymes themselves, especially in the methionine residues, that may render one or multiple isoforms inactive. Current work in the lab is looking at the effect of reducing agents on α-mannosidase activity in the presence of $H_2O_2$ and TNFα. Future studies will use proteomics to look at the physical changes TNFα and $H_2O_2$ may have on the enzymes themselves.

Consistent with our previous data showing a role for HM N-glycans in mediating $CD16^+$ monocyte adhesion, we wanted to see if the treatment of PEG-catalase, which we show to reduce surface N-glycans, would abrogate $CD16^+$ monocyte adhesion to TNFα-treated ECs. Our adhesion data still needs repeating, but so far suggests that treatment with PEG-catalase, and therefore the reduction of surface N-glycans, does in fact abrogate $CD16^+$ monocyte adhesion to the inflamed endothelium. In addition to showing a role for the neutralization of $H_2O_2$ in reducing surface HM N-glycans and increasing α-mannosidase activity, these data also suggest a role in altering immune cell trafficking.

The major sources of TNFα-induced $H_2O_2$ originate from the ER and the mitochondria (32). Since the α-mannosidases reside in the ER-Golgi secretory pathway, we started by looking at $H_2O_2$-producing enzymes in those organelles: NOX-4 and ERO1α. Both enzymes were inhibited by small molecule inhibitors, but only inhibition of ERO1α abrogated TNFα-induced inhibition of α-mannosidase activity and decreased surface HM epitopes. Based on DCF measurements and western blot analysis, we know that EN460 is decreasing $H_2O_2$ production by keeping ERO1α in the reduced form. Further, preliminary data with a BiP antibody for ER stress indication shows that EN460 is not inducing ER stress at the concentrations used.

Finally, we examined the effect of other reactive species that may be generated during inflammation, including peroxynitrite ($ONOO^-$) and hypochlorous acid (HOCl). Neither of these species changed α-mannosidase activity over an hour, corroborating our hypothesis that this inhibition is indeed $H_2O_2$ dependent. However, we note that one hour is a long time point to treat with species as reactive as $ONOO^·$. Future studies will examine earlier time points, or use slow-releasing agents such as SIN-1, and the impact these species may have on activity.

Taken together, the data presented herein demonstrate mechanism of regulating surface endothelial N-glycans during inflammation by decreased class I α-mannosidase activity, and present a novel role for $H_2O_2$ in mediating N-glycosylation. Understanding the regulation of N-glycans provides potential therapeutic targets in the treatment of inflammation.

# References

1. Stanley P, Schachter H, Taniguchi N. N-Glycans. In: nd, Varki A, Cummings RD, Esko JD, Freeze HH, Stanley P, et al., editors. Essentials of Glycobiology. Cold Spring Harbor (NY)2009.

2. Galkina E, Ley K. Immune and inflammatory mechanisms of atherosclerosis (*). Annu Rev Immunol. 2009;27:165-97.

3. Renkonen J, Tynninen O, Hayry P, Paavonen T, Renkonen R. Glycosylation might provide endothelial zip codes for organ-specific leukocyte traffic into inflammatory sites. Am J Pathol. 2002;161(2):543-50.

4. Dennis JW, Granovsky M, Warren CE. Protein glycosylation in development and disease. Bioessays. 1999;21(5):412-21.

5. Jimenez D, Roda-Navarro P, Springer TA, Casanovas JM. Contribution of N-linked glycans to the conformation and function of intercellular adhesion molecules (ICAMs). J Biol Chem. 2005;280(17):5854-61.

6. Scott D, Dunn T, Ballestas M, Litovsky S, Patel RP. Identification of a high-mannose ICAM-1 glycoform: effects of ICAM-1 hypoglycosylation on monocyte adhesion and outside in signaling. Am J Physiol Cell Physiol. 2013;305(2):C228-37.

7. Chacko BK, Scott D, Chandler RT, Patel RP. Endothelial surface N-Glycans mediate monocyte adhesion and are targets for anti-inflammatory effects of peroxisome proliferator-activated receptor Y ligands. J Biol Chem. 2011;286(44):38738-47.

8. Garcia-Vallejo JJ, Van Dijk W, Van Het Hof B, Van Die I, Engelse MA, Van Hinsbergh VW, et al. Activation of human endothelial cells by tumor necrosis factor-alpha results in profound changes in the expression of glycosylation-related genes. J Cell Physiol. 2006;206(1):203-10.

9. Kobata A, Amano J. Altered glycosylation of proteins produced by malignant cells, and application for the diagnosis and immunotherapy of tumours. Immunol Cell Biol. 2005;83(4):429-39.

10. Croci DO, Cerliani JP, Dalotto-Moreno T, Mendez-Huergo SP, Mascanfroni ID, Dergan-Dylon S, et al. Glycosylation-dependent lectin-receptor interactions preserve angiogenesis in anti-VEGF refractory tumors. Cell. 2014;156(4):744-58.

11. Stowell SR, Ju T, Cummings RD. Protein glycosylation in cancer. Annu Rev Pathol. 2015;10:473-510.

12. de Leoz ML, Young LJ, An HJ, Kronewitter SR, Kim J, Miyamoto S, et al. High-mannose glycans are elevated during breast cancer progression. Mol Cell Proteomics. 2011;10(1):M110 002717.

13. Talabnin K, Talabnin C, Ishihara M, Azadi P. Increased expression of the high-mannose M6N2 and NeuAc3H3N3M3N2F tri-antennary N-glycans in cholangiocarcinoma. Oncol Lett. 2018;15(1):1030-6.

14. Regal-McDonald K, Xu B, Barnes JW, Patel RP. High-mannose intercellular adhesion molecule-1 (ICAM-1) enhances CD16+ monocyte adhesion to the endothelium. Am J Physiol Heart Circ Physiol. 2019.

15. Collins T, Read MA, Neish AS, Whitley MZ, Thanos D, Maniatis T. Transcriptional regulation of endothelial cell adhesion molecules: NF-kappa B and cytokine-inducible enhancers. FASEB J. 1995;9(10):899-909.

16. Aebi M. N-linked protein glycosylation in the ER. Biochim Biophys Acta. 2013;1833(11):2430-7.

17. Breitling J, Aebi M. N-linked protein glycosylation in the endoplasmic reticulum. Cold Spring Harb Perspect Biol. 2013;5(8):a013359.

18. Hashii N, Kawasaki N, Itoh S, Nakajima Y, Kawanishi T, Yamaguchi T. Alteration of N-glycosylation in the kidney in a mouse model of systemic lupus erythematosus: relative quantification of N-glycans using an isotope-tagging method. Immunology. 2009;126(3):336-45.

19. Wong MY, Chen K, Antonopoulos A, Kasper BT, Dewal MB, Taylor RJ, et al. XBP1s activation can globally remodel N-glycan structure distribution patterns. Proc Natl Acad Sci U S A. 2018;115(43):E10089-E98.

20. Scott DW, Vallejo MO, Patel RP. Heterogenic Endothelial Responses to Inflammation: Role for Differentital N-Glycosylation and Vascular Bed of Origin. J American Heart Association. 2013;2(4).

21. Fujiyama K, Sakuradani S, Moran DG, Yoshida T, Seki T. Effect of alpha1,2-mannosidic linkage located in a alpha1,3-branch of Man6GlcNAc2 oligosaccharide on enzyme activity of recombinant human Man9-mannosidase produced in Escherichia coli. J Biosci Bioeng. 2001;91(4):419-21.

22. Isoyama-Tanaka J, Dohi K, Misaki R, Fujiyama K. Improved expression and characterization of recombinant human Golgi alpha1,2-mannosidase I isoforms (IA2 and IC) by Escherichia coli. J Biosci Bioeng. 2011;112(1):14-9.

23. Lipari F, Gour-Salin BJ, Herscovics A. The Saccharomyces cerevisiae processing alpha 1,2-mannosidase is an inverting glycosidase. Biochem Biophys Res Commun. 1995;209(1):322-6.

24. Shah N, Kuntz DA, Rose DR. Comparison of kifunensine and 1-deoxymannojirimycin binding to class I and II alpha-mannosidases demonstrates different saccharide distortions in inverting and retaining catalytic mechanisms. Biochemistry. 2003;42(47):13812-6.

25. Herscovics A. Structure and function of Class I alpha 1,2-mannosidases involved in glycoprotein synthesis and endoplasmic reticulum quality control. Biochimie. 2001;83(8):757-62.

26. Shah N, Kuntz DA, Rose DR. Golgi alpha-mannosidase II cleaves two sugars sequentially in the same catalytic site. Proc Natl Acad Sci U S A. 2008;105(28):9570-5.

27. Majzunova M, Dovinova I, Barancik M, Chan JY. Redox signaling in pathophysiology of hypertension. J Biomed Sci. 2013;20:69.

28. Schulz E, Gori T, Munzel T. Oxidative stress and endothelial dysfunction in hypertension. Hypertens Res. 2011;34(6):665-73.

29. Howden R. Nrf2 and cardiovascular defense. Oxid Med Cell Longev. 2013;2013:104308.

30. Scott DW, Chen J, Chacko BK, Traylor JG, Orr AW, Patel RP. Role for endothelial N-glycan mannose residues in monocyte recruitment during atherogenesis. Arterioscler Thromb Vasc Biol. 2012;32(8).

31. Kevil CG, Patel RP, Bullard DC. Essential role of ICAM-1 in mediating monocyte adhesion to aortic endothelial cells. Am J Physiol Cell Physiol. 2001;281(5):C1442-7.

32. Chen X, Andresen BT, Hill M, Zhang J, Booth F, Zhang C. Role of Reactive Oxygen Species in Tumor Necrosis Factor-alpha Induced Endothelial Dysfunction. Curr Hypertens Rev. 2008;4(4):245-55.

33. Woo CH, Eom YW, Yoo MH, You HJ, Han HJ, Song WK, et al. Tumor necrosis factor-alpha generates reactive oxygen species via a cytosolic phospholipase A2-linked cascade. J Biol Chem. 2000;275(41):32357-62.

34. Young CN, Koepke JI, Terlecky LJ, Borkin MS, Boyd Savoy L, Terlecky SR. Reactive oxygen species in tumor necrosis factor-alpha-activated primary human keratinocytes: implications for psoriasis and inflammatory skin disease. J Invest Dermatol. 2008;128(11):2606-14.

35. Gaggini F, Laleu B, Orchard M, Fioraso-Cartier L, Cagnon L, Houngninou-Molango S, et al. Design, synthesis and biological activity of original pyrazolo-pyrido-diazepine, -pyrazine and -oxazine dione derivatives as novel dual Nox4/Nox1 inhibitors. Bioorg Med Chem. 2011;19(23):6989-99.

36. Blais JD, Chin KT, Zito E, Zhang Y, Heldman N, Harding HP, et al. A small molecule inhibitor of endoplasmic reticulum oxidation 1 (ERO1) with selectively reversible thiol reactivity. J Biol Chem. 2010;285(27):20993-1003.

37. Cioffi DL, Pandey S, Alvarez DF, Cioffi EA. Terminal sialic acids are an important determinant of pulmonary endothelial barrier integrity. Am J Physiol Lung Cell Mol Physiol. 2012;302(10):L1067-77.

38. Zeng H, Pappas C, Belser JA, Houser KV, Zhong W, Wadford DA, et al. Human pulmonary microvascular endothelial cells support productive replication of highly pathogenic avian influenza viruses: possible involvement in the pathogenesis of human H5N1 virus infection. J Virol. 2012;86(2):667-78.

39. Thorpe PE, Ran S. Mapping zip codes in human vasculature. Pharmacogenomics J. 2002;2(4):205-6.

\

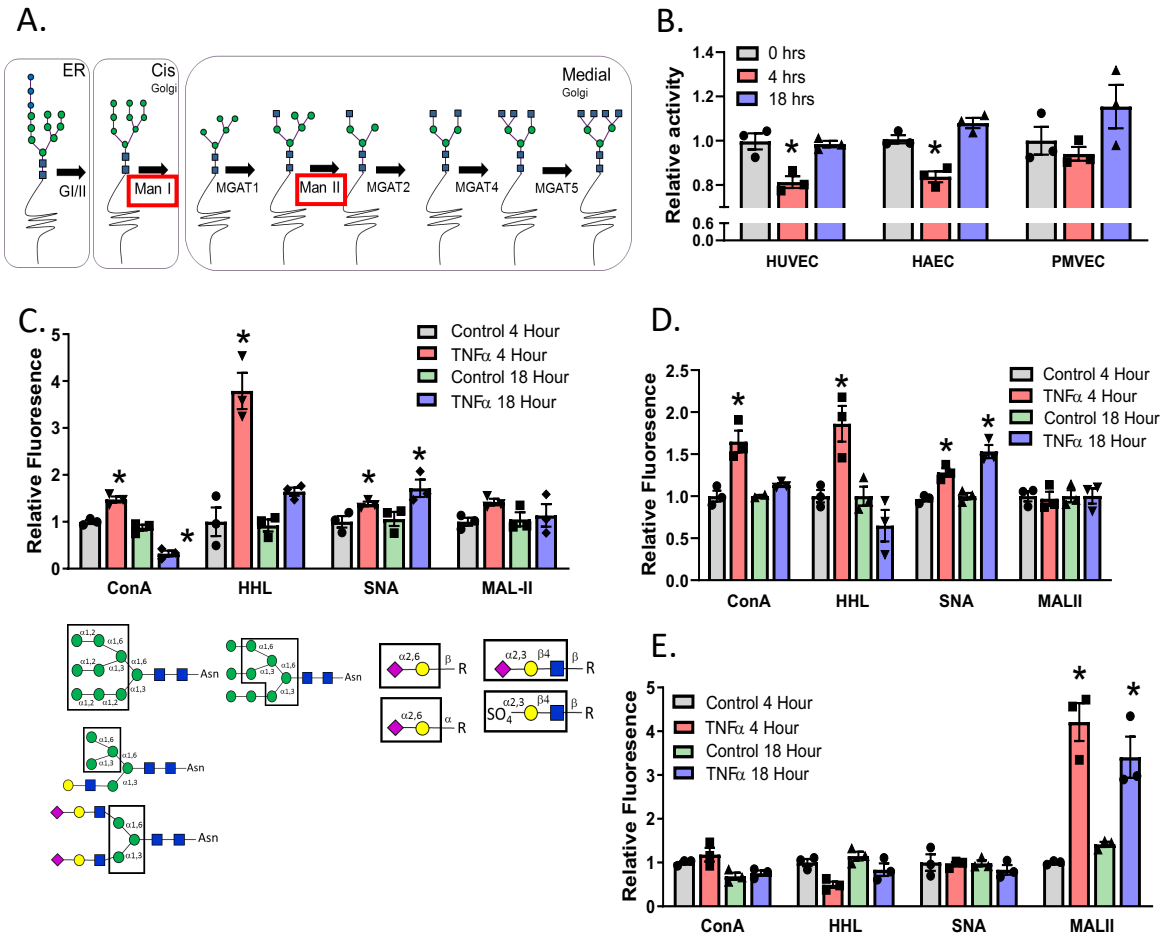
A.
ER
Cis
Golgi
Medial
Golgi
GI/II
Man I
MGAT1
Man II
MGAT2
MGAT4
MGAT5
B.
Relative activity
0 hrs
4 hrs
18 hrs
HUVEC
HAEC
PMVEC
C.
Relative Fluoresence
Control 4 Hour
TNFα 4 Hour
Control 18 Hour
TNFα 18 Hour
ConA
HHL
SNA
MAL-II
Asn
R
D.
Relative Fluoresence
Control 4 Hour
TNFα 4 Hour
Control 18 Hour
TNFα 18 Hour
ConA
HHL
SNA
MALII
E.
Relative Fluoresence
Control 4 Hour
TNFα 4 Hour
Control 18 Hour
TNFα 18 Hour
ConA
HHL
SNA
MALII

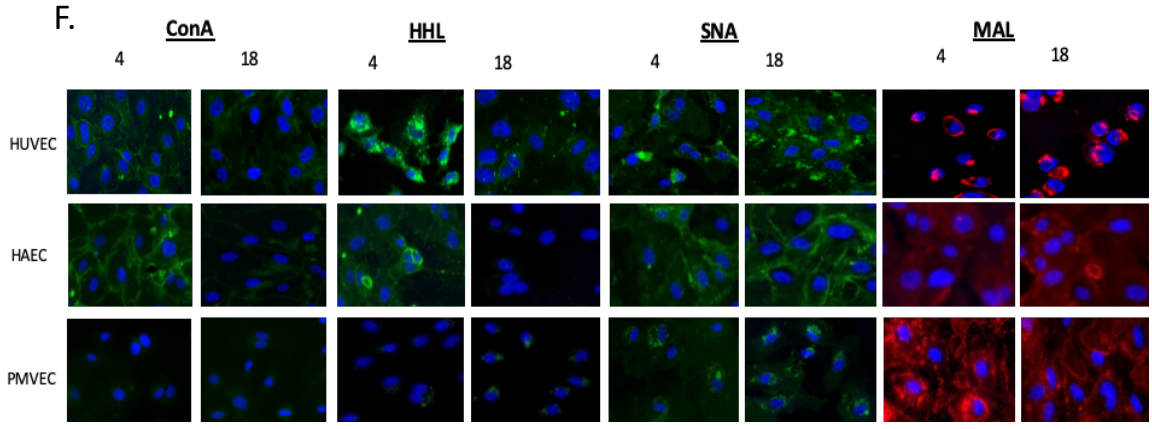
F.
ConA
HHL
SNA
MAL
4
18
4
18
4
18
4
18
HUVEC
HAEC
PMVEC

**Figure 1. TNFα inhibition of α-mannosidase activity and HM N-glycan formation occurs early. A.** N-glycan schematic and location of α-mannosidase enzymes highlighted in red boxes. **B.** Relative α-mannosidase activity in HUVECs, HAECs, and PMVECs during 0, 4, and 18 hour TNFα treatment. *=p≤0.05 compared to each group control by one-way ANOVA. Data are mean ± SEM, n=3. **C – E**. Relative fluorescence of 4 different lectins across HUVECs, HAECs, and PMVECs during 0, 4, and 18 hour TNFα treatment. Sugar structures recognized by each lectin are below the legend. *=p≤0.05 compared to respective controls per lectin. Data are mean ± SEM, n=3. **F.** Representative images of lectin staining across cell lines treated with TNFα for 4 and 18 hours. Green (ConA, HHL, and SNA) and red (MAL-II) represent positive lectin staining. Blue staining is a DAPI nuclear stain.

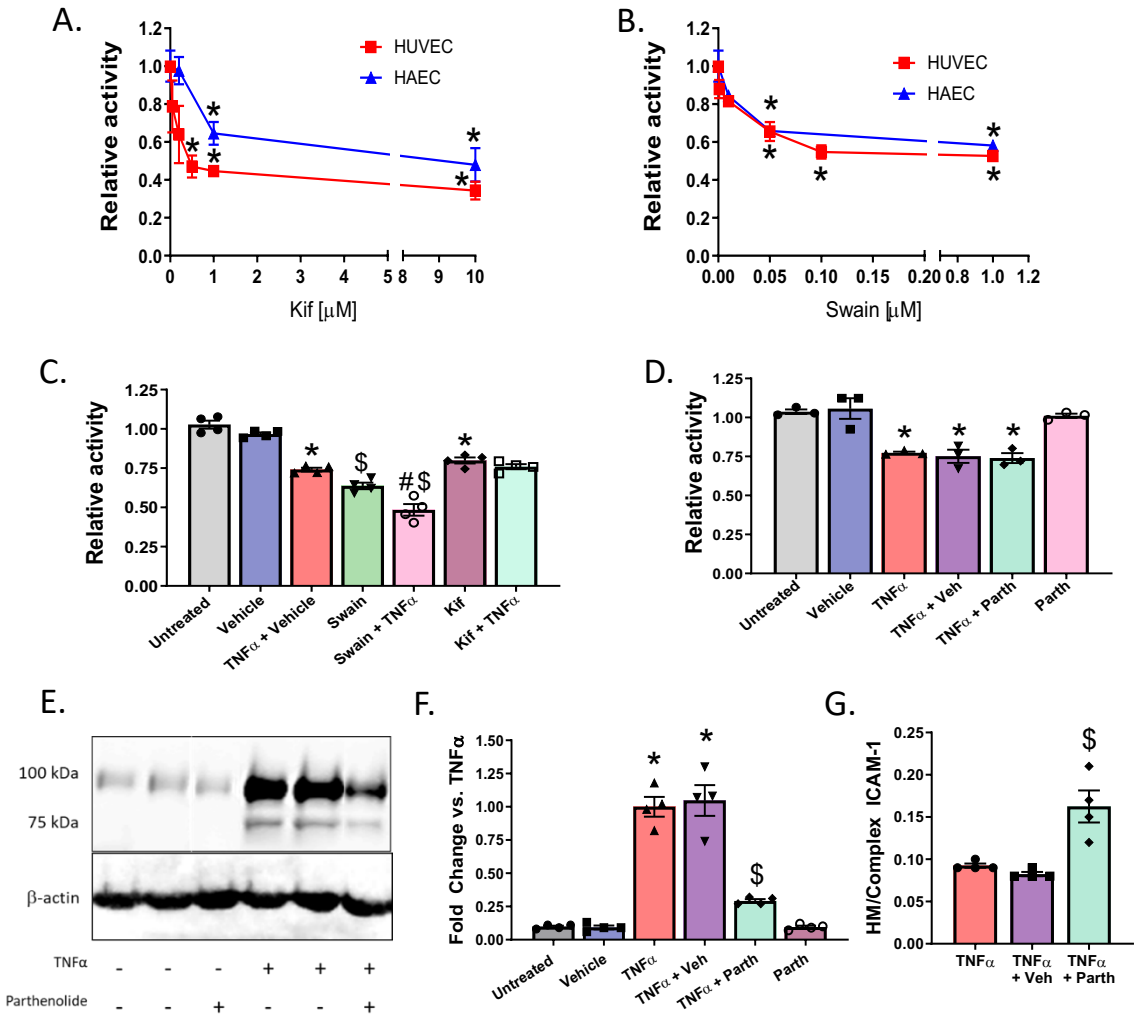


**Figure 2. TNFα inhibition of α-mannosidase activity is class-I dependent. A.** HUVECs and HAECs were treated for 2 hours with increasing doses of Kif and total α-mannosidase activity measured. *=p<0.05 compared to untreated cells. Data are mean ± SEM, n=3. **B.** HUVECs and HAECs were treated for 2 hours with increasing doses of Swain and total α-mannosidase activity measured. *=p<0.05 compared to untreated cells. Data are mean ± SEM, n=3. **C.** HUVECs were pretreated with 1μM Kif or Swain for 2 hours prior to TNFα treatment and α-mannosidase activity measured. *=p≤0.05 compared to control; $=p≤0.05 compared to TNFα; #=p≤0.05 compared to Swain alone. Data are mean ± SEM, n=4. **D.** α-mannosidase activity measured in cells pretreated with 5μM Parthenolide prior to TNFα treatment. *=p≤0.05 compared to control. Data are mean ± SEM, n=3. **E.** Western blot image and **F.** analysis of ICAM-1 N-glycoforms in cells treated as described in (**D**). *=p≤0.05 compared to control; $=p≤0.05 compared to TNFα. Data are mean ± SEM, n=4. **G.** Analysis of ratio of HM-ICAM-1 to complex ICAM-1 from (**E**). $=p≤0.05 compared to TNFα. Data are mean ± SEM, n=4.

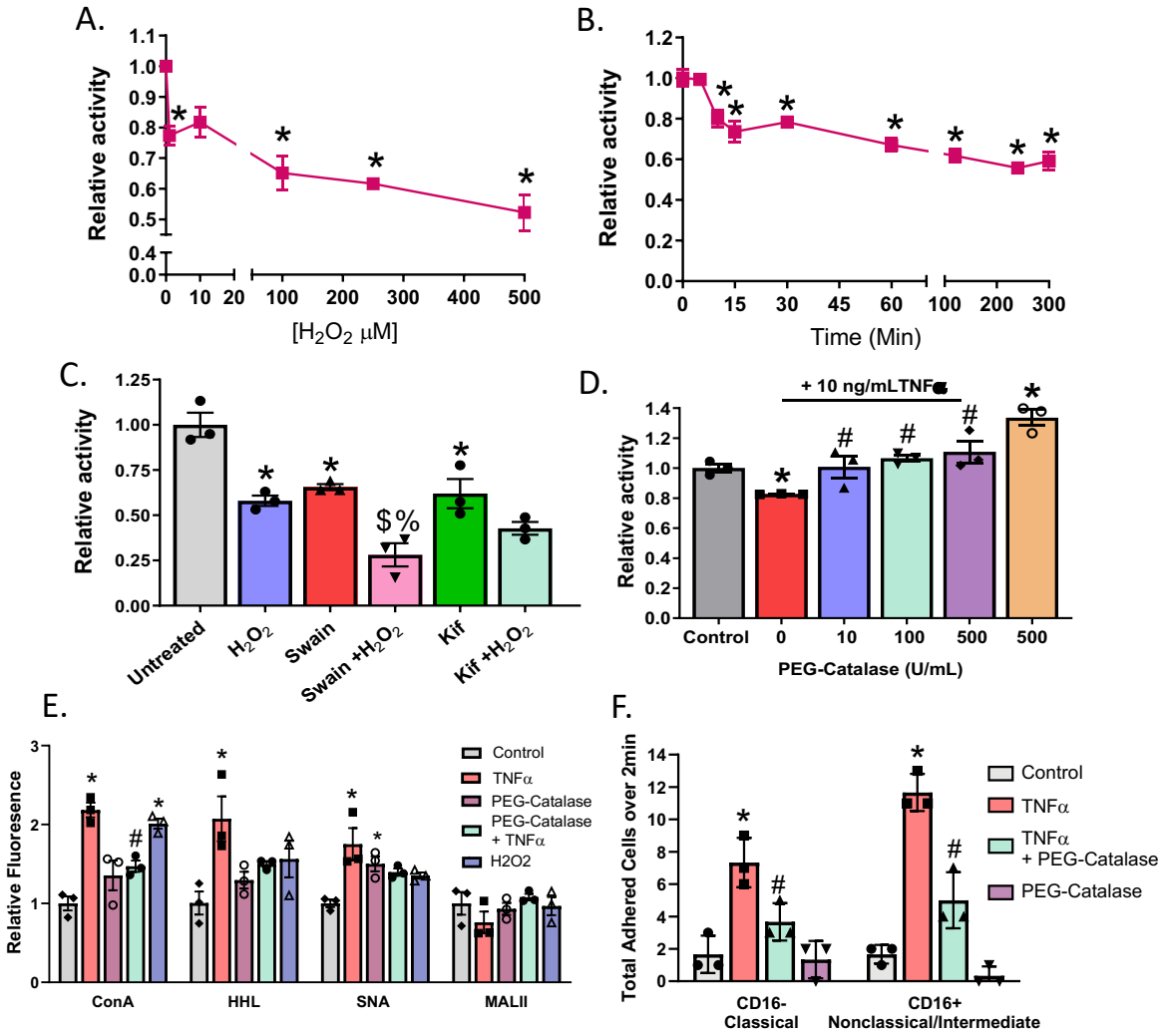


**Figure 3. Hydrogen peroxide inhibits α-mannosidase activity in a time and dose dependent manner**. **A.** HUVECs were treated with increasing doses of exogenous $H_2O_2$ for 1 hour and α-mannosidase activity measured. *=p≤0.05 compared to untreated control. Data are mean ± SEM, n=3. **B.** HUVECs were treated with 100 μM exogenous $H_2O_2$ from 0-300 min and α-mannosidase activity measured. *=p≤0.05 compared to untreated control. Data are mean ± SEM, n=3. **C**. HUVECs were pretreated with 1 μM Kif or Swain prior to 100 μM $H_2O_2$ treatment and α-mannosidase activity measured. *=p≤0.05 compared to untreated control; $=p≤0.05 compared to Swain; %=p≤0.05 compared to $H_2O_2$. Data are mean ± SEM, n=3. **D.** HUVECs were simultaneously treated with increasing concentrations of PEG-catalase along with TNFα treatment and α-mannosidase activity measured. *=p≤0.05 compared to control; #=p≤0.05 compared to TNFα alone. Data are mean ± SEM, n=3. **E**. HUVECs were treated as described in **C & D** and lectin staining with ConA, HHL, SNA, and MAL-II was performed. *=p<0.05 compared to control; #=p≤0.05 compared to TNFα. Data are mean ± SEM, n=3. **F.** HUVECs were treated as described in **E** and subject to monocyte adhesion assay as described in methods. *=p≤0.05 compared to control; #=p≤0.05 compared to TNFα alone. Data are mean ± SEM, n=3.

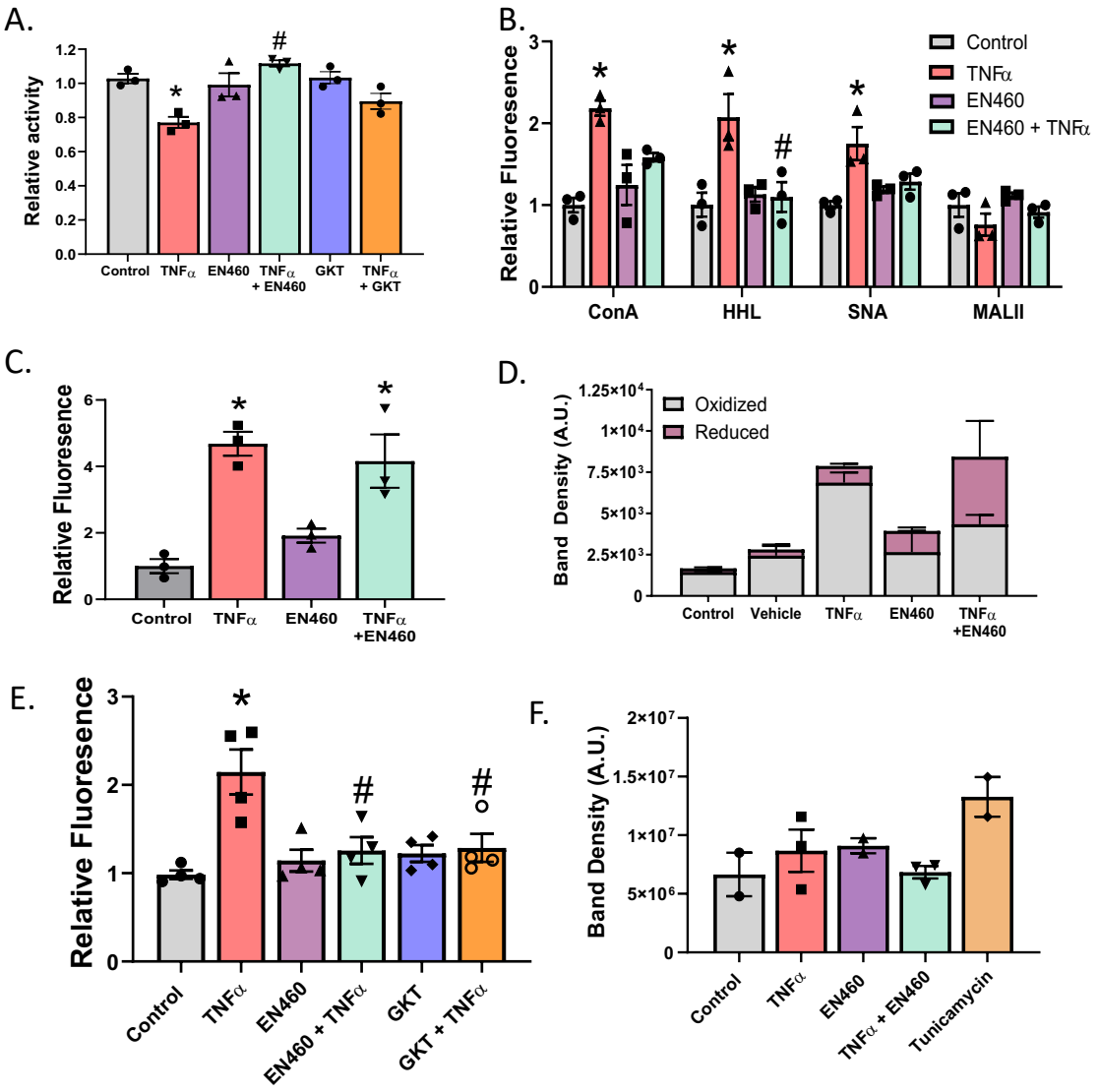


**Figure 4. ERO1-α inhibition abrogates TNFα-inhibtion of α-mannosidase activity and HM N-glycan formation**. **A.** HUVECs were pretreated with either 10 μM GKT137831 or 5 μM EN460 to inhibit NOX4 and ERO1-α, respectively, and α-mannosidase activity measured. *=p<0.05 compared to control; #=p≤0.05 compared to TNFα. Data are mean ± SEM, n=3. **B.** Lectin stain of cells treated in **A.** *=p≤0.05 compared to control; #=p≤0.05 compared to TNFα. **C.** HUVECs were treated as described in **A** and surface ICAM-1 was measured via ELISA. *=p≤0.05 compared to control. Data are mean ± SEM, n=3. **D.** HUVECs were treated as described in **A** and oxidized and reduced ERO1α measured via western blot. Data are mean ± SEM, n=3. **E.** HUVECs were treated as described in (A) and subject to DCFDA assay to measure ROS production. *=p<0.05 compared to control; #=p≤0.05 compared to TNFα. Data are mean ± SEM, n=4. **F.** HUVECs were treated as described and some were treated with 1 μM Tunicamycin 1 hour prior to lysis and western blot analysis for the ER stress marker BiP. Data are mean ± SEM, n=2-3.

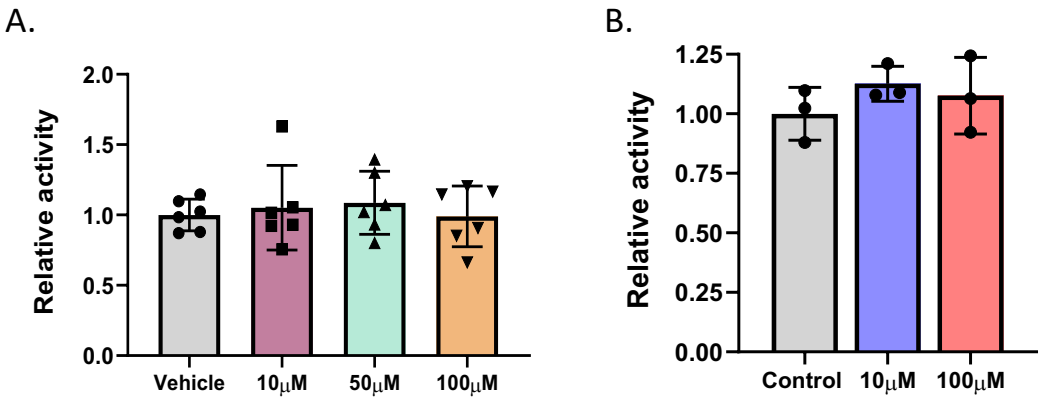


**Figure 5. HOCl and $ONOO^-$ have no effect on α-mannosidase activity. A.** HUVECs were treated with 0,10, 50, and 100 μM HOCl for 1 hour and α-mannosidase activity measured. Data are mean ± SEM, n=6. **B.** HUVECs were treated with 0, 10, or 100 uM $ONOO^-$ for 1 hour and α-mannosidase activity measured. Data are mean ± SEM, n=3.

# DISCUSSION

The studies presented herein explore the role of N-glycans in disease and their regulation by inflammatory stimuli. I presented data in the previous chapters to demonstrate i) the role of HM-ICAM-1 in monocyte adhesion, specifically of different subsets associated with disease, ii) the presence of ICAM-1 N-glycoforms *in vivo* in human and mouse models of endothelial dysfunction, and iii) the regulation α-mannosidases that impact N-glycan formation.

First, we looked at the effects of HM epitopes on monocyte adhesion to the endothelium (**chapter 2**). As discussed earlier, monocytes come in several flavors: classical, nonclassical, and intermediate. These more pro-inflammatory intermediate monocytes are independently associated with atherosclerosis, peripheral artery disease, and adverse cardiac events (69, 70, 115), and our studies wanted to elucidate the mechanisms behind recruitment of these specific subsets to the endothelium.

Our study separated $CD16^-$ (classical) and $CD16^+$ (nonclassical and intermediate) monocytes and looked at adhesion to a HM-rich endothelial surface, as well as a HM-ICAM-1 expressed in a Cos-1 cell line. The selective increase of $CD16^+$ monocyte adhesion to HM-rich endothelial cells and HM-ICAM-1 expressing Cos-1 cells demonstrates, for the first time, a role for HM-ICAM-1 in recruiting monocyte subsets. This observation was strengthened by demonstrating that $CD16^+$ monocyte adhesion could be abrogated with the use of ICAM-1 antibodies directed to the glycosylated domain 3 (Mac-1 binding site), while antibodies directed to the un-glycosylated domain 1 (LFA-1 binding site) had no effect.

Taken together, these studies and others (79, 106, 109, 110) demonstrate a key role of HM-ICAM-1 in the recruitment of specific monocytes. Requisite for this model is that ligands on $CD16^+$ monocytes show specificity for HM epitopes. Interestingly, CD16 itself may regulate Mac-1 activation and binding to ICAM-1. In neutrophils, CD16 binds to Mac-1 via sugar-based interactions; enzymatic digestion of HM N-glycans or competition with D-mannose on CD16 abrogate binding to Mac-1 (116-120). Interestingly, these CD16-Mac-1 interactions are absent in $CD16^+$ monocytes due to monocyte CD16A lacking Asn 82, on which N-glycans are formed in the neutrophil CD16B. I hypothesize therefore that lack of HM/hybrid N-glycans on monocytic CD16A allows endothelial HM N-glycans on ICAM-1 to bind Mac-1 and selectively recruit $CD16^+$ monocytes. Consistent with this hypothesis, neutrophil adhesion to endothelial ICAM-1 were independent of HM-structures (79).

It is also worth noting that our model does not imply that ICAM-1 harbors either HM or complex N-glycans. ICAM-1 contains 8 N-glycosylation sites, and each site can be differentially modified with any variety of N-glycan structures, from HM structures to hybrid to complex, sialylated structures. Referring to HM-ICAM-1 means that there are HM epitopes in key N-glycan sites on ICAM-1 that are responsible for monocyte adhesion; i.e., in domain 3.

With understanding the role of HM-ICAM-1 in recruiting monocytes, we wanted to explore its translational potential by looking at its presence *in vivo.* In **chapter 3**, we demonstrate the presence of a HM form of ICAM-1 in both human and mouse atherosclerotic lesions, as well as in CKD patients with failed maturation of AVFs for dialysis. The expression of HM-ICAM-1 increased in human lesions with disease severity, suggesting

the more severe the disease, the more HM epitopes will be present. HM-ICAM-1 was also present in two different mouse models of atherosclerosis: one with a HFD regimen for 12 weeks and another with partial carotid ligation and HFD for 1 week. In both human and mouse studies, HM-ICAM-1 expression positively correlated with CD68 macrophage staining, suggesting a strong association between the two.

Further, identifying HM-ICAM-1 in failed AVFs of dialysis patients indicates that these observations are not only applicable to atherosclerosis, but other models of endothelial dysfunction as well. The rate of AVF failure can be as high as 40%, and in many cases is due in part to the restenosis of the vessel by similar mechanisms as seen in atherosclerotic plaque development (121). While complex, sialylated ICAM-1 was also present in all of these models, the presence of HM-ICAM-1 is most intriguing, since it is thought that protein N-glycoforms must be in the complex form to be expressed on the cell surface.

The regulation of N-glycosylation during inflammation to form those HM epitopes was the subject of **chapter 4.** We were able to show a temporal regulation of α-mannosidase activity and subsequent HM N-glycan formation in ECs. The transient inhibition of α-mannosidase activity (4 hour TNFα treatment) suggests that *in vitro* conditions differ from *in vivo,* as we showed the presence of HM-ICAM-1 in advanced human atherosclerotic lesions. Part of this may be explained by the continuous inflammatory signaling seen in human atherosclerosis; I hypothesize that if we continually added inflammatory stimuli to endothelial cells, we would see a sustained inhibition of α-mannosidase activity and HM-N-glycan formation. Importantly, this inhibition of α-mannosidase ac-

tivity or HM N-glycan formation was not recapitulated in PMVECs, providing some evidence to support the N-glycan "zip code" hypothesis. From there, we were able to identify that class I α-mannosidases were being inhibited by TNFα, which corroborated our lectin staining and western blotting showing an increase specifically in HM residues, as measured by HHL and ConA. Finally, we showed that TNFα was inhibiting α-mannosidase activity through $H_2O_2$, demonstrating for the first time to our knowledge a role for reactive species in regulating N-glycans.

The work shown in this dissertation is summarized in **figure 7:** inflammatory signaling will decrease α-mannosidase activity, in part by the production of $H_2O_2$, and ICAM-1 will then be expressed on the cell surface in a HM glycoform. Vascular beds where ICAM-1 is modified with a HM sugar in domain 3 will specifically recruit $C16^+$ monocytes via Mac-1 and this will exacerbate atherosclerosis. Without the correct sugars, $CD16^+$ monocytes will not be recruited and vessels will remain protected, giving rise to a heterogeneous endothelial "zip code" using N-glycans as the specific recruiting factor.

## Project limitations

Of course, this project has not been without its limitations. First and foremost, our reagents and assays to measure and understand N-glycosylation are limited. One such example lies in the lectins. Lectins are powerful tools used to identify sugars, but their specificity is still somewhat debated. In the past, *Concanavalin A* (ConA) has been used to identify high-mannose (HM) structures; yet in addition to mannose, ConA can also recognize terminal glucose and galactose residues. To complement ConA, we also *used Hip-*

*peastrum Hybrid lectin* (HHL), which is specific for HM epitopes. Further, we complemented *Sambucus Nigra* (SNA), which recognizes α-2-6-sialylation, with *Maackia Amurensis lectin II* (MAL-II), which recognizes α-2-3-sialylation, to differentiate between the two types of sialic acid linkages. By employing these lectins, we were able to explore specific N-glycoforms of ICAM-1 and their impact in disease. Exactly which sites on ICAM-1 are modified and how will be the focus of future investigation. Using tools such as digestion enzymes like PNGaseF and EndoH to digest all and HM N-glycans, respectively, we can identify how much of ICAM-1 harbors HM N-glycans using mass spec analysis. From there, we can use site-directed mutagenesis to mutate N-glycan sites on ICAM-1 and measure the N-glycans still present to determine which sites are modified and how (122).

With the identification of which sites on ICAM-1 are HM during inflammation, we may then be able to develop a glyan-specific antibody that targets HM-ICAM-1 specifically, rather than all of ICAM-1. While glycan-specific antibodies have not yet become commercially available, there are companies (e.g., Antibody Solutions) working on their development by using glycosylated peptides, so perhaps glycan-specific antibodies may become available in the near future. The ability to target this form of ICAM-1 would leave the normally fully processed ICAM-1 intact, evading immune responses that were seen with the ICAM-1 clinical trials discussed earlier.

Human monocytes exist in three subsets, as discussed in the introduction. Yet our studies on monocytes (**chapter 2**) had only two subsets separated: $CD16^-$ and $CD16^+$. There are several reasons for this. First, the only currently viable way to separate all three

subsets is via flow cytometry based on CD14 and CD16 levels. While possible, using antibodies to those or other markers (e.g. CX3CR1) may unintentionally activate our monocytes. In fact, the ability to separate monocytes into the three subsets to then be able to use them for functional studies *in vitro* remains a limitation in the field because of the possibility of antibody activation and the amount of whole blood needed to isolate enough monocytes for functional assays.

Along those lines, we did ensure that our results were not skewed based on our own sorting method, discussed in **chapter 2**. Future studies to look at the intermediate monocyte adhesion vs. the nonclassical adhesion would shed more insight into these subsets and their behavior. Because intermediate monocytes are correlated with cardiovascular disease, and the nature of the non-classical monocytes are largely patrolling, I hypothesize that the intermediate monocytes are the key $CD16^{+}$ monocytes contributing to plaque development.

As alluded to above, studying N-glycosylation enzymes is no easy task, and the α-mannosidases are some of the more complicated enzymes in the pathway due to several reasons. First, α-mannosidases exist not only in two classes, but in 4-5 different isoforms per class. Over the years, the nomenclature of the isoforms and locations of said isoforms have changed, and the information about these enzymes can be confusing and even contradictory just from the terminology alone. The nomenclature is now standardized, which will help understanding in the future. Second, these enzymes are difficult to purify. Class II α-mannosidases have been purified from jack bean, but there are no purified forms of class I α-mannosidases, nor of the isoforms of either class. Finally, these enzymes have a level of functional redundancy, as they are all capable of cleaving the

same terminal mannose linkages. Some isoforms may act on some proteins, while others will not, and this can change depending on cell type and protein turnover (94). Luckily, there are some tools at hand to evaluate α-mannosidases. We were able to directly measure total α-mannosidase activity using fluorescent substrates such a resorufin-α-d-mannopyranoside, and we can employ class I and II small molecule inhibitors in conjunction with inflammatory stimuli treatment to tease out which class of α-mannosidases is being impacted by inflammation.

Finally, the lack of antibodies to the α-mannosidase enzymes limited this project to studying the activity of the enzymes only, instead of being able to look at their expression levels. However, ongoing work in the lab is knocking down the class I α-mannosidase isoforms in Cos1 cell lines to determine the impact on N-glycans. More studies are required to determine if the inhibition seen by TNFα is indeed at the transcript, expression, or activity level. As discussed in **chapter 4**, based on the quick nature of inhibition using $H_2O_2$, I hypothesize that the inhibition is directly on the activity itself rather than at the transcript level.

It also seems that newer, more specific antibodies are becoming increasingly available for these enzymes – I have had success with an antibody from Novus Biologicals for MAN1A1. If this development continues, it will provide even more insight into the mechanism behind α-mannosidase inhibition during inflammation.

## Conclusions and future directions

The idea of adhesion molecule N-glycosylation selectively mediating monocyte adhesion as presented in this dissertation also has implications when discussing endothelial heterogeneity. Differences are observed between vascular beds; for example, the pulmonary endothelium does not respond the same way as an aortic endothelium or venous endothelium to inflammatory stimuli (see **chapter 4**) (28-30, 43). While inflammation increases adhesion molecule expression in both cell lines, aortic endothelial cells have increased surface hypoglycosylation whereas pulmonary endothelial cells do not (43). Combined with the data presented that HM-ICAM-1 recruits $CD16^+$ monocytes, this endothelial 'N-glycan zip code' may represent one mechanism that mediates selective monocyte subset recruitment to specific vascular beds (41, 44).

The only therapies we currently have for the treatment of atherosclerosis outside of lifestyle changes are drugs to lower cholesterol levels and blood pressure, although recent anti-inflammatory strategies demonstrate efficacy, as highlighted by IL-1β antagonism in the Canakinumab anti-inflammatory thrombosis outcomes study (CANTOS) (123-125) . I hypothesize that the key to inflammatory monocyte subset adhesion to specific vascular beds during inflammation is an endothelial N-glycan zip code; where high-mannose N-glycoforms of adhesion molecules, specifically ICAM-1, are only expressed in at-risk vessels and specifically recruit inflammatory $CD16^+$ monocytes. The proposed model provides druggable targets previously unexplored; namely the idea of interfering with monocyte-endothelial adhesion by targeting the N-glycans.

One such method could be inhibition with mannose itself. Mannose therapy has already been shown to slow cancer tumor growth in mice and improve metabolism and

attenuate obesity onset (126, 127). The model presented herein proposes another benefit to mannose therapy; that it may specifically abrogate inflammatory monocyte accumulation while maintaining the integrity of the innate immune system. My hypothesis is that mannose therapy would compete with HM-ICAM-1 for $CD16^+$ monocytes, blocking the Mac-1 ligand and reducing $CD16^+$ monocyte adhesion. At the same time, mannose therapy would not affect endothelial cells that do not express HM-ICAM-1, nor would it inhibit $CD16^-$ adhesion, thereby maintaining an innate immune response.

Much of the work presented herein demonstrate the importance of endothelial N-glycans in disease progression using *ex vivo* and *in vitro* models. Ongoing work is focusing on the impact on HM N-glycans, and blocking HM N-glycans, in atherosclerosis development *in vivo*. For those purposes, we are beginning to use a partial carotid ligation mouse model that incorporates the use of a topical pluronic gel containing the class I α-mannosidase inhibitor Kifunensine (Kif) to form HM structures in the injured carotid artery. Preliminary data from this model show larger lesions in Kif-treated animals, as well as a positive correlation with CD68 macrophage staining. We also plan to incorporate mannose supplementation into this model moving forward to see if it will decrease lesion size and macrophage infiltrations.

Glycobiology is essential to life as we know it, and glycans play key roles in all aspects of health and disease. As science and medicine continue to advance, it would be unsurprising to find many N-glycan dependent niches similar to what I have outlined in this dissertation applicable to other diseases, especially cancer and autoimmune diseases such as lupus. The emergence of data demonstrating the importance of N-glycans will pro-

pel the field forward, and more pertinent therapeutics targeting the appropriate N-glycoforms of proteins or the N-glycosylation pathway can be developed for the treatment of not only atherosclerosis, but other inflammatory-based diseases as well.

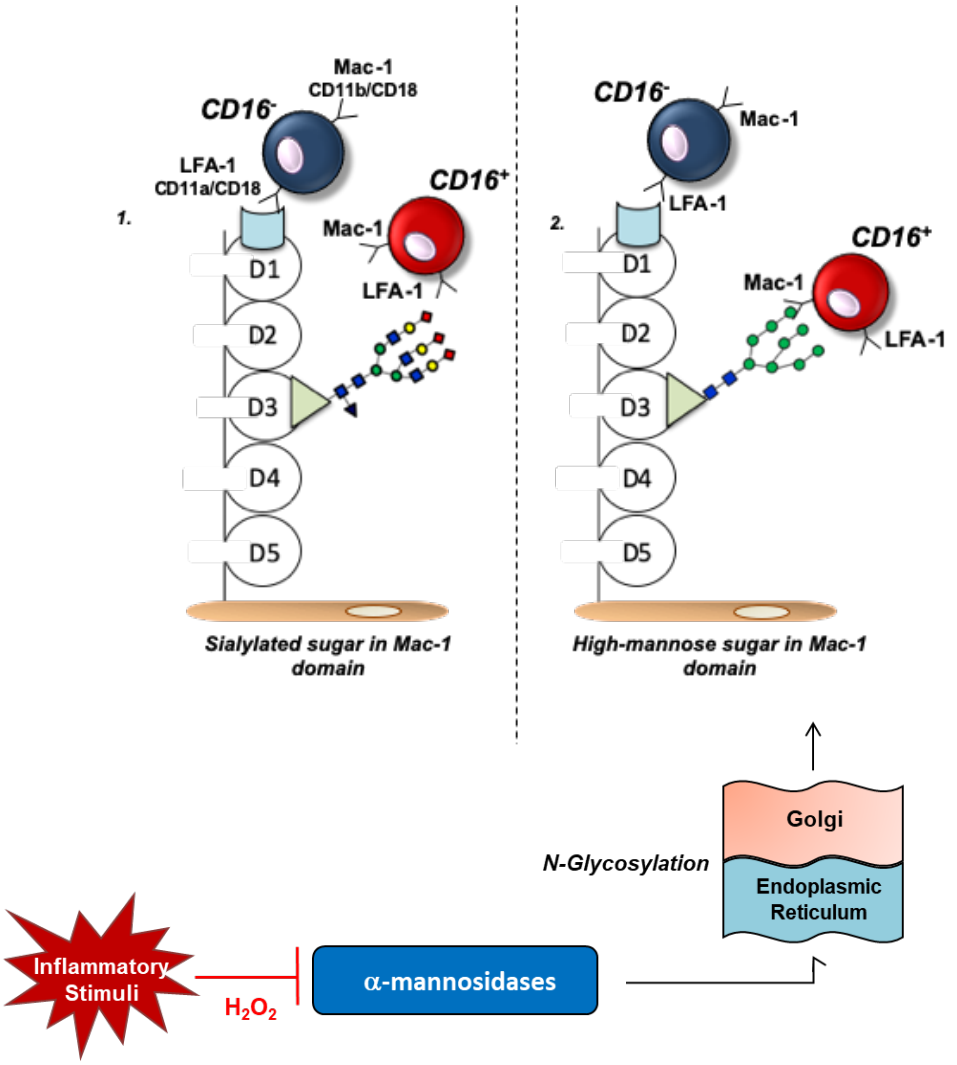


**Figure 7**. **Formation of HM N-glycans on the cell surface recruit CD16$^{+}$ monocytes**. Inflammatory stimuli produce $H_2O_2$ that inhibits α-mannosidase activity, decreasing N-glycosylation and causing a HM-ICAM-1 on the cell surface. CD16$^{+}$ monocytes will adhere to LFA-1 or Mac-1 binding domain, but adhere more frequently to Mac-1 when there is a high-mannose N-glycan in the Mac-1 binding domain. CD16$^{-}$ monocytes will adhere to LFA-1 or Mac-1 regardless of the N-glycan modification.

# General References

1. Ikeda U, Takahashi M, Shimada K. Monocyte-endothelial cell interaction in atherogenesis and thrombosis. Clin Cardiol. 1998;21(1):11-4.

2. Mestas J, Ley K. Monocyte-endothelial cell interactions in the development of atherosclerosis. Trends Cardiovasc Med. 2008;18(6):228-32.

3. Faruqi RM, DiCorleto PE. Mechanisms of monocyte recruitment and accumulation. Br Heart J. 1993;69(1 Suppl):S19-29.

4. Bevilacqua MP. Endothelial-leukocyte adhesion molecules. Annu Rev Immunol. 1993;11:767-804.

5. Diamond MS, Staunton DE, de Fougerolles AR, Stacker SA, Garcia-Aguilar J, Hibbs ML, et al. ICAM-1 (CD54): a counter-receptor for Mac-1 (CD11b/CD18). J Cell Biol. 1990;111(6 Pt 2):3129-39.

6. Dunne JL, Collins RG, Beaudet AL, Ballantyne CM, Ley K. Mac-1, but not LFA-1, uses intercellular adhesion molecule-1 to mediate slow leukocyte rolling in TNF-alpha-induced inflammation. J Immunol. 2003;171(11):6105-11.

7. Dustin ML, Springer TA. Lymphocyte function-associated antigen-1 (LFA-1) interaction with intercellular adhesion molecule-1 (ICAM-1) is one of at least three mechanisms for lymphocyte adhesion to cultured endothelial cells. J Cell Biol. 1988;107(1):321-31.

8. Forchhammer L, Loft S, Roursgaard M, Cao Y, Riddervold IS, Sigsgaard T, et al. Expression of adhesion molecules, monocyte interactions and oxidative stress in human endothelial cells exposed to wood smoke and diesel exhaust particulate matter. Toxicol Lett. 2012;209(2):121-8.

9. Deanfield JE, Halcox JP, Rabelink TJ. Endothelial function and dysfunction: testing and clinical relevance. Circulation. 2007;115(10):1285-95.

10. Esper RJ, Nordaby RA, Vilarino JO, Paragano A, Cacharron JL, Machado RA. Endothelial dysfunction: a comprehensive appraisal. Cardiovasc Diabetol. 2006;5:4.

11. Hadi HA, Suwaidi JA. Endothelial dysfunction in diabetes mellitus. Vasc Health Risk Manag. 2007;3(6):853-76.

12. Mauro D, Nerviani A. Endothelial Dysfunction in Systemic Lupus Erythematosus: Pathogenesis, Assessment and Therapeutic Opportunities. Rev Recent Clin Trials. 2018;13(3):192-8.

13. Shi C, Pamer EG. Monocyte recruitment during infection and inflammation. Nat Rev Immunol. 2011;11(11):762-74.

14. Idzkowska E, Eljaszewicz A, Miklasz P, Musial WJ, Tycinska AM, Moniuszko M. The role of different monocyte subsets in the pathogenesis of atherosclerosis and acute coronary syndromes. Scan J of Immun. 2015;82(3):163-73.

15. Castier Y, Lehoux S, Hu Y, Foteinos G, Tedgui A, Xu Q. Characterization of neointima lesions associated with arteriovenous fistulas in a mouse model. Kidney Int. 2006;70(2):315-20.

16. Rekhter M, Nicholls S, Ferguson M, Gordon D. Cell proliferation in human arteriovenous fistulas used for hemodialysis. Arterioscler Thromb. 1993;13(4):609-17.

17. Liu BC, Li L, Gao M, Wang YL, Yu JR. Microinflammation is involved in the dysfunction of arteriovenous fistula in patients with maintenance hemodialysis. Chin Med J (Engl). 2008;121(21):2157-61.

18. Ramirez R, Carracedo J, Merino A, Soriano S, Ojeda R, Alvarez-Lara MA, et al. CD14+CD16+ monocytes from chronic kidney disease patients exhibit increased adhesion ability to endothelial cells. Contrib Nephrol. 2011;171:57-61.

19. Bourdillon MC, Poston RN, Covacho C, Chignier E, Bricca G, McGregor JL. ICAM-1 deficiency reduces atherosclerotic lesions in double-knockout mice (ApoE(-/-)/ICAM-1(-/-)) fed a fat or a chow diet. Arterioscler Thromb Vasc Biol. 2000;20(12):2630-5.

20. Collins RG, Velji R, Guevara NV, Hicks MJ, Chan L, Beaudet AL. P-Selectin or intercellular adhesion molecule (ICAM)-1 deficiency substantially protects against atherosclerosis in apolipoprotein E-deficient mice. J Exp Med. 2000;191(1):189-94.

21. Patel SS, Thiagarajan R, Willerson JT, Yeh ET. Inhibition of alpha4 integrin and ICAM-1 markedly attenuate macrophage homing to atherosclerotic plaques in ApoE-deficient mice. Circulation. 1998;97(1):75-81.

22. Argenbright LW, Letts LG, Rothlein R. Monoclonal antibodies to the leukocyte membrane CD18 glycoprotein complex and to intercellular adhesion molecule-1 inhibit leukocyte-endothelial adhesion in rabbits. J Leukoc Biol. 1991;49(3):253-7.

23. Investigators EAST. Use of anti-ICAM-1 therapy in ischemic stroke. Neurology. 2001;57(8):1428-34.

24. Salmela K, Wramner L, Ekberg H, Hauser I, Bentdal O, Lins LE, et al. A randomized multicenter trial of the anti-ICAM-1 monoclonal antibody (enlimomab) for the prevention of acute rejection and delayed onset of graft function in cadaveric renal transplantation: a report of the European Anti-ICAM-1 Renal Transplant Study Group. Transplantation. 1999;67(5):729-36.

25. Boyette LB, Macedo C, Hadi K, Elinoff BD, Walters JT, Ramaswami B, et al. Phenotype, function, and differentiation potential of human monocyte subsets. PLoS One. 2017;12(4):e0176460.

26. Ingersoll MA, Spanbroek R, Lottaz C, Gautier EL, Frankenberger M, Hoffmann R, et al. Comparison of gene expression profiles between human and mouse monocyte subsets. Blood. 2010;115(3):e10-9.

27. Shantsila E, Wrigley B, Tapp L, Apostolakis S, Montoro-Garcia S, Drayson MT, et al. Immunophenotypic characterization of human monocyte subsets: possible implications for cardiovascular disease pathophysiology. J Thromb Haemost. 2011;9(5):1056-66.

28. Aird WC. Endothelial cell heterogeneity. Cold Spring Harb Perspect Med. 2012;2(1):a006429.

29. Aird WC. Phenotypic heterogeneity of the endothelium: II. Representative vascular beds. Circ Res. 2007;100(2):174-90.

30. Aird WC. Phenotypic heterogeneity of the endothelium: I. Structure, function, and mechanisms. Circ Res. 2007;100(2):158-73.

31. Cejkova S, Kralova-Lesna I, Poledne R. Monocyte adhesion to the endothelium is an initial stage of atherosclerosis development. Cor et Vasa. 2015;58(4):e419-25.

32. Chi Z, Melendez AJ. Role of cell adhesion molecules and immune-cell migration in the initiation, onset and development of atherosclerosis. Cell Adh Migr. 2007;1(4):171-5.

33. Galkina E, Ley K. Immune and inflammatory mechanisms of atherosclerosis (*). Annu Rev Immunol. 2009;27:165-97.

34. Carlos TM, Harlan JM. Leukocyte-endothelial adhesion molecules. Blood. 1994;84(7):2068-101.

35. Galkina E, Ley K. Vascular adhesion molecules in atherosclerosis. Arterioscler Thromb Vasc Biol. 2007;27(11):2292-301.

36. Tak PP, Firestein GS. NF-kappaB: a key role in inflammatory diseases. J Clin Invest. 2001;107(1):7-11.

37. Devaux B, Scholz D, Hirche A, Klovekorn WP, Schaper J. Upregulation of cell adhesion molecules and the presence of low grade inflammation in human chronic heart failure. Eur Heart J. 1997;18(3):470-9.

38. Nagel T, Resnick N, Atkinson WJ, Dewey CF, Jr., Gimbrone MA, Jr. Shear stress selectively upregulates intercellular adhesion molecule-1 expression in cultured human vascular endothelial cells. J Clin Invest. 1994;94(2):885-91.

39. Swirski FK, Weissleder R, Pittet MJ. Heterogeneous in vivo behavior of monocyte subsets in atherosclerosis. Arterioscler Thromb Vasc Biol. 2009;29(10):1424-32.

40. Wong KL, Yeap WH, Tai JJY, Ong SM, Dang TM, Wong SC. The three human monocyte subsets: implications for health and disease. Immunologic Research. 2012;53(1):41-57.

41. Renkonen J, Tynninen O, Hayry P, Paavonen T, Renkonen R. Glycosylation might provide endothelial zip codes for organ-specific leukocyte traffic into inflammatory sites. Am J Pathol. 2002;161(2):543-50.

42. Croci DO, Cerliani JP, Dalotto-Moreno T, Mendez-Huergo SP, Mascanfroni ID, Dergan-Dylon S, et al. Glycosylation-dependent lectin-receptor interactions preserve angiogenesis in anti-VEGF refractory tumors. Cell. 2014;156(4):744-58.

43. Scott DW, Vallejo MO, Patel RP. Heterogenic Endothelial Responses to Inflammation: Role for Differentital N-Glycosylation and Vascular Bed of Origin. J American Heart Association. 2013;2(4).

44. Thorpe PE, Ran S. Mapping zip codes in human vasculature. Pharmacogenomics J. 2002;2(4):205-6.

45. Kochanek KD, Murphy SL, Xu J, Arias E. Deaths: Final Data for 2017. National Vital Statistics Report. 2019;68(9).

46. Benjamin EJ, Muntner P, Alonso A, Bittencourt MS, Callaway CW, Carson AP, et al. Heart Disease and Stroke Statistics-2019 Update: A Report From the American Heart Association. Circulation. 2019;139(10):e56-e528.

47. Hansson GK, Libby P. The immune response in atherosclerosis: a double-edged sword. Nat Rev Immunol. 2006;6(7):508-19.

48. Libby P. History of Discovery: Inflammation in Atherosclerosis. Arterioscler Thromb Vasc Biol. 2012;32(9):2045-51.

49. Libby P. Inflammation in atherosclerosis. Nature. 2002;420(6917):868-74.

50. Remmerie A, Scott CL. Macrophages and lipid metabolism. Cell Immunol. 2018;330:27-42.

51. Blair HC, Sepulveda J, Papachristou DJ. Nature and nurture in atherosclerosis: The roles of acylcarnitine and cell membrane-fatty acid intermediates. Vascul Pharmacol. 2016;78:17-23.

52. van Furth R, Cohn ZA. The origin and kinetics of mononuclear phagocytes. J Exp Med. 1968;128(3):415-35.

53. van Furth R, Raeburn JA, van Zwet TL. Characteristics of human mononuclear phagocytes. Blood. 1979;54(2):485-500.

54. Ziegler-Heitbrock L. Blood Monocytes and Their Subsets: Established Features and Open Questions. Front Immunol. 2015;6:423.

55. Wong KL, Tai JJ, Wong WC, Han H, Sem X, Yeap WH, et al. Gene expression profiling reveals the defining features of the classical, intermediate, and nonclassical human monocyte subsets. Blood. 2011;118(5):e16-31.

56. Ancuta P, Rao R, Moses A, Mehle A, Shaw SK, Luscinskas FW, et al. Fractalkine preferentially mediates arrest and migration of CD16+ monocytes. J Exp Med. 2003;197(12):1701-7.

57. Cros J, Cagnard N, Woollard K, Patey N, Zhang SY, Senechal B, et al. Human CD14dim monocytes patrol and sense nucleic acids and viruses via TLR7 and TLR8 receptors. Immunity. 2010;33(3):375-86.

58. Smedman C, Ernemar T, Gudmundsdotter L, Gille-Johnson P, Somell A, Nihlmark K, et al. FluoroSpot Analysis of TLR-Activated Monocytes Reveals Several Distinct Cytokine-Secreting Subpopulations. Scand J Immunol. 2012;75(2):249-58.

59. Zawada AM, Rogacev KS, Rotter B, Winter P, Marell RR, Fliser D, et al. SuperSAGE evidence for CD14++CD16+ monocytes as a third monocyte subset. Blood. 2011;118(12):e50-61.

60. Auffray C, Fogg D, Garfa M, Elain G, Join-Lambert O, Kayal S, et al. Monitoring of blood vessels and tissues by a population of monocytes with patrolling behavior. Science. 2007;317(5838):666-70.

61. Rossol M, Kraus S, Pierer M, Baerwald C, Wagner U. The CD14(bright) CD16+ monocyte subset is expanded in rheumatoid arthritis and promotes expansion of the Th17 cell population. Arthritis Rheum. 2012;64(3):671-7.

62. Belge KU, Dayyani F, Horelt A, Siedlar M, Frankenberger M, Frankenberger B, et al. The proinflammatory CD14+CD16+DR++ monocytes are a major source of TNF. J Immunol. 2002;168(7):3536-42.

63. Skrzeczynska-Moncznik J, Bzowska M, Loseke S, Grage-Griebenow E, Zembala M, Pryjma J. Peripheral blood CD14high CD16+ monocytes are main producers of IL-10. Scand J Immunol. 2008;67(2):152-9.

64. Babaev VR, Bobryshev YV, Sukhova GK, Kasantseva IA. Monocyte/macrophage accumulation and smooth muscle cell phenotypes in early atherosclerotic lesions of human aorta. Atherosclerosis. 1993;100(2):237-48.

65. Bobryshev YV. Monocyte recruitment and foam cell formation in atherosclerosis. Micron. 2006;37(3):208-22.

66. Bobryshev YV, Lord RS. Ultrastructural recognition of cells with dendritic cell morphology in human aortic intima. Contacting interactions of Vascular Dendritic Cells in athero-resistant and athero-prone areas of the normal aorta. Arch Histol Cytol. 1995;58(3):307-22.

67. Libby P. Changing concepts of atherogenesis. J Intern Med. 2000;247(3):349-58.

68. Lusis AJ. Atherosclerosis. Nature. 2000;407(6801):233-41.

69. Rogacev KS, Cremers B, Zawada AM, Seiler S, Binder N, Ege P, et al. CD14++CD16+ monocytes independently predict cardiovascular events: a cohort study of 951 patients referred for elective coronary angiography. J Am Coll Cardiol. 2012;60(16):1512-20.

70. Wildgruber M, Aschenbrenner T, Wendorff H, Czubba M, Glinzer A, Haller B, et al. The "Intermediate" CD14(++)CD16(+) monocyte subset increases in severe peripheral artery disease in humans. Sci Rep. 2016;6:39483.

71. Heine GH, Ulrich C, Seibert E, Seiler S, Marell J, Reichart B, et al. CD14(++)CD16+ monocytes but not total monocyte numbers predict cardiovascular events in dialysis patients. Kidney Int. 2008;73(5):622-9.

72. Kapinsky M, Torzweski M, Buchler C, Duong CQ, Rother G, Schmitz G. Enzymatically degraded LDL preferentially binds to $CD14^{high}$ CD16+ monocytes and induces foam cell formation mediated only in part by the class B scavenger-receptor CD36. Arterioscler Thromb Vasc Biol. 2001;21:1004-10.

73. Merino A, Buendia P, Martin-Malo A, Aljama P, Ramirez R, Carracedo J. Senescent CD14+CD16+ monocytes exhibit proinflammatory and proatherosclerotic activity. J Immunol. 2011;186(3):1809-15.

74. Zawada AM, Fell LH, Untersteller K, Seiler S, Rogacev KS, Fliser D, et al. Comparison of two different strategies for human monocyte subsets gating within the large-scale prospective CARE FOR HOMe Study. Cytometry A. 2015;87(8):750-8.

75. Weber C, Shantsila E, Hristov M, Caligiuri G, Guzik T, Heine GH, et al. Role and analysis of monocyte subsets in cardiovascular disease. Joint consensus document of the European Society of Cardiology (ESC) Working Groups "Atherosclerosis & Vascular Biology" and "Thrombosis". Thromb Haemost. 2016;116(4):626-37.

76. Ziegler-Heitbrock L. The CD14+ CD16+ blood monocytes: their role in infection and inflammation. J Leukoc Biol. 2007;81(3):584-92.

77. Starikova EA, Lebedeva AM, Freidlin IS. [CD14++CD16- and CD14+CD16+ human monocytes adhesion to endothelial cells]. Tsitologiia. 2010;52(5):380-3.

78. Aspinall AI, Curbishley SM, Lalor PF, Weston CJ, Blahova M, Liaskou E, et al. CX(3)CR1 and vascular adhesion protein-1-dependent recruitment of CD16(+) monocytes across human liver sinusoidal endothelium. Hepatology. 2010;51(6):2030-9.

79. Regal-McDonald K, Xu B, Barnes JW, Patel RP. High-mannose intercellular adhesion molecule-1 (ICAM-1) enhances CD16+ monocyte adhesion to the endothelium. Am J Physiol Heart Circ Physiol. 2019.

80. Poston RN, Haskard DO, Coucher JR, Gall NP, Johnson-Tidey RR. Expression of intercellular adhesion molecule-1 in atherosclerotic plaques. Am J Pathol. 1992;140(3):665-73.

81. van der Wal AC, Das PK, Tigges AJ, Becker AE. Adhesion molecules on the endothelium and mononuclear cells in human atherosclerotic lesions. Am J Pathol. 1992;141(6):1427-33.

82. Garcia-Vallejo JJ, Van Dijk W, Van Het Hof B, Van Die I, Engelse MA, Van Hinsbergh VW, et al. Activation of human endothelial cells by tumor necrosis factor-alpha results in profound changes in the expression of glycosylation-related genes. J Cell Physiol. 2006;206(1):203-10.

83. Davenpeck KL, Sterbinsky SA, Bochner BS. Rat neutrophils express alpha4 and beta1 integrins and bind to vascular cell adhesion molecule-1 (VCAM-1) and mucosal addressin cell adhesion molecule-1 (MAdCAM-1). Blood. 1998;91(7):2341-6.

84. Ding ZM, Babensee JE, Simon SI, Lu H, Perrard JL, Bullard DC, et al. Relative contribution of LFA-1 and Mac-1 to neutrophil adhesion and migration. J Immunol. 1999;163(9):5029-38.

85. Gerhardt T, Ley K. Monocyte trafficking across the vessel wall. Cardiovasc Res. 2015;107(3):321-30.

86. Lefort CT, Ley K. Neutrophil arrest by LFA-1 activation. Front Immunol. 2012;3:157.

87. Tacke F, Alvarez D, Kaplan TJ, Jakubzick C, Spanbroek R, Llodra J, et al. Monocyte subsets differentially employ CCR2, CCR5, and CX3CR1 to accumulate within atherosclerotic plaques. J Clin Invest. 2007;117(1):185-94.

88. Deniset JF, Kubes P. Intravital Imaging of Myeloid Cells: Inflammatory Migration and Resident Patrolling. Microbiol Spectr. 2016;4(6).

89. Hickey MJ, Forster M, Mitchell D, Kaur J, De Caigny C, Kubes P. L-selectin facilitates emigration and extravascular locomotion of leukocytes during acute inflammatory responses in vivo. J Immunol. 2000;165(12):7164-70.

90. Li N, Yang H, Wang M, Lu S, Zhang Y, Long M. Ligand-specific binding forces of LFA-1 and Mac-1 in neutrophil adhesion and crawling. Mol Biol Cell. 2018;29(4):408-18.

91. Shimaoka M, Xiao T, Liu JH, Yang Y, Dong Y, Jun CD, et al. Structures of the alpha L I domain and its complex with ICAM-1 reveal a shape-shifting pathway for integrin regulation. Cell. 2003;112(1):99-111.

92. Rodgers SD, Camphausen RT, Hammer DA. Sialyl Lewis(x)-mediated, PSGL-1-independent rolling adhesion on P-selectin. Biophys J. 2000;79(2):694-706.

93. Stec M, Weglarczyk K, Baran J, Zuba E, Mytar B, Pryjma J, et al. Expansion and differentiation of CD14+CD16(-) and CD14+ +CD16+ human monocyte subsets from cord blood CD34+ hematopoietic progenitors. J Leukoc Biol. 2007;82(3):594-602.

94. Stanley P, Schachter H, Taniguchi N. N-Glycans. In: nd, Varki A, Cummings RD, Esko JD, Freeze HH, Stanley P, et al., editors. Essentials of Glycobiology. Cold Spring Harbor (NY)2009.

95. Khoury GA, Baliban RC, Floudas CA. Proteome-wide post-translational modification statistics: frequency analysis and curation of the swiss-prot database. Sci Rep. 2011;1.

96. Lau KS, Partridge EA, Grigorian A, Silvescu CI, Reinhold VN, Demetriou M, et al. Complex N-glycan number and degree of branching cooperate to regulate cell proliferation and differentiation. Cell. 2007;129(1):123-34.

97. Holdbrooks AT, Britain CM, Bellis SL. ST6Gal-I sialyltransferase promotes tumor necrosis factor (TNF)-mediated cancer cell survival via sialylation of the TNF receptor 1 (TNFR1) death receptor. J Biol Chem. 2018;293(5):1610-22.

98. Glavey SV, Huynh D, Reagan MR, Manier S, Moschetta M, Kawano Y, et al. The cancer glycome: carbohydrates as mediators of metastasis. Blood Rev. 2015;29(4):269-79.

99. Herscovics A. Structure and function of Class I alpha 1,2-mannosidases involved in glycoprotein synthesis and endoplasmic reticulum quality control. Biochimie. 2001;83(8):757-62.

100. Lipari F, Gour-Salin BJ, Herscovics A. The Saccharomyces cerevisiae processing alpha 1,2-mannosidase is an inverting glycosidase. Biochem Biophys Res Commun. 1995;209(1):322-6.

101. Shah N, Kuntz DA, Rose DR. Golgi alpha-mannosidase II cleaves two sugars sequentially in the same catalytic site. Proc Natl Acad Sci U S A. 2008;105(28):9570-5.

102. Shah N, Kuntz DA, Rose DR. Comparison of kifunensine and 1-deoxymannojirimycin binding to class I and II alpha-mannosidases demonstrates different

saccharide distortions in inverting and retaining catalytic mechanisms. Biochemistry. 2003;42(47):13812-6.

103. Tremblay LO, Herscovics A. Cloning and expression of a specific human alpha 1,2-mannosidase that trims Man9GlcNAc2 to Man8GlcNAc2 isomer B during N-glycan biosynthesis. Glycobiology. 1999;9(10):1073-8.

104. Fujiyama K, Sakuradani S, Moran DG, Yoshida T, Seki T. Effect of alpha1,2-mannosidic linkage located in a alpha1,3-branch of Man6GlcNAc2 oligosaccharide on enzyme activity of recombinant human Man9-mannosidase produced in Escherichia coli. J Biosci Bioeng. 2001;91(4):419-21.

105. Isoyama-Tanaka J, Dohi K, Misaki R, Fujiyama K. Improved expression and characterization of recombinant human Golgi alpha1,2-mannosidase I isoforms (IA2 and IC) by Escherichia coli. J Biosci Bioeng. 2011;112(1):14-9.

106. Scott D, Dunn T, Ballestas M, Litovsky S, Patel RP. Identification of a high-mannose ICAM-1 glycoform: effects of ICAM-1 hypoglycosylation on monocyte adhesion and outside in signaling. Am J Physiol Cell Physiol. 2013;305(2):C228-37.

107. Staunton DE, Marlin SD, Stratowa C, Dustin ML, Springer TA. Primary structure of ICAM-1 demonstrates interaction between members of the immunoglobulin and integrin supergene families. Cell. 1988;52(6):925-33.

108. Liu G, Place AT, Chen Z, Brovkovych VM, Vogel SM, Muller WA, et al. ICAM-1-activated Src and eNOS signaling increase endothelial cell surface PECAM-1 adhesivity and neutrophil transmigration. Blood. 2012;120(9):1942-52.

109. Scott DW, Chen J, Chacko BK, Traylor JG, Orr AW, Patel RP. Role for endothelial N-glycan mannose residues in monocyte recruitment during atherogenesis. Arterioscler Thromb Vasc Biol. 2012;32(8).

110. Diamond MS, Staunton DE, Marlin SD, Springer TA. Binding of the integrin Mac-1 (CD11b/CD18) to the third immunoglobulin-like domain of ICAM-1 (CD54) and its regulation by glycosylation. Cell. 1991;65(6):961-71.

111. Kevil CG, Patel RP, Bullard DC. Essential role of ICAM-1 in mediating monocyte adhesion to aortic endothelial cells. Am J Physiol Cell Physiol. 2001;281(5):C1442-7.

112. Ramos TN, Bullard DC, Barnum SR. ICAM-1: Isoforms and Phenotypes. J Immunol. 2014;192(10):4469-74.

113. Jimenez D, Roda-Navarro P, Springer TA, Casanovas JM. Contribution of N-linked glycans to the conformation and function of intercellular adhesion molecules (ICAMs). J Biol Chem. 2005;280(17):5854-61.

114. Chacko BK, Scott D, Chandler RT, Patel RP. Endothelial surface N-Glycans mediate monocyte adhesion and are targets for anti-inflammatory effects of peroxisome proliferator-activated receptor Y ligands. J Biol Chem. 2011;286(44):38738-47.

115. Wildgruber M, Czubba M, Aschenbrenner T, Wendorff H, Hapfelmeier A, Glinzer A, et al. Increased intermediate CD14(++)CD16(++) monocyte subset levels associate with restenosis after peripheral percutaneous transluminal angioplasty. Atherosclerosis. 2016;253:128-34.

116. Edberg JC, Kimberly RP. Cell type-specific glycoforms of Fc gamma RIIIa (CD16): differential ligand binding. J Immunol. 1997;159(8):3849-57.

117. Kimberly RP, Tappe NJ, Merriam LT, Redecha PB, Edberg JC, Schwartzman S, et al. Carbohydrates on human Fc gamma receptors. Interdependence of the classical IgG and nonclassical lectin-binding sites on human Fc gamma RIII expressed on neutrophils. J Immunol. 1989;142(11):3923-30.

118. Preynat-Seauve O, Villiers CL, Jourdan G, Richard MJ, Plumas J, Favier A, et al. An interaction between CD16 and CR3 enhances iC3b binding to CR3 but is lost during differentiation of monocytes into dendritic cells. Eur J Immunol. 2004;34(1):147-55.

119. Xia Y, Borland G, Huang J, Mizukami IF, Petty HR, Todd RF, 3rd, et al. Function of the lectin domain of Mac-1/complement receptor type 3 (CD11b/CD18) in regulating neutrophil adhesion. J Immunol. 2002;169(11):6417-26.

120. Zhou M, Todd RF, 3rd, van de Winkel JG, Petty HR. Cocapping of the leukoadhesin molecules complement receptor type 3 and lymphocyte function-associated antigen-1 with Fc gamma receptor III on human neutrophils. Possible role of lectin-like interactions. J Immunol. 1993;150(7):3030-41.

121. Schinstock CA, Albright RC, Williams AW, Dillon JJ, Bergstralh EJ, Jenson BM, et al. Outcomes of arteriovenous fistula creation after the Fistula First Initiative. Clin J Am Soc Nephrol. 2011;6(8):1996-2002.

122. Tsai PL, Chen SF. A Brief Review of Bioinformatics Tools for Glycosylation Analysis by Mass Spectrometry. Mass Spectrom (Tokyo). 2017;6(Spec Iss):S0064.

123. Everett BM, Cornel JH, Lainscak M, Anker SD, Abbate A, Thuren T, et al. Anti-Inflammatory Therapy With Canakinumab for the Prevention of Hospitalization for Heart Failure. Circulation. 2019;139(10):1289-99.

124. Ridker PM, MacFadyen JG, Thuren T, Everett BM, Libby P, Glynn RJ, et al. Effect of interleukin-1beta inhibition with canakinumab on incident lung cancer in patients with atherosclerosis: exploratory results from a randomised, double-blind, placebo-controlled trial. Lancet. 2017;390(10105):1833-42.

125. Kosmas CE, Silverio D, Sourlas A, Montan PD, Guzman E, Garcia MJ. Anti-inflammatory therapy for cardiovascular disease. Ann Transl Med. 2019;7(7):147.

126. Sharma V, Smolin J, Nayak J, Ayala JE, Scott DA, Peterson SN, et al. Mannose Alters Gut Microbiome, Prevents Diet-Induced Obesity, and Improves Host Metabolism. Cell Rep. 2018;24(12):3087-98.

127. Gonzalez PS, O'Prey J, Cardaci S, Barthet VJA, Sakamaki JI, Beaumatin F, et al. Mannose impairs tumour growth and enhances chemotherapy. Nature. 2018;563(7733):719-23.

# APPENDIX A

## COPYRIGHT STATEMENT AMERICAN JOURNAL OF PHYSIOLOGY

COPYRIGHT STATEMENT

## Reuse by Authors of Their Work Published by APS

The APS Journals are copyrighted for the protection of authors and the Society. The Mandatory Submission Form serves as the Society's official copyright transfer form. Author's rights to reuse their APS-published work are described below:

| | |
|---|---|
| Republication in New Works | Authors may republish parts of their final-published work (e.g., figures, tables), without charge and without requesting permission, provided that full citation of the source is given in the new work. |
| Meeting Presentations and Conferences | Authors may use their work (in whole or in part) for presentations (e.g., at meetings and conferences). These presentations may be reproduced on any type of media in materials arising from the meeting or conference such as the proceedings of a meeting or conference. A copyright fee will apply if there is a charge to the user or if the materials arising are directly or indirectly commercially supported[1]. Full citation is required. |
| Theses and Dissertations | Authors may reproduce whole published articles in dissertations and post to thesis repositories without charge and without requesting permission. Full citation is required. |
| Open Courseware | Authors may post articles, chapters or parts thereof to a public access courseware website. Permission must be requested from the APS[1]. A copyright fee will apply to a book chapter and during the first 12 months of a journal article's publication. Full citation is required. |

# APPENDIX B

# INSTITUTIONAL REVIEW BOARD APPROVAL

THE UNIVERSITY OF ALABAMA AT BIRMINGHAM
Office of the Institutional Review Board for Human Use

470 Administration Building
701 20th Street South
Birmingham, AL 35294-0104
205.934.3789 | Fax 205.934.1301 |
irb@uab.edu

## APPROVAL LETTER

**TO:** Patel, Rakesh Pravinchandra

**FROM:** University of Alabama at Birmingham Institutional Review Board
Federalwide Assurance # FWA00005960
IORG Registration # IRB00000196 (IRB 01)
IORG Registration # IRB00000726 (IRB 02)

**DATE:** 09-Jul-2019

**RE:** IRB-090504006
Role of hemoglobin b93cys residue in nitric oxide bioactivity

---

The IRB reviewed and approved the Continuing Review submitted on 17-Jun-2019 for the above referenced project. The review was conducted in accordance with UAB's Assurance of Compliance approved by the Department of Health and Human Services.

| | |
|---|---|
| **Type of Review:** | Expedited |
| **Expedited Categories:** | 2 |
| **Determination:** | Approved |
| **Approval Date:** | 09-Jul-2019 |
| **Approval Period:** | One Year |
| **Expiration Date:** | 08-Jul-2020 |

It was noted that this protocol has been open to enrollment for 5 years or more. The IRB requires that you submit an updated Human Subjects Protocol (HSP) every 5 years. You will need to submit an updated HSP (including any changes or revisions since the start of the study) at the time of your next renewal and indicate that this is a "5-year renewal". See the IRB website for the most recent form http://www.uab.edu/irb/forms/hsp.doc.

**Documents Included in Review:**

- continuing review